

**NASA TECHNICAL  
TRANSLATION**

NASA TT F-790



**NASA TT F-790**



**LOAN COPY: RETU  
AFWL TECHNICAL L  
KIRTLAND AFB, N. M.**

**HEAT TRANSFER IN THE ATMOSPHERE**

*Edited by Ye. M. Feygel'son and L. R. Tsvang*

*"Nauka" Press, Moscow, 1972*



**NATIONAL AERONAUTICS AND SPACE ADMINISTRATION • WASHINGTON, D. C. • JULY 1974**



0069090

1. Report No. NASA TT F-790		2. Government Accession No.		3. Recipient's Catalog No.	
4. Title and Subtitle HEAT TRANSFER IN THE ATMOSPHERE				5. Report Date July 1974	
				6. Performing Organization Code	
7. Author(s) Ye. M. Feygel'son and L.R. Tsvang, Editors				8. Performing Organization Report No.	
				10. Work Unit No.	
9. Performing Organization Name and Address Linguistic Systems, Inc. 116 Austin Street Cambridge, MA 02139				11. Contract or Grant No. NASW-2482	
				13. Type of Report and Period Covered TRANSLATION	
12. Sponsoring Agency Name and Address NATIONAL AERONAUTICS AND SPACE ADMINISTRATION WASHINGTON, D.C. 20546				14. Sponsoring Agency Code	
15. Supplementary Notes Translation of "Teploobmen v Atmosfere," Moscow, "Nauka" Press, 1972, pp 1-147					
16. Abstract  Investigations of radiant and turbulent heat transfer in the atmosphere are presented in this collection.  Data concerning radiant heat transfer in the troposphere in a cloudless sky, in stratiform and broken cloud cover, were obtained by means of aircraft and ground measurements, numerical experiments, and theoretical analysis. Turbulent heat fluxes were measured from aircraft in the boundary layer of the atmosphere in conditions of a clear sky and in convective cloud cover. The basic quantitative relationships of radiant heat transfer were considered depending upon cloud cover—the principal regulator of the transfer of radiation, and also as a function of other factors. Various methods of calculating the radiant influx of heat are compared. Methods of considering radiant heat transfer in problems of the general circulation of the atmosphere and weather forecasting are presented.					
17. Key Words (Suggested by Author(s))			18. Distribution Statement  Unclassified - unlimited  STAR Category 13		
19. Security Classif. (of this report) Unclassified	20. Security Classif. (of this page) Unclassified	21. No. of Pages 210	22. Price* \$5.75		



Investigations of radiant and turbulent heat transfer in the atmosphere are presented in this collection.

Data concerning radiant heat transfer in the troposphere in a cloudless sky, in stratiform and broken cloud cover, were obtained by means of aircraft and ground measurements, numerical experiments, and theoretical analysis. Turbulent heat fluxes were measured from aircraft in the boundary layer of the atmosphere in conditions of a clear sky and in convective cloud cover. The basic quantitative relationships of radiant heat transfer were considered depending upon cloud cover—the principal regulator of the transfer of radiation, and also as a function of other factors. Various methods of calculating the radiant influx of heat are compared. Methods of considering radiant heat transfer in problems of the general circulation of the atmosphere and weather forecasting are presented.

The collection is intended for specialists in the physics of the atmosphere, dynamic meteorology, the physics of clouds, oceanology, and also for graduate and undergraduate students of the appropriate specialties.

Responsible editors:  
Ye. M. Feygel'son and L. R. Tsvang





## Preface

The physics of the atmosphere and meteorology are located on the threshold of a great event—the Global Atmospheric Experiments organized by the International Scientific Union for 1975. A large amount of research work for validation of the statements of specific measurements precedes the performance of the experiments. In this collection, certain results of such work of a collective of specialists on actinometry and turbulence from the Institute of the Physics of the Atmosphere (IFA) of the USSR Academy of Sciences, in actinometry of the Institute of Physics and Astronomy of the Academy of Sciences of Estonia (IFA AN ESSR) and the Ukrainian Hydrometeorological Institute of the GUGMS (Main Administration of the Hydrometeorological Service) (Ukr NIGMI) are presented in this collection. /3\*

The general task assigned to the combined collective may be formulated thus: "Investigation of radiation and turbulent heat transfer in the atmosphere in the reaction with cloud cover for the purpose of developing physically valid methods of calculating the influx of heat in problems of the dynamics of the atmosphere".

The work began in 1966 and in this collection the basic results obtained in 1966-1969 are presented. Data from individual investigations were published basically in the Izvestiya AN SSSR, Seriya FAO (Bulletin of the USSR Academy of Sciences, Physics of the Atmosphere and Ocean Series) in subject collections published by the IFA AN ESSR, in the transactions of the Ukr NIGMI, and other publications. The purpose of the collection is to give a general concept of the totality of all the works performed with an adequately brief explanation of particular results.

The diverse problems of the physics of the atmosphere, meteorology, climatology, and engineering require information concerning the basic mechanisms of heat transfer and their interrelationships in the earth's atmosphere. In particular, such information is necessary for one of the main contemporary problems of the physics of the atmosphere and meteorology—investigations of the global large-scale dynamics of the atmosphere (general circulation of the atmosphere) for the purpose of validation and improvement of the methods of long-range weather forecasting. This problem requires a consideration of the basic energy resources of the atmosphere and, among them, the influx of solar radiation—the primary moving force of atmospheric motion—in reaction with long-wave (thermal) cooling and other forms of heat transfer.

In the investigation of the unsteady-state dynamic regime of the atmosphere, sources of heat must be considered with an allowance for their basic feedback. For radiation, obviously, the main /4

---

\*Numbers in righthand margin indicate pagination of foreign text.

regulator is the cloud cover, determining the feedback of the radiation field with the other meteorological fields. Therefore, the unsteady-state process of heat transfer must be studied in interrelationship with the cloud cover. In this collection great attention is devoted to the investigation of the variability of radiation fields in connection with the variability of cloud cover.

Three states of the atmosphere are considered: cloudless conditions, an atmosphere with stratoformous, and with convective cloud cover. In each case individually, two radiation fields are investigated: short-wave (solar) ( $0.4 \leq \lambda \leq 4.0$  microns) and long-wave (thermal) ( $4.0 \leq \lambda \leq 100$  microns) radiation, since their role in heat transfer and reaction with the atmosphere and, consequently, also methods of determination, differ. Turbulent heat fluxes are considered only in cloudless conditions and in convective cloud cover in the boundary layer of the atmosphere.

Much space in the collection is devoted to the investigation of the quantitative relationships of the behavior of heat fluxes and influxes as a function of the factors determining them: profiles of temperature and humidity, the turbidity (pollution) of the atmosphere, water content and droplet composition of clouds, and their arrangement in space. The statistical structure of radiant fluxes is considered.

All the material in the collection is divided into four parts, individual sections of which were written by the authors indicated in the table of contents. The following system of symbols has been accepted for citations to articles of this collection: in brackets the number of the part is indicated in Roman numerals, and then, in arabic numerals the sequence number of the article in the collection (see the Table of Contents).

In conclusion, the authors thank Academician A. M. Obukhov, Academician of the Estonian SSR Academy of Sciences A. Ya. Kipper, Candidate of Physical and Mathematical Sciences K. T. Logvinov, and also Professor G. V. Rozenberg, Doctor of Physical and Mathematical Sciences Yu. K. Ross, Candidate of Physical and Mathematical Sciences A. V. Tkachenko for supporting the work and constant good will.

Airborne work in the study of radiation heat transfer in clouds was basically performed aboard aircraft of the Ukr NIGMI from the base at the meteorological test area of this institute. The authors thank the chief of the meteorological test area of the Ukr. NIGMI, Comrade A. I. Furman, and the collective of pilots and airborne aerologists who provided for the performance of this work.

# TABLE OF CONTENTS

	page
Preface	v
List of Symbols	xi
I. LONG-WAVE RADIATION	1
1. L. M. Gradus, Kh. Yu. Niylik, and Ye. M. Feygel'son, Integral Function of the Transmission of Thermal Radiation	1
2. L. V. Petrova and Ye. M. Feygel'son, Features of Long-Wave Radiant Influx in Stratoformous Cloud Cover (Numerical Experiment)	7
3. Ye. M. Feygel'son, A Cloud as a Heat Sink	16
4. A. S. Ginzburg and Ye. M. Feygel'son, Some Approximate Methods of Calculating Radiant Heat Transfer in a Cloudless Atmosphere	26
5. A. S. Ginzburg and Kh. Yu. Niylik, Comparison of Various Methods of Calculating the Field of Long-Wave Radiation	30
6. Kh. Yu. Niylik, Estimate of the Error in Calculation of Fluxes and Influxes of Thermal Radiation Due to Errors of Initial Meteorological Parameters	39
7. Kh. Yu. Niylik, On Calculations of the Thermal Radiation of the Atmosphere in Broken Cloud Cover	46
8. N. I. Goysa, V. D. Oppengeym, and Ye. M. Feygel'son, Vertical Profiles of Fluxes of Long-Wave Radiation in a Cloudy Atmosphere	50
II. SHORT-WAVE RADIATION	54
9. O. A. Avaste, Transfer of Solar Radiation in the Atmosphere	54
10. O. A. Avaste, L. D. Krasnokotskaya, and Ye. M. Feygel'son, On the Calculation of the Integral Flux and Influx of Solar Radiation	67
11. L. D. Krasnokotskaya and L. M. Romanova, Reflection Transmission, and Absorption of Radiation by Clouds in the Absorption Bands of Water Vapor	72

	page
12. N. I. Goysa and V. M. Shoshin, Experimental Investigations of Fluxes of Solar Radiation in the Lower Troposphere in St and Sc Clouds	78
13. N. I. Goysa and V. M. Shoshin, Average Vertical Structure of the Field of Short-Wave Radiation in Stratoform St and Sc Cloud Cover	92
III. TURBULENT AND RADIANT HEAT TRANSFER IN THE BOUNDARY LAYER OF THE ATMOSPHERE	100
14. L. R. Tsvang, On the Closing of the Equation of Heat Influx in the Boundary Layer of the Atmosphere (According to Experimental Data)	100
15. V. D. Oppengeym and G. P. Faraponova, Determination of the Radiation Heat Flux in the Boundary Layer of the Atmosphere	107
IV. STATISTICAL STRUCTURE OF RADIATION FIELDS IN CLOUDS	111
16. Yu. R. Mullamaa, V. K. Pyldmaa, and M. A. Sulev, Some Problems of the Methodology of Measurement of Average Fluxes of Short-Wave Radiation in Cloud Cover	111
17. V. K. Pyldmaa, On the Accuracy of the Averaging of Total Radiation Fluxes	119
18. R. G. Timanovskaya and Ye. M. Feygel'son, On the Methodology of the Study of the Statistical Structure of Ground Fluxes of Solar Radiation in Cloudy Conditions	125
19. V. K. Pyldmaa and R. G. Timanovskaya, Total Radiation at the Surface of the Earth in Various Conditions of Cloud Cover	131
20. R. G. Timanovskaya and Ye. M. Fegyel'son, Some Parameters of Cumulus Clouds Observed by Photographs of the Sky and From Ground Actinometric Measurements	138
21. R. G. Timanovskaya and Ye. M. Feygel'son, Fluxes of Solar Radiation at the Surface of the Earth in Cumulus Cloud Cover	146
22. M. A. Sulev, Spatial Structure of the Field of Short-Wave Radiation in Stratocumulus and Cumulus Cloud Cover	156

	page
23. Yu. R. Mullamaa, V. K. Pyldmaa, and M. A. Sulte, Structure of the Field of Cumulus Clouds	161
24. Yu. R. Mullamaa, On the Transmission of Solar Radiation by Stratoformous Cloud Cover as a Function of the Statistical Characteristics of its Structure	166
25. O. A. Avaste, Yu. R. Mullamaa, Kh. Yu. Niylik, and M. A. Sulev, On the Coverage of the Sky by Clouds	173
Conclusion	182
Abstracts of articles	190



- $A_k$  - short-wave albedo  
 $B$  - total radiation balance  
 $B_k$  - balance of short-wave radiation  
 $B_d$  - balance of long-wave radiation  
 $\Delta B$  - total radiation heat influx to the layer  
 $\Delta B_d$  - influx of long-wave radiation  
 $\Delta B_k$  - influx of short-wave radiation  
 $\delta$  - transmission function for diffuse radiation  
 $D\downarrow$  - downflux (descending flow) of scattered radiation  
 $D\uparrow$  - upflux (up flow) of scattered radiation  
 $E_\lambda$  - black-body radiation on the wavelength  $\lambda$   
 $E = \sigma T^4$   
 $F$  - effective radiation  
 $F\downarrow$  - downflux of long-wave radiation  
 $F\uparrow$  - upflux of long-wave radiation  
 $f$  - linear frequency  
 $H$  - altitude of upper boundary of the atmosphere  
 $I_0$  - solar constant  
 $M$  - number of observations, readings, cases, realizations  
 $m$  - mass of air  
 $m_x$  - mass of substance  $x$  ( $x=v$  water vapor;  $w$ -droplet water,  $u$ -carbon dioxide gas);  $m_x$  is calculated at a given value of  $\rho_x$  according to the formula  

$$m_x(z) = \int_0^z \rho_x(z) dz$$
  
 $n$  - quantity of relative cloud cover  
 $n_0$  - quantity of cloud cover in the direction of the zenith or nadir  
 $n_\vartheta$  - quantity of cloud cover in the direction  $\vartheta$   
 $P$  - probability  
 $\Phi$  - transparency of the layer or transmission of radiation by the layer



- p - probability density
- Q - flux of total solar radiation, i.e., sum of the fluxes of descending direct and scattered solar radiation
- $Q_0$  - average diurnal fluctuation of the total radiation at the surface of the earth for a cloudless sky for a given calendar day and geographical point
- $Q^*=Q/Q_0$  - relative total radiation flux
- R - long-wave radiant heat influx to an element of volume
- $r(x), r(t)$  - standardized autocorrelation function of variability of radiant fluxes in space and in time, respectively
- $\ell_1, t_1$  - correlation radius, determined from the condition  $r(\ell_1)=r(t_1)=0.5$  /6
- $\ell_2, t_2$  - the same, at the condition  $r(\ell_2)=r(t_2)=0.1$
- S - flux of direct radiation of the sun to a surface perpendicular to the beams
- S' - flux of direct radiation of the sun to a horizontal surface
- $S(\omega)$  or  $S(f)$  - spectral density
- $S_0$  - average diurnal fluctuation of the direct radiation flux to a perpendicular plane at the surface of the earth with a cloudless sky for a given calendar day and geographical point
- $S^*=S/S_0$  - relative flux of direct solar radiation
- $s_\odot$  - duration of sunlight
- T - absolute temperature ( $t^\circ \text{C}$  is the temperature in degrees Centigrade)
- t - time
- U - relative humidity
- u - content of  $\text{CO}_2$
- V - variability factor
- v - velocity (speed, rate)
- x, y, z - spatial coordinates
- $z_{n.g.}$  - height of lower boundary of cloud
- $z_{v.g.}$  - height of upper boundary of cloud

$\vartheta$  - zenith angle  
 $\vartheta_{\odot}$  - zenith angle of the sun  
 $\lambda$  - wave-length  
 $\nu$  - wave number  
 $\rho$  - density of the air  
 $\rho_x$  - content of the substance x in a unit of volume of the air (see  $m_x$ )  
 $\sigma^2$  - dispersion  
 $\tau$  - optical thickness  
 $\omega$  - angular frequency  
 $n_{\Lambda}$  - averaged quantity of the relative cloud cover

## I. LONG-WAVE RADIATION<sup>†</sup>

### INTEGRAL FUNCTION OF THE TRANSMISSION OF THERMAL RADIATION

L. M. Gradus, Kh. Yu. Niylik, and Ye. M. Feygel'son

For calculation of fluxes of thermal radiation in the troposphere an integral transmission function was constructed [1], considering absorption by droplet water. This transmission function requires the assignment of the distribution of the density of droplet water or the water content of the cloud in space and in time, together with the corresponding distributions of the gaseous absorbing substances. By means of such a function it turns out to be possible to describe the continuous transition from cloudless conditions to cloudy conditions and vice versa, thus tracing the variation of the radiation influx in the process of the development and destruction of clouds. We also succeeded in constructing a continuous profile of the influx in the entire layer of the troposphere, including the cloud layer. Prior assumptions concerning the nature of the radiation of the cloud boundaries turn out to be unnecessary. /7\*

According to definition, an integral transmission function for directional radiation of frequency  $\nu$  is described by the formula

$$\Phi(m_v, m_c, m_w) = \int_0^{\infty} \gamma_\nu(\bar{T}) \Phi_\nu(m_v) \Phi_\nu(m_c) \Phi_\nu(m_w) d\nu. \quad (1)$$

Here  $m_v$  and  $m_c$  are the effective masses of water vapor and carbon dioxide gas, considering the variation of the pressure in the air layer under consideration;  $m_w$  is the true mass of droplet water in this same layer;  $\Phi_\nu(x)$  is the spectral transmission function of the corresponding substance ( $x=m_v$ ,  $m_c$ , or  $m_w$ )

---

<sup>†</sup>The content of the 1-4th and 8th articles of this part were presented in a more complete form in Ye. M. Feygel'son's monograph "Luchistiy teploobmen i oblaka" (Radiant Heat Transfer and Clouds) (Gidrometeoizdat, 1970).

\*Numbers in the right margin indicate pagination of foreign text.

$$\gamma_v(\bar{T}) = \frac{E_v(\bar{T})}{E(\bar{T})};$$

$\bar{T}$  is the average temperature.

According to formula (1) numerical integration was done at  $\Delta\nu = 25 \text{ cm}^{-1}$  in the interval (25-2800  $\text{cm}^{-1}$ ) at  $T = 260$  kelvins. The values of the transmission functions  $\Phi_{\Delta\nu}(m_v)$  and  $\Phi_{\Delta\nu}(m_c)$  from [2] were used, and the function  $\Phi_{\Delta\nu}(m_w)$  was assumed in the form /8

$$\Phi_{\Delta\nu}(m_w) = \exp[-\alpha_{\Delta\nu} m_w], \quad (2)$$

where  $\alpha_{\Delta\nu}$  is the absorption factor of the droplet water, calculated according to data from [3] and [4] for two characteristic distributions of cloud droplets by dimension.

The tables of the integral transmission function of gaseous components obtained for a case of  $m_w = 0$  are given in [5].

In [1], attention is called to the feasibility of the approximation of the function  $\Phi(m_v, m_c, m_w)$ , by formulas with separation of the variables that are convenient for calculation. For this the natural separation of the predominating part of the spectrum (0-550  $\text{cm}^{-1}$ ) and (800-2800  $\text{cm}^{-1}$ ) was used, in which, at cloudless conditions, only water vapor is absorbed. The transmission function at  $m_w = 0$  was represented in the form

$$\Phi(m_v, m_c, 0) = \Phi_1(m_v) + \Phi_2(m_v, m_c), \quad (3)$$

where

$$\Phi_1(m_v) = \int_0^{550 \text{ cm}^{-1}} \gamma_v(\bar{T}) \Phi_v(m_v) dv + \int_{800}^{2800} \gamma_v(\bar{T}) \Phi_v(m_v) \Phi_v(m_c) dv. \quad (4)$$

It was further assumed that:

$$\Phi_2(m_v, m_c) = \Phi_2(m_v) \Phi_3(m_c), \quad (5)$$

where

$$\Phi_2(m_v) = \int_{550}^{800} \gamma_v(\bar{T}) \Phi_v(m_v) dv, \quad (6)$$

$$\Phi_3(m_c) = \left[ \frac{\int_{550}^{800} \gamma_v(\bar{T}) \Phi_v(m_v) \cdot \Phi_v(m_c) dv}{\int_{550}^{800} \gamma_v(\bar{T}) \Phi_v(m_v) dv} \right] \quad (7)$$

The line over the righthand part of the last equation signifies averaging with respect to  $m_v$  ( $0 \leq m_v \leq 1$  cm) of the expression enclosed in the brackets, that depends only slightly upon  $m_v$ .

As a result the integral transmission function of the gaseous components was presented in the form

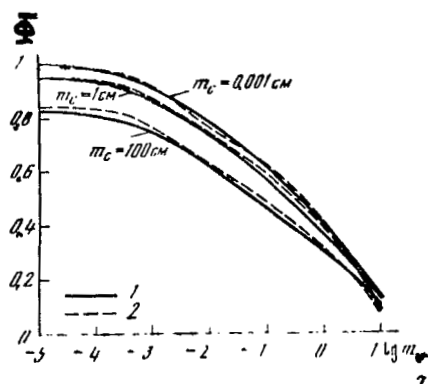
$$\Phi(m_v, m_c) = \Phi_1(m_v) + \Phi_2(m_v) \Phi_3(m_c), \quad (8)$$

and each of the functions in the righthand part of ratio (8) was approximated by exponential functions: /9

$$\Phi_n(m_n) = \sum_{k=1}^3 a_k^{(n)} e^{-a_k^{(n)} m_n}, \quad (9)$$

where

$$m_1 = m_2 = m_v; \quad m_3 = m_c.$$



Integral transmission function of directional radiation.

1- accurate values; 2- approximation by formulas (8) and (9).

The error of the approximation may be estimated according to the data in the drawing.

The parameters of formula (9) at  $m_v \leq 1$  cm;  $m_c \leq 300$  cm are given in the table; in the parentheses the value of the parameters are given at  $m_v \leq 10$  cm and  $m_c \leq 500$  cm.

n	k					
	$\alpha_k^{(n)}$			$\alpha_k^{(n)} \text{ cm}^{-1}$		
	1	2	3	1	2	3
1	0,192 (0,192)	0,210 (0,204)	0,347 (0,294)	474 (431,6)	11,2 (10,5)	0,300 (0,147)
2	0,044	0,192	0,000	2,900	0,226	
3	0,322	0,400	0,278	0,562	0,012	0,00015

The transmission function at  $m_w \neq 0$  was presented in the form

$$\varphi(m_v; m_c; m_w) = e^{-\alpha m_w} [\Phi_1(m_v) + \Phi_2(m_v) \cdot \Phi_3(m_c)], \quad (10)$$

where  $\alpha$  is the average absorption factor of the droplet water, /10 determined according to the formula

$$\alpha = \left[ \frac{1}{m_w} \ln \frac{\Phi(m_v; m_c; 0)}{\Phi(m_v; m_c; m_w)} \right],$$

where the averaging is performed according to  $m_v$ ,  $m_c$ , and  $m_w$  within limits of 0-1 cm, 0-300 cm, and 0-0.001 cm, respectively. The error due to the use of the averaged value of  $\alpha$  in comparison with the calculated value according to formula (1) does not exceed 10%.

The following values of the coefficient  $\alpha$  are recommended for stratoform clouds of various types:

$$\alpha = \begin{cases} 500 \text{ cm}^2 \text{g}^{-1} & \text{in Sc and As clouds} \\ 2000 \text{ cm}^2 \text{g}^{-1} & \text{in St and Ns clouds.} \end{cases}$$

In conclusion, we will indicate that the use of the function  $\delta(m_v, m_c, m_w)$  is feasible in multi-level problems of cloud

formation, when the magnitude of  $m_w(z)$  is calculated. At  $m_w = 0$ , this function is one of the variations of the integral transmission function of the gaseous components compared in [1] with other functions of such a type. Possible advantages of the variation described are the use of newer spectral data and the construction of adequately precise approximation formulas.

## REFERENCES

1. Gradus, L. M., Kh. Yu. Niylysk, and Ye. M. Feygel'son, "An integral transmission function for cloud conditions", Izv. AN SSSR, seriya FAO, 4, No. 4, 1968.
2. Davis, P. A., and W. Viezee, "A Model for computing infrared transmission through atmospheric water vapour and carbon dioxide", J. Geophys. Res., 69, No. 18, 1964.
3. Shifrin, K. S. and I. L. Zel'manovick, Tablitsy po svetorasseyaniyu (Tables of Light Diffusion), Leningrad, Gidrometeoizdat, 1968.
4. Herman, B. M., "Infrared absorption scattering and total attenuation cross-sections for water spheres", Quart. J. Roy. Meterol. Soc., 88, No. 376, 1962.
5. Niylysk, Kh. Yu. and L. E. Sammel, Integral'naya funktsiya propuskaniya atmosfery dlya raschetov polya teplovogo izlucheniya v atmosfere. Tablitsy radiatsionnykh kharakteristik atmosfery (Integral function of atmospheric passage for the study of the heat radiation field in the atmosphere. Tables of the radiation characteristics of the atmosphere), Tartu, AN Estonian SSR Press, Institute of Astronomy and Physics, 1969.



FEATURES OF LONG-WAVE RADIANT INFLUX  
IN STRATOFORMOUS CLOUD COVER  
(Numerical Experiment)

L. V. Petrova and Ye. M. Feygel'son

The non-monotonic behavior of influx as a function of altitude in conditions of stratiform cloud cover makes it necessary to study it as a function of geometrical conditions (level of location, thickness and quantity of cloud layers), of physical properties of the cloud (water content and dimensions of the droplets), and of the distribution of temperature and humidity. /11

To ascertain these dependences, a numerical experiment was performed which made it possible to investigate the effect of each of the factors listed above separately. Such an experiment turned out to be possible after an integral transmission function for cloud conditions was constructed [I.1], making it possible to calculate the continuous vertical profile of the long-wave radiant influx under the cloud, in the cloud, and above it, with consideration of the properties of the cloud layer. The statement of the problem and a brief summary of the results are given below. The results of the numerical experiment are explained in detail in refs. [1,2].

Conditions of the experiment. The influx  $R(z)$  was calculated in the interval  $0 \leq z \leq H$  at  $H = 10$  km with a spacing  $\Delta z = 50$  m on the "Minsk-2" electronic computer according to the formula

$$R(z) = -\frac{d}{dz} \left\{ E(0) \delta(m_v, m_w, m_c) + \int_0^H E(z') \frac{d \delta(|m_v - m'_v|; |m_w - m'_w|; |m_c - m'_c|)}{dz'} dz' \right\}. \quad (1)$$

Here  $R(z)$  is the influx at the given distributions of humidity  $\rho_v(z)$ , water content  $\rho_w(z)$ , and temperature  $T(z)$  assigned, with respect to altitude;  $m_v, m_w, m_c$  represent the mass of the water vapor, droplet water, and carbon dioxide gas in the air column  $(0, z)$ ;  $m'_v, m'_w$ , and  $m'_c$  are the same in the column  $(0, z')$ . In accordance with [I.1] the function  $\delta(m_v, m_w, m_c)$  was presented in the form  $\delta(m_v, m_w, m_c) = e^{-k\alpha m_w} \times \delta(m_v, m_c)$ , where  $\alpha$  is the absorption factor of the droplet water, depending upon the form of cloud cover;  $k$  is a diffusivity parameter, by means of which the scattering of long-wave radiation in the cloud is roughly

considered;  $\delta(m_v, m_c)$  is the transmission function of the gaseous components from ref. [3].

In the performance of the numerical experiment, all the parameters of the atmosphere were fixed in sequence except one, according to which the tabulation was conducted within limits approximately corresponding to the real variation of this parameter.

A basic model of the atmosphere was assumed in which the distributions of the temperature and humidity were assigned by the formulas: /12

$$T(z) = T(0) - \gamma Z \quad (2)$$

at  $\gamma = 6^\circ \text{ km}^{-1}$ ,  $T(0) = 273^\circ \text{ K}$ ,  $0 \leq z \leq H$ ,  $H = 10 \text{ km}$

$$\rho_v(z) = \begin{cases} f[T(z)] & \text{at } z_1 \leq z \leq z_2, \\ f[T(z_1)] e^{a_1(z_1-z)} & \text{at } 0 \leq z \leq z_1, \\ f[T(z_2)] e^{-a_2(z-z_2)} & \text{at } z_2 \leq z \leq H. \end{cases} \quad \begin{matrix} (3) \\ (3') \\ (3'') \end{matrix}$$

Here  $z_1 \equiv z_{n.g.}$  and  $z_2 \equiv z_{v.g.}$  are the boundaries of the cloud;  $f(T)$  is the humidity in conditions of saturation at the temperature  $T$ . The constants  $a_1$  and  $a_2$  were selected so that outside the interval  $(z_1, z_2)$  no saturation was achieved, and the magnitude of the humidity was close to the observed value.

The properties of the cloud in the basic model were determined by the parameters: water content (absolute humidity)  $\rho_w = 0.2 \text{ g/m}^3$ ; gradient of absolute humidity at the boundaries

$$\frac{d\rho_w}{dz_i} = 4 \text{ g} \cdot \text{m}^{-3} \cdot \text{km}^{-1};$$

average absorption factor of droplet water,  $\alpha = 1300 \text{ cm}^2/\text{g}$ ;  $k = 1.66$ ;  $z_{n.g.} = 2 \text{ km}$ ,  $z_{v.g.} = 3 \text{ km}$ .

In a cloudless atmosphere the temperature distribution was described by formula (2), and the humidity by formula (3''), at  $a_2 = 0.45 \text{ km}^{-1}$  and  $z_2 = 0$ .

In the table the profiles of radiant influx in cloudy and cloudless conditions, calculated for the basic model, are compared. It is apparent that in the cloud layer a unique profile /13

z, km	R(z), cal/m <sup>3</sup> .min		z, km	R(z), cal/m <sup>3</sup> .min	
	cloudy atmosph.	cloud- less at.		cloudy atmosph.	cloud- less at.
0,05	-0,141	-0,313	2,4	-0,03121	-0,158
0,2	-0,0795	-0,255	2,6	-0,04656	-0,156
0,5	-0,0427	-0,218	2,8	-0,0127	-0,155
1	-0,0116	-0,189	2,85	-0,111	-0,155
1,2	-0,02692	-0,182	2,9	-0,968	-0,155
1,3	0,02507	-0,178	2,95	-8,47	-0,155
1,5	0,0182	-0,173	3 - z <sub>vp</sub>	-18,8	-0,155
1,8	0,0493	-0,166	3,05	-0,307	-0,155
2 - z <sub>ng</sub>	0,108	-0,162	3,1	-0,288	-0,155
2,05	3,77	-0,162	3,5	0,243	-0,155
2,1	1,72	-0,161	4	-0,232	-0,156
2,15	0,195	-0,160	4,5	-0,227	-0,158
2,2	0,0222	-0,160	5	-0,221	-0,159
2,25	0,0252	-0,159	6	-0,200	
2,3	0,0224	-0,159			

of the radiation influx is formed, with characteristic peaks of heating and cooling near the lower and upper boundaries of the cloud, respectively.

In the layer under the cloud, radiation influx is one or one-and-one-half orders of magnitude less than at the same levels in cloudless conditions. In the depths of the cloud the influx is close to zero. In the layer over the cloud with a growth of  $z$  the magnitude of the influx approaches that corresponding to cloudless conditions, remaining approximately 30% greater than the latter at  $z \leq 5$  km.

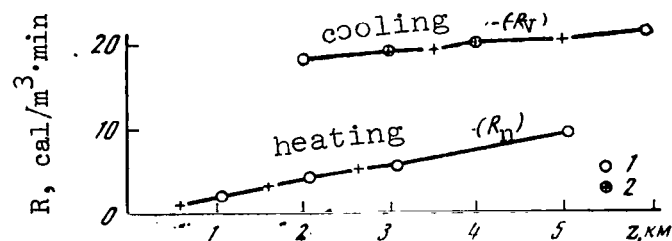


Fig. 1. Behavior of the quantities  $R_n$  and  $R_v$  in a case of a moving cloud (1) and an expanding cloud (2).

Profile of radiant influx as a function of geometrical factors. The change in  $R(z)$  as a function of the level of the cloud layer was considered as well as the change in its thickness as a function of the number of cloud layers.

The numerical experiment demonstrated that the layers of extreme heating and cooling are localized within the cloud near the boundaries and move together with them in uplifting or expansion of the cloud layer. The maximum cooling at the upper boundary,  $R_v$ , is always greater in absolute magnitude than maximum heating at the lower boundary  $R_n$ . However, with an increase in the levels of the boundaries the quantity  $R_n$  increases much faster than  $|R_v|$ , so that the difference  $|R_v| - R_n$  decreases with a rise of the cloud. In the expansion of the cloud this difference decreases or increases depending upon the direction of expansion.

The behavior of the peaks of the extreme influx is apparent in Fig. 1, where on one curve the values of  $R_n$  are plotted, and on the other the values of  $R_v$  as a function of the levels of the boundaries with a rise of the cloud from 1-2 km to 5-6 km and in expansion from a thickness of 0.5 km to 4.5 km.

With several cloud layers, their mutual arrangement turns out to be more essential than the thickness of each of them: a nearby thin upper cloud suppresses radiation cooling of the lower cloud more strongly than a distant and thick cloud.

At the external boundaries of the cloud system—the lower at the lower cloud and the upper at the upper cloud—heating and cooling are determined by the level of these boundaries and are indifferent to the number of layers. /14

Radiation influxes near the internal boundaries are considerable and exceed influxes at the same levels in the absence of clouds, inside clouds, or in the layers under or between the clouds.

Effect of the physical properties of the cloud. In [I.3] it is demonstrated that the radiation influx near the cloud boundary essentially depends upon the gradient of the absolute humidity and upon the absorption factor of the droplet water. Radiation influxes were calculated at different values of the parameters indicated. The absolute humidity was assumed according to the formula

$$\rho_w(z) = \delta(z - z_{ng})^a (z_{vg} - z)^b, \quad (4)$$

which makes it possible to vary the parameters  $\rho_{w,max}$ , the maximum absolute humidity (water content) of the cloud, and  $d\rho_w/dz_1$  ( $i = 1, 2$ ) independently.

Calculations demonstrated that with a growth  $d\rho_w/dz_1$  with the condition  $\rho_{w,max} = \text{const}$  the radiation heating (or cooling) layer narrows; the magnitude of the maximum heating (or cooling) increases and the level approaches the corresponding boundary.

The variations of the radiation influx in the vicinity of the upper boundary of the cloud are illustrated in Fig. 2, where the distribution of the absolute humidity in each case is also given.

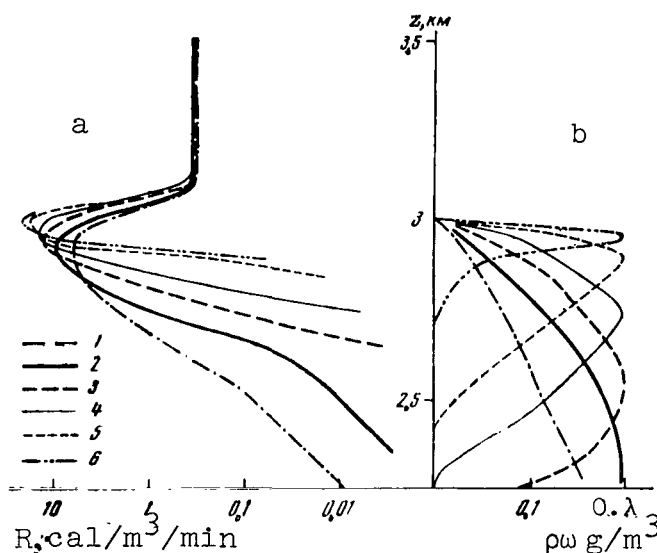


Fig. 2. Radiation cooling in the vicinity of the upper boundary of a cloud (a) and the absolute humidity, calculated according to formula (4) at  $\rho_{w,max} = 0.2 \text{ g/m}^3$  (b).

1-  $d\rho_w/dz_{v.g.} = 0.2 \text{ g/m}^3 \cdot \text{km}$ ; 2-  $0.5 \text{ g/m}^3 \cdot \text{km}$ ; 3-  $1 \text{ g/m}^3 \cdot \text{km}$ ; 4-  $2 \text{ g/m}^3 \cdot \text{km}$ ; 5-  $4 \text{ g/m}^3 \cdot \text{km}$ ; 6-  $10 \text{ g/m}^3 \cdot \text{km}$ .

The relation between influx and droplet spectrum is expressed in terms of the average absorption factor  $\alpha$  of the droplet water [1.1]. To ascertain the dependence of the influx upon this parameter, calculations were performed at different

/15

values of  $\alpha$ . It was ascertained that with a growth of  $\alpha$  the cooling and heating peaks behave just as they do with a growth of  $dp_w/dz_1$ . This effect is explained in [1.3] and [4].

The variation of the parameter  $\alpha$  is perceptible in a layer with a thickness of 500-700 m under the cloud and more than 100 m over the cloud.

Temperature and humidity. The variations of the influx as a function of the variation of the temperature profile and the humidity profile as a whole were considered, and also as a function of the distribution of these quantities. In particular, the influxes were calculated at temperature and humidity inversions. The influx in the boundary layer of the atmosphere as a function of the temperature difference  $\Delta T = T_s - T(0)$  was estimated, where  $T_s$  is the temperature of the soil.

The calculations have demonstrated that the variations of the influx due to the variation of the average temperature and humidity within the limits of possible climatic values are small in comparison with the variations introduced by the cloud cover.

Real irregular temperature and humidity oscillations cause oscillations of the influx in cloudless conditions comparable with its average magnitude.

In ascertaining the dependence of the influx upon inversions of the quantities indicated it was observed that the temperature inversions have a stronger effect upon the behavior of the radiation influx than humidity inversions, if both take place in a narrow layer similar to real atmospheric inversions

The behavior of the influx in the temperature inversion layer qualitatively resembles that observed near the cloud boundaries, but the intensity of peaks of heating and cooling is considerably less.

The calculations of the influx at various values of the parameter  $\Delta T$  and a standard distribution of temperature and humidity demonstrated that in summer in the mid-day hours over dry land, when the temperature difference between the soil and the air may reach values of  $\Delta T = 20-30^\circ$  the boundary layer of the atmosphere to a level  $z = 1$  km is heated by long-wave radiation of the soil. In the layer  $250 \text{ m} \leq z \leq 500 \text{ m}$  this heating is comparable with a cooling at  $\Delta T = 0$ , and in the layer  $z < 250 \text{ m}$  appreciably exceeds the latter. Near the earth's surface at  $\Delta T = 30^\circ$ ,

exceptionally strong heating occurs, comparable with radiation cooling at the surface of the boundary of the cloud layer.

Thin cloud cover. The radiation effect of thin cloud cover was considered separately. The enormous absorbing capability of droplet water makes this effect quite noticeable. In Fig. 3 the cooling peaks of thin ( $\rho_w = 0.01 \text{ g/m}^3$ ) and dense ( $\rho_w = 0.2 \text{ g/m}^3$ ) clouds are compared at the same gradients of the absolute humidity at the boundaries  $d\rho_w/dz_1 = 0.2 \text{ g/m}^3 \cdot \text{km}$ ; for comparison, a case of influx in cloudless conditions and at  $\rho_w = 0.2 \text{ g/m}^3$  at  $d\rho_w/dz_1 = 4 \text{ g/m}^3 \cdot \text{km}$  is also given. In Fig. 3 the similarity of the profiles of the influx in the vicinity of the upper boundary of thin and thick clouds is shown at the same gradient of the absolute humidity and the decisive difference of the case of a weak cloud from conditions of a cloudless atmosphere is shown. /16

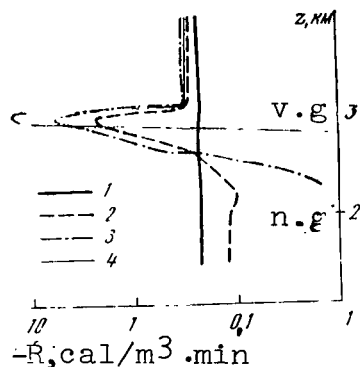


Fig. 3. Profile of the influx in the vicinity of the boundary of a cloud layer. 1- cloudless conditions; 2-  $\rho_w = \text{const} = 0.01 \text{ g/m}^3$ ,  $d\rho_w/dz_1 = 0.1 \text{ g/m}^3 \cdot \text{km}$ ; 3-  $\rho_w = 0.2 \text{ g/m}^3$ ,  $d\rho_w/dz_1 = 0.2 \text{ g/m}^3 \cdot \text{km}$ ; 4-  $\rho_w = 0.2 \text{ g/m}^3$ ,  $d\rho_w/dz_1 = 4 \text{ g/m}^3 \cdot \text{km}$ .

According to data from calculations, cloud cover with an absolute humidity  $\rho_w \leq 0.05 \text{ g/m}^3$  should be considered as thin in the radiation sense.

In the range of absolute humidity from  $0.01$  to  $0.03 \text{ g/m}^3$  the influx acquires qualitative criteria that are characteristic for clouds. In the range of  $0.03$ - $0.05 \text{ g/m}^3$  the numerical values of the influx become close to those observed in conditions of thick cloud cover.

With a further increase in the absolute humidity, the influx becomes sensitive to this parameter and varies only as a function of the gradient of the absolute humidity at the cloud boundaries.



#### REFERENCES

1. Petrova, L. V. and Ye. M. Feygel'son, "Radiation heat transfer in developing cloud cover", Izv. AN SSSR, seriya FAO, 2, No. 4, 1966.
2. Petrova, L. V., "Certain problems of the formation of a long-wave radiation influx in continuous cloud cover", Izv. AN SSSR, seriya FAO, 4, No. 10, 1968.
3. Shekhter, F. N., "On the calculation of radiant fluxes in the atmosphere", Trudy GGO, No. 22 (84), 1950.
4. Feygel'son, Ye. M., "Influx of long-wave radiation in cloud conditions", Izv. AN SSSR, seriya FAO, 4, No. 5, 1968.

## A CLOUD AS A HEAT SINK

Ye. M. Feygel'son

The absorption capacity of droplet water in the thermal radiation range may be roughly estimated according to the formula  $\ln \delta(\rho_w l) = \alpha \rho_w l = 1$  [I.1]. With the absolute humidity (water content)  $\rho_w$  of stratoformous clouds being of the order of  $10^{-7}$  g per  $\text{cm}^3$  and the absorption factor  $\alpha$  of the order of  $500\text{--}2000 \text{ cm}^2/\text{g}$  the length  $l$  of the free run of the radiation in the cloud turns out to be of the order of 200–50 m. The length of the free run of radiation in a cloudless atmosphere, estimated according to the condition  $-\ln \delta(\rho_v l) = -1$ , turns out to be of the order of the thickness of the homogeneous atmosphere.

From these estimates it follows that a real stratoformous cloud is a radiator comparable with the thickness of the atmosphere as a whole. In addition, this radiator has a number of characteristics: it is strictly localized in space and may be compared to a heat sink. As a matter of fact, an even finer localization occurs, since only the boundary layers of the cloud are radiationally active—a radiant drainage of heat originates at the upper boundary of the cloud and a source of heat at the lower boundary [I.2].

The internal part of the cloud is passive in relationship to the transfer of thermal radiation and in this sense is in a regime of thermodynamic equilibrium.

Finally, a cloud layer reacts differently with the underlying surface and with the atmosphere over it than does a cloudless layer of equal thickness with boundaries at the same altitude. In the first case the "atmospheric window" (8–12 microns) is lacking, and therefore the radiation of the earth's surface is compensated basically by the counterradiation of the cloud, and the atmosphere over the cloud turns out to be isolated from the thermal radiation of the earth.

As a consequence of these characteristics, in stratoformous cloud cover the vertical distribution of the radiant influx  $-R(z)$  is characterized by extreme heterogeneity. In Fig. 1 two examples of the vertical profile of the influx are demonstrated, calculated for an atmosphere containing a cloud layer with an absolute humidity equal to  $0.2 \text{ g/m}^3$ , a gradient of the absolute humidity of  $4 \text{ g/m}^3$  at the boundaries with an average absorption

factor of the droplet water of  $1300 \text{ cm}^2/\text{g}$ . The naturally defined regions of the characteristic behavior of the influx are cross-hatched; the values of the integral influx to the layer are given:

$$\int_{z_{j-1}}^{z_j} R(z) dz$$

for each region (upper numbers) and those of the same magnitude for standard cloudless conditions (lower numbers).

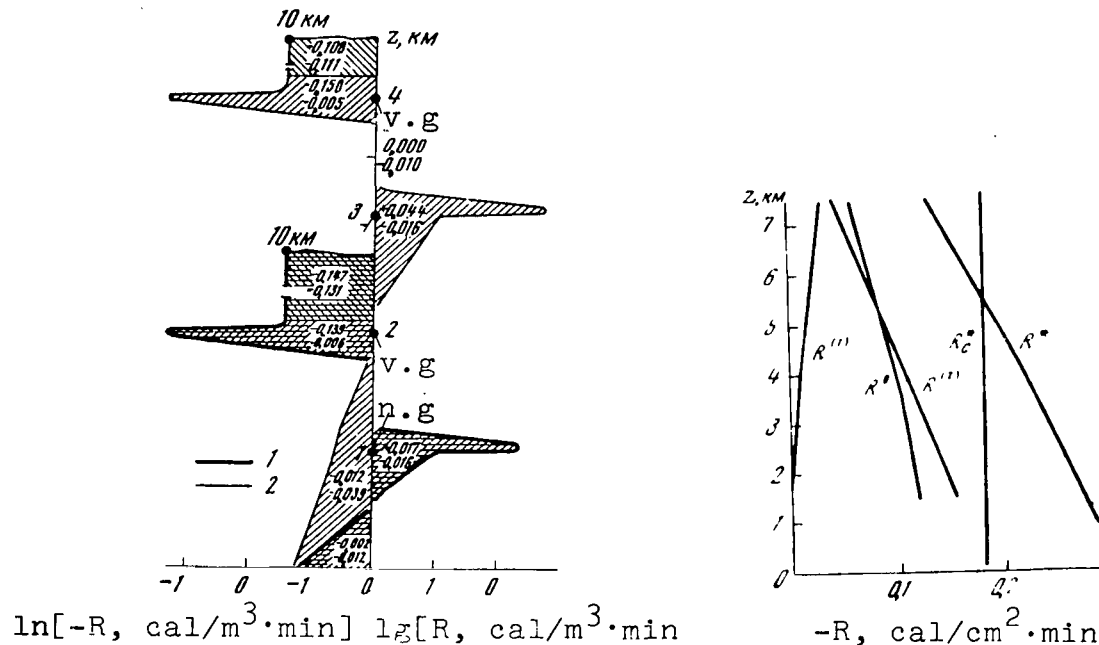


Fig. 1. Vertical profile of the influx in a stratoformous cloud.  
1- cloud in a layer of 1-2 km; 2- cloud in a layer of 3-4 km.

The behavior of integral influxes as a function of the altitude of the cloud corresponds to the quantitative relationships described in [1,2] and [I.2]. Here we direct attention only to the following circumstances: cooling of the same order as the entire atmosphere over the cloud corresponds to a narrow layer within the cloud at the upper boundary; this cooling is not compensated by adequately great heating at the lower boundary. /18

In a case of a cloudy atmosphere, the weight of the individual layers in the general radiation influx is not proportional to the thickness of the layers. We may ignore the influx to the entire layer under the cloud and to the greater part of the cloud layer, but we cannot ignore the cooling of the narrow upper part of the cloud. The latter, together with the cooling of the atmosphere above the cloud, constitutes almost all the radiation cooling of the atmosphere as a whole.

In refs. [1,2] and [I.2] are presented the results of an investigation of the properties of a cloud as a heat sink by methods of numerical experiment and asymptotic analysis. The radiation regime of the cloud as a whole and that of its boundary parts are considered separately, and also the layers under the cloud and over the cloud.

Cooling and heating near the cloud boundaries. In [2] the following approximate expressions of the extreme influxes were obtained, i.e., maximum cooling  $R_v$  under the upper boundary of the cloud, and maximum heating  $R_n$  over the lower boundary:

$$R_v \approx - \sqrt{\alpha \left| \frac{d\rho_w}{dz_{vg}} \right|} E(z_{vg}) \delta(m_v^* - m_{2,v}), \quad (1)$$

$$R_n \approx \sqrt{\alpha \frac{d\rho_w}{dz_{ng}}} [E(0) - E(z_{ng})] \delta(m_1, v). \quad (2)$$

Here  $m_{1,v}$ ,  $m_{2,v}$ , and  $m_v^*$  represent the constant of water vapor in the layers  $(0, z_{n.g.})$ ,  $(0, z_{v.g.})$ , and  $(0, H)$ ;  $H$  is the upper boundary of the atmosphere.

Levels of maximum heating and cooling  $z^{(1)}$  are found at distances  $|z^{(1)} - z_1|$  from the cloud boundaries, and

$$|z_i - z^{(i)}| \approx \frac{1}{\sqrt{\alpha \left| \frac{d\rho_w}{dz_i} \right|}}. \quad (3)$$

Here and below

$$z_i = \begin{cases} z_{n.g.} & i = 1, \\ z_{v.g.} & i = 2. \end{cases}$$

In expressions (1)-(3) the dependences of the influx upon the properties of the cloud and upon the atmosphere outside the cloud are differentiated, which is convenient for calculations, investigations, and solutions of the reverse problems. In this case, the quantities  $\alpha$  and  $dp_w/dz_1$ , which are difficult to determine enter into (1)-(3) in the form of one parameter, expressing /19 the effective absorption capability of the cloud.

The ratios obtained make it possible to establish the following features of the behavior of extreme influxes, depending basically upon the absorption capability of the droplet water, the gradient of the absolute humidity at the boundaries, the temperature at the upper boundary, and the temperature difference between the levels  $z = 0$  and  $z = z_{n.g.}$ , and also upon the content of the water vapor in the atmosphere above and below the cloud.

With an increase in the effective absorption capability of the boundary parts of the cloud, the layers of the extreme influx narrow, are extended, and are pressed close to the cloud boundaries.

If in the vicinity of both boundaries of the low cloud the absorption capability is the same, then cooling at the upper boundary exceeds heating at the lower boundary by an order of magnitude.

In the uplifting of the cloud, cooling and heating may increase or decrease as a consequence of the opposite variations of the temperature and the transmission function. It is natural to expect, nevertheless, that both processes will be intensified as a consequence of the rapid growth of the quantity  $\mathcal{D}(m_v^* - m_{2,v})$  at small masses of the water vapor in the layer above the cloud and a slow decrease of  $\delta(m_{1,v})$  at large masses in the layer under the cloud. For these reasons, in uplifting of the cloud cooling will be preserved at a higher rate than heating.

The error of formulas (1)-(2) does not exceed 25% when

$$0.2 \leq \frac{dp_w}{dz_1} \leq 4 \text{ g/m}^3 \text{ km} \quad \text{and} \quad 450 \leq \alpha \leq 3000 \text{ cm}^2/\text{g} [2].$$

Formula (3) makes it possible to calculate the half-width of the layer of the extreme influx with an accuracy to 50 m.

Relations (1)-(3) make it possible to estimate, in approximation the integral influxes  $M_v$  and  $M_n$  in the boundary layers of the cloud:

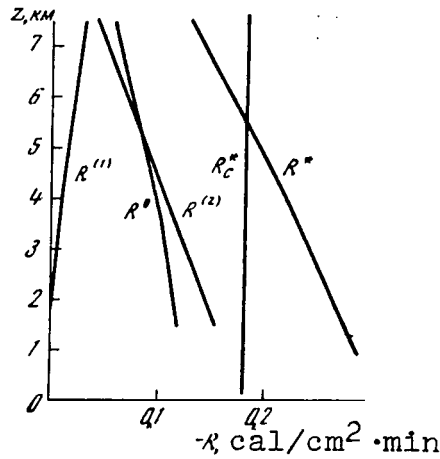


Fig. 2. Influxes to the layers under the cloud ( $R^{(1)}$ ), in the cloud ( $R^{(0)}$ ), and over the cloud ( $R^{(2)}$ ), and also to the entire layer of the atmosphere ( $R^*$ ), as a function of the level of the arrangement of the cloud layer;  $R_c^*$  is the influx to the entire column of a cloudless atmosphere.

$$M_v \approx (z_v - z^{(2)}) R_v = -E(z_2) \delta(m_v^* - m_{2,v}), \quad (4)$$

$$M_n \approx (z^{(1)} - z_{ng}) R_n = [E(0) - E(z_{n,g})] \delta(m_{1,v}). \quad (5)$$

The quantities  $M_v$  and  $M_n$  do not depend upon the properties of the cloud, which is easily explained. Both peaks of the extreme influx originate as a consequence of the rapid change in the fluxes of the radiation entering the cloud, caused by the great absorption capability of the droplet water [1.8]. The rate of variation of these fluxes ( $R_v$  and  $R_n$ ) and the width of the layer in which they are formed ( $|z_1 - z^{(1)}|$ ) are determined by the properties of the boundary layers of the cloud—the parameters  $d\rho_w/dz_1$  and  $\alpha$ . However, at any values of these parameters, the entering fluxes vary from the magnitude determined by conditions outside the cloud (the flux arriving at the cloud), up to black-body radiation (the flux inside the cloud). The influxes to the boundary layers, i.e., the quantities  $M_v$  or  $M_n$  are determined by these limiting values, not dependent upon the properties of the cloud.

Influx to thick layers. The separation of the atmosphere into layers in accordance with the features of the profile of the influx may turn out to be inconvenient or too detailed for problems of large-scale dynamics. Since over the cloud the influx varies only weakly, and under the cloud it is small, and the cloud frequently is compressed to a surface in calculations, a division into layers under the cloud, in the cloud, and over the cloud appears natural.

In Fig. 2 the influxes to the entire column of the layers under the cloud, in the cloud, and over the cloud are presented as a function of the level of the cloud layer with a thickness of 1 km, and also their sum

$$R^* = R^{(1)} + R^{(0)} + R^{(2)}.$$

For a comparison, the influx  $R_C^*$  to the entire thickness of the atmosphere in conditions of a clear sky is given, at the same distribution of the temperature and humidity.

It is apparent that as the cloud rises influxes to the layers /21 in the cloud and above the cloud, and also to the entire column of the atmosphere, decrease with respect to absolute magnitude.

The influx to the layer under the cloud is negligible for clouds of the lower and medium levels. In clouds of the lower and medium levels a cloudy atmosphere as a whole is essentially colder than a cloudless atmosphere.

The influx to a cloud layer is close, with respect to magnitude, to the influx to the layer over a cloud at any thickness of the latter. The sum  $(R^{(0)} + R^{(2)})$  basically determines the cooling of the atmosphere as a whole.

Thus, approximately half of the total radiation cooling of the atmosphere falls to the cloud layer which is a high-capacity heat sink. This sink is formed due to the layer of extreme cooling at the upper boundary of the cloud and is noticeably corrected  $R^{(0)}$  due to the heating layer at the lower boundary. The quantity  $R^{(0)}$  may be calculated, in approximation, according to the formula

$$R^{(0)} \approx -E(z_{v,g}) \delta(m_v^* - m_{2,v}) + [E(0) - E(z_{n,g})] \delta(m_{1,v}). \quad (6)$$

The expression of the influx to the entire column of the atmosphere over the cloud obtained in this approximation has the form

$$R^{(2)} = -E(H) [1 - \delta(m_v^* - m_{2,v})], \quad (7)$$

and for the layer under the cloud we obtain

$$R^{(1)} = 0. \quad (8)$$

The error of formula (6) in a case of dense clouds with a gradient of the absolute humidity at the boundaries of the order of 1-10 g per m<sup>3</sup>/km does not exceed 15%, and that of formula (7), 50% [3]†

Multi-layer cloud cover. In conditions of multi-layer cloud cover the upper cloud essentially suppresses the radiation effect of the cloud layers located below; nevertheless, this effect remains considerable [1.2]. The mutual radiation effect of the cloud layers is basically determined by the distance between them and not by their physical properties. In [3] influxes to layers defined in a case of one-layer, two-layer, and three-layer cloud cover are compared. The necessity of considering the number and arrangement of the layers in the determination of general cooling and its distribution inside the atmosphere is observed. Each cloud layer—even an internal layer—is considerably greater than the space between the clouds. Cooling of the external cloud layer is especially great.

If we calculate the fraction of cooling falling to the share of the cloud layer, inter-cloud layer, and the layer above the cloud, it is ascertained that the role of cooling concentrated in the clouds rapidly increases with an increase in the number of layers and, accordingly, the contribution of the other layers decreases. Such data are given in the table for a case of clouds located in layers (1-2 km), (5-6 km), and (7-8 km). /22

Nature of layers	Fraction of cooling, %		
	Form of cloud cover		
	1-layer (1-2 km)	2-layer (1-2 km), (5-6 km)	3-layer (1-2 km), (5-6 km), (7-8 km)
Layer under and between clouds	0	3	4
In the clouds	43	62	80
Above the cloud	57	35	16

† If we assume in (7) that  $H \approx 5$  km (the upper boundary of the atmosphere for water vapor) the error of this formula sharply decreases.



Approximate expressions of the integral influxes in a case of a k-layer cloud cover take the form

$$R_k^{(1)} = 0, \quad k = 0, 1, \dots, n-1,$$

where  $R_k^{(1)}$  is the influx to the k-th inter-cloud layer,  $k = 0$  is the layer under the cloud:

$$R_k^{(0)} = [E(z_{v.g.}^{(k-1)}) - E(z_{n.g.}^{(k)})] \delta(m_{1,v}^{(k)} - m_{2,v}^{(k-1)}) - [E(z_{v.g.}^{(k)}) - E(z_{n.g.}^{(k+1)})] \delta(m_{1,v}^{(k+1)} - m_{2,v}^{(k)}). \quad (9)$$

Here  $z_{n.g.}^{(k)}$  and  $z_{v.g.}^{(k)}$  represent the lower and upper boundaries of the k-th cloud layer;  $m_{1,v}^{(k)}$ ,  $m_{2,v}^{(k)}$  are the corresponding masses of the water vapor;  $E(z_1^{n+1}) = 0$ . Expression  $R^{(2)}$  remains as before.

A cloud as a black radiator. In the calculation of the radiation effect of clouds it is usually assumed that they transmit fluxes of black-body radiation<sup>†</sup>  $\sigma T^4(z_{n.g.})$  to the space outside v.g.

the cloud. Such an assumption deprives us of the opportunity of considering optically thin clouds and tracing the conversions of radiant fluxes inside the cloud.

In [1-3], [I.2], and in this article the results of an investigation free from prior assumptions concerning the nature of the radiation of cloud boundaries are considered. Therefore, it turned out to be possible to determine the radiation effect of weak cloud cover [I.2] and [2] to investigate powerful boundary effects, and also to estimate the error of the "black" approximation [2,3]. The latter turned out to be of the order of 50% at a small magnitude of  $|z - z_{n.g.}|$ , where  $z > z_{v.g.}$  or  $z < z_{n.g.}$ . With a growth of  $|z - z_{n.g.}|$  v.g.

the error of the "black" approximation rapidly decreases.

It is estimated in [3] as a measure of the dependence of the quantities  $R^{(1)}$ ,  $R^{(0)}$ ,  $R^{(2)}$ , and  $R^*$  upon the parameters of the cloud cover  $\alpha$ ,  $d\rho_w/dz_1$  at  $\rho_{w,max}$ . It is understood that the weak

---

<sup>†</sup> Calculation of fluxes with this assumption is further called the "black" approximation.

dependence upon these parameters signifies a good accuracy of the "black" approximation. It was ascertained that in a variation of  $\frac{dp_w}{dz_i}$  within limits of (0.2-4) g/m<sup>3</sup> km, corresponding to real limits of variations of the gradient of the absolute humidity, the influxes  $R^{(2)}$  and  $R^*$  vary by 5%; the influx  $R^{(0)}$  by 20%; and finally the influx  $R^{(1)}$  varies by several orders of magnitude. The variation of the parameter  $\alpha$  within limits of (500-3000 cm<sup>2</sup>/g) [I.1] is felt even less in the integral influxes.

These estimates refer to values of  $\rho_w \geq 0.03$  g/m<sup>3</sup> at  $z_{v.g.} - z_{n.g.} \geq 0.5$  km, which makes it possible to consider clouds with a water reserve  $m_w \geq 0.0015$  g/cm to be optically dense, permitting the use of the "black" approximation with the accuracy indicated.

The "black" approximation may thus be considered to be practically accurate in the calculation of an influx to the entire column of the atmosphere or to its part over the cloud. The influx to the cloud column is also determined with an accuracy satisfying the requirements of the majority of practical problems. Finally, the influx to the layer under the cloud as a whole can not be calculated in the "black" approximation, which is not so very essential in the majority of cases, since this influx is small.

#### REFERENCES

1. Petrova, L. V., "Certain problems of the formation of the long-wave radiation influx in continuous cloud cover", Izv. AN SSSR, seriya FAO, No. 10, 1968.
2. Feygel'son, Ye. M., "Influx of long-wave radiation in cloud conditions", Izv. AN SSSR, seriya FAO, No. 5, 1968.
3. Petrova, L. V. and Ye. M. Feygel'son, "Radiation cooling of thick layers", Izv. AN SSSR, seriya FAO, No. 6, 1969.

SOME APPROXIMATE METHODS OF CALCULATING  
RADIANT HEAT TRANSFER IN A CLOUDLESS ATMOSPHERE

A. S. Ginzburg and Ye. M. Feygel'son

In this work simplified methods of calculating one-sided and effective fluxes of radiation are discussed, and also methods of calculating influxes of heat, intended for problems of dynamic meteorology not requiring a high degree of accuracy.

One-sided ascending  $F\uparrow$  and descending  $F\downarrow$  heat fluxes in the spectral range  $\Delta\lambda$  have the form

$$F_{\uparrow\Delta\lambda}(z) = E_{\Delta\lambda}(0) D_{\Delta\lambda}(0, z) + \int_0^z E_{\Delta\lambda}(z') \frac{dD_{\Delta\lambda}(z', z)}{dz'} dz', \quad (1)$$

$$F_{\downarrow\Delta\lambda}(z) = E_{\Delta\lambda}(H) D_{\Delta\lambda}(z, H) + \int_z^H E_{\Delta\lambda}(z') \frac{dD_{\Delta\lambda}(z, z')}{dz'} dz', \quad (2)$$

where  $E_{\Delta\lambda}(0)$  is the radiation of the underlying surface;  $E_{\Delta\lambda}(H)$  is /24 the downflow at the upper boundary  $H$  of the atmosphere;  $D(z_1, z_2)$  is the transmission function of the layer  $(z_1, z_2)$ . The effective flux is calculated as the difference of one-sided fluxes  $F = F\uparrow - F\downarrow$ , and the influx of heat as the derivative with respect to altitude of the effective flux  $R = dF/dz$ . The calculation of fluxes in narrow spectral intervals of the order of  $25 \text{ cm}^{-1}$  and then summation throughout the spectrum is the most accurate method of calculating the field of the natural radiation of the atmosphere. However, such "spectral" calculations are too complex and can supply only reference data. The use of the integral transmission function (application of radiation nomograms)—the so-called "integral" calculations, serves as a natural and generally known method of simplifying the calculations. Expressions for fluxes and the influx in this case have the same form as for the corresponding spectral quantities if we assume that  $\Delta\lambda = (0, \infty)$  in (1) and (2).

We will write an expression for the influx of heat:

$$R(z) = -\frac{d}{dz} \left[ E(0) D(0, z) - E(H) D(z, H) + \int_0^z E(z') \frac{dD(z, z')}{dz'} dz' \right].$$

In the materials of the Global Atmospheric Processes Research Program (GARP) [1] it is indicated that up to this time the necessary accuracy of the calculation of radiant heat transfer in problems of dynamics has not been determined. Therefore the assumption is expressed that it is advisable to construct a number of approximate methods with their successive complications. In [1] these methods are given in the following order: 1) the use of climatic data; 2) the consideration of only the radiation departing beyond the limits of the atmosphere, i.e., cooling into space; 3) the consideration of cooling to space with an empirical consideration of local heat transfer; 4) "integral" calculations; 5) spectral methods.

In ref. [2] the second and third of the methods listed are considered and an approximate method is proposed, considering cooling into space and heat transfer with the underlying surface. Heat fluxes in this case are equal to

$$F_{\uparrow 1}(z) = E(0) D(0, z) + E(z) [1 - D(0, z)], \quad (4)$$

$$F_{\uparrow 1}(z) = E(H) D(z, H) + E(z) [1 - D(z, H)]. \quad (5)$$

Expressions (4) and (5) also may be obtained under the assumption of a  $\delta$ -shaped nature of the first derivative of the integral transmission function from expressions (1) and (2). The heat influx in this approximation has the form

$$R_1(z) = - \frac{d}{dz} [(E(0) - E(z)) D(0, z) - (E(H) - E(z)) D(z, H)]. \quad (6)$$

In the assumption of a  $\delta$ -shaped nature of the second derivative of the transmission function, in [2] the following expression /25 for the radiation heat influx is derived directly from relation (3):

$$R_2(z) = - \left[ (E(0) - E(z)) \frac{dD(0, z)}{dz} - (E(H) - E(z)) \frac{dD(z, H)}{dz} \right] \quad (7)$$

The approximate methods proposed in [2] are not sensitive to the value and local variations of the humidity and temperature far from the level under consideration. This circumstance is not an obstacle for the use of these approximations, since for problems of dynamics only large-scale features of the distributions of temperature and humidity are essential. The accuracy of calculations according to formulas (4)-(7) are estimated in [1.5]. Here we only note that the approximate methods considered may be extended to a case of cloud conditions. The approximation  $R_2$  makes

it possible to describe the continuous profile of the influx inside the cloud layer and outside it. For this, in the integral transmission function  $D$  it is necessary to consider the absorption of droplet water. In the approximation  $R_1$  it is convenient to describe the heat influx to the layers under the cloud, in the cloud and above the cloud. In this case we should consider that the cloud radiates as a black body and serves as the underlying surface for the layer above the cloud and as the upper boundary of the atmosphere for the layer under the cloud.

#### REFERENCES

1. GARP Conference Report, Stockholm, July 1967.
2. Ginzburg, A. S. and Ye. M. Feygel'son, "Approximate methods of calculating radiant flux and heat influxes in the troposphere", Izv. AN SSSR, seriya FAO, No. 5, 1970.

# COMPARISON OF VARIOUS METHODS OF CALCULATING THE FIELD OF LONG-WAVE RADIATION

A. S. Ginzburg and Kh. Yu. Niylik

In many problems of the dynamics of the atmosphere, a necessity arises for the calculation of radiant fluxes and influxes of heat, and the requirements for accuracy vary. In this work, results of successively more simplified calculations of fluxes and radiant flux of heat are compared, considered, for example in [1] and [1.4]. The results of calculations by different methods are given for three models of the atmosphere, differing in vertical profiles of temperature and humidity at altitudes  $0 \leq z \leq 10$  km

/26

Model A (the ARDC-59 standard atmosphere):<sup>†</sup>

$$\begin{aligned} T(0) &= 288.2^\circ\text{K}; & \gamma &= 6.5 \text{ degrees/km}; \\ U(0) &= 58\%; & m_v^* &= 1.38 \text{ g/cm}^2. \end{aligned}$$

Model B (moist summer in mid latitudes):

$$\begin{aligned} T(0) &= 293.2^\circ \text{ K}; & \gamma &= 6.5 \text{ degrees/km}; \\ U(0) &= 100\%; & m_v^* &= 3.25 \text{ g/cm}^2 \end{aligned}$$

Model C (dry winter in mid latitudes):

$$\begin{aligned} T(0) &= 258.2^\circ \text{ K}; & \gamma &= 4 \text{ degrees/km}; \\ U(0) &= 20\%; & m_v^* &= 0.06 \text{ g/cm}^2 \end{aligned}$$

More complete data concerning these models of the atmosphere may be found in [2].

All the calculations, aside from the case stipulated below, are performed according to the following scheme. The effective absorbing mass of the water vapor in the column of air ( $z_1, z_2$ ) is calculated according to the formula

$$m_v(z_1, z_2) = \int_{z_1}^{z_2} \rho_v(z) \frac{P(z)}{P(0)} dz,$$

or, which is the same thing, according to the formula,

---

<sup>†</sup>Here  $\gamma$  is the temperature gradient in the troposphere,  $m_v^*$  is the effective mass of water vapor in the entire column of the atmosphere.



$$m_v(z_1, z_2) = \frac{1}{gP(0)} \int_{P_1}^{P_2} q(P) PdP$$

(here  $q$  is the specific humidity). In an analogous formula for the effective mass  $m_u(z_1, z_2)$  of carbon dioxide gas the volumetric concentration of  $CO_2$  is assumed to be constant and equal to 0.03%. According to the masses of the absorbing substances the spectral or integral transmission function is determined, and then at the given temperature distribution the ascending flux  $F\uparrow(z)$  and descending flux  $F\downarrow(z)$  is calculated, in calories per  $cm^2$  per minute at  $z = 0, 1, 2, 4, 6$ , and 10 km. If we know the one-sided fluxes, we may determine the effective radiation flux  $F(z) = F\uparrow(z) - F\downarrow(z)$  and the heat influx to the layer  $(z_1, z_2)$  equal to  $F(z_1) - F(z_2)$ . The average heat influx to the elementary volume in the layer  $(z_1, z_2)$  is equal to

$$R = \frac{F(z_1) - F(z_2)}{z_2 - z_1} \cdot 10^{-5} \frac{\text{cal}}{\text{cm}^3 \cdot \text{min}} = 10 \frac{F(z_1) - F(z_2)}{z_2 - z_1} \frac{\text{cal}}{\text{m}^3 \cdot \text{min}}. \quad (1)$$

In the comparison of various methods, results of spectral calculations performed at the IFA AN ESSR [2,3] serve as the reference data. The errors of all other calculations are given relative to these quantities. The calculations of the spectral intensities of the descending and ascending thermal radiation are performed by means of transmission functions for narrow spectral ranges with a width of the order of  $25 \text{ cm}^{-1}$  within limits of  $225\text{--}2000 \text{ cm}^{-1}$  (5-44 microns). Then the quantities obtained are integrated with respect to directions and summed over the spectrum. At the real temperature of the atmosphere outside the interval of  $225\text{--}2000 \text{ cm}^{-1}$  about 6% of the radiation of a "black" body is located, and therefore to obtain integral fluxes a correction factor 1.06 is used. Table 1, where the fraction of radiation of a "black" body  $\Delta E$ , located outside the interval of  $225\text{--}2000 \text{ cm}^{-1}$  at various temperatures is indicated, shows how accurate this factor is. The values of the fluxes and influxes obtained in such a manner are designated below by the subscript "sp".

TABLE 1

$T, ^\circ K$	220	240	260	280	300
$\Delta E, \%$	9	8	6	6	5

Then the calculation of one-sided heat fluxes is considered, performed directly by means of the integral transmission function from [4] for the interval  $2975-25 \text{ cm}^{-1}$ , and also the effective radiation and the heat influx determined by these fluxes. The quantities obtained are designated by the subscript "int". We should note that the initial data for the construction of the transmission function in [4] coincide with the initial data for spectral calculations in [2,3] in the region of  $833-225 \text{ cm}^{-1}$  and differ somewhat in the region  $2000-833 \text{ cm}^{-1}$ . The effect of these divergences on the magnitude of the transmission function is shown in Table 2, where the transmission functions of water vapor in the region  $2000-225 \text{ cm}^{-1}$  are compared.

TABLE 2

$m_v$	0,001	0,01	0,1	1,0	10
$D_{sp}$	0.905	0.772	0.599	0.394	0.125
$D_{int}$	0.913	0.784	0.614	0.403	0.136

$D_{sp}$  is constructed according to data used in [2,3],  $D_{int}$  corresponds to ref. [4]. Tentative estimates demonstrate that the divergences in the transmission functions indicated lead to differences in the magnitudes of the fluxes of ascending and descending radiation of the order of 0.5-1%. In "spectral" calculations the radiation and absorption of heat by the atmospheric ozone is taken into consideration, which is not considered in the construction of the integral transmission function in [5]. /28

The effect of absorption by ozone on the magnitude of the transmission function is estimated in Table 3, where the integral transmission function is given at various contents of ozone in the atmosphere (in cm). The content of  $\text{CO}_2$  everywhere is 120 cm.

TABLE 3

Ozone content	$m_v$					
	0,05	0,1	0,5	1,0	2,0	5,0
0	0.471	0.424	0.306	0.246	0.177	0.092
0.1	0.442	0.399	0.284	0.224	0.153	0.082
0.4	0.422	0.379	0.267	0.208	0.147	0.074

The error of the calculation of the fluxes of descending thermal radiation without consideration of ozone does not exceed 3-4% in the troposphere, on the average. The error in the values of the ascending fluxes is negligible. The comments made demonstrate that the "spectral" and "integral" calculations were performed in several different conditions and a comparison of them is not entirely correct. However, the estimates given testify to the small effect of inaccuracy of the initial data on the results of the calculations. In the future this will make it possible to compare the results of the simplified "integral" calculations directly with the "spectral" magnitudes.

In [I.1] an approximation of the integral transmission function was constructed for the interval  $25-2800\text{ cm}^{-1}$ . The initial data there are the same as in [4]. One-sided fluxes according to approximate formulas (4) and (5) from [I.4] are calculated by means of this approximation. The corresponding values of the fluxes and influxes are designated by the subscript "1". We note that the error of approximation does not exceed 4-6%, and the error of the fluxes  $F_{\uparrow, \downarrow}$  caused by this does not exceed 1-2%.

In Table 4 the values of fluxes of descending and ascending radiation are given (in  $\text{cal/cm}^2/\text{min}$ ), calculated by the three methods described above for three models of the atmosphere.

The table demonstrates the surprisingly good agreement between the quantities  $F_{\uparrow, \downarrow, \text{int}}$  and  $F_{\uparrow, \downarrow, \text{sp}}$ . Apparently, such a coincidence is explained by the compensation of the error associated with the use of the approximate method of calculating the fluxes and the error of the integral transmission function (see Tables 1 and 3). The flux of descending radiation calculated in the approximation "1" turns out to be systematically greater, and the ascending radiation systematically less than the corresponding fluxes in more accurate calculations. This quantitative relationship follows also from a comparison of formulas (1) with (4) and (2) with (5) in [I.4]. The errors of calculation of  $F_{\downarrow 1}$  and especially of  $F_{\uparrow 1}$  increase with a growth of the optical density of the atmosphere, and in this case the relative error of  $F_{\downarrow 1}$  is approximately constant with respect to altitude and on the average is equal to 5%. The error of calculation of  $F_{\uparrow 1}$  in the lower layers is close to zero, and in the upper layers of the troposphere reaches 20-30; on the average this error is equal to 5-6%.

In the calculation of the flux of effective radiation the relative error naturally increases and amounts to 5% on the average

TABLE 4

$z, \text{km}$	$F_{\downarrow \text{sp}}$	$F_{\downarrow \text{int}}$	$F_{\downarrow 1}$	$F_{\uparrow \text{sp}}$	$F_{\uparrow \text{int}}$	$F_{\uparrow 1}$
Model A						
0	0.407	0.409	0.423	0.558	0.560	0.561
1	0.346	0.347	0.365	0.536	0.529	0.529
2	0.291	0.291	0.308	0.507	0.498	0.493
4	0.207	0.204	0.215	0.462	0.443	0.429
6	0.138	0.135	0.134	0.424	0.402	0.376
10	0.044	0.040	0.043	0.379	0.354	0.292
Model B						
0	0.484	0.483	0.511	0.598	0.600	0.600
1	0.405	0.412	0.438	0.568	0.569	0.568
2	0.341	0.344	0.364	0.537	0.528	0.521
4	0.247	0.246	0.261	0.485	0.463	0.445
6	0.172	0.168	0.177	0.440	0.415	0.379
10	0.072	0.068	0.074	0.384	0.356	0.277
Model C						
0	0.194	0.191	0.192	0.356	0.361	0.361
1	0.170	0.166	0.165	0.349	0.352	0.352
2	0.147	0.143	0.142	0.340	0.342	0.341
4	0.108	0.105	0.107	0.325	0.324	0.320
6	0.076	0.073	0.079	0.312	0.309	0.300
10	0.038	0.031	0.027	0.294	0.292	0.267

for  $F_{\text{int}}$ , and for  $F_1$ , 15% with relationship to  $F_{\text{sp}}$  and 12% with relationship to  $F_{\text{int}}$ . In the calculation of the influx the error increases more and more and amounts to 14% on the average for  $R_{\text{int}}$ , and for  $R_1$  about 25-30%. (All the magnitudes of the radiation influx were calculated according to formula (1)).  $R_{\text{int}}$  and  $R_1$  decrease the absolute magnitude of the influx, and  $|R_1|$  in the upper layers of Models A and B is several orders of magnitude less than  $|R_{\text{sp}}|$  and  $|R_{\text{int}}|$ , which is a consequence of the large error of  $F_{\uparrow 1}$  at the corresponding levels (see Table 5 where the fluxes of effective radiation are given in  $\text{cal/cm}^2 \text{ min}$  and the average influxes of heat in  $\text{cal/m}^3 \text{ min}$ ).

In the previous article the approximate method of calculating  $R_2$  /30 the influx of heat to the elementary volume at a given level, was considered (see expression (7) in [I.4]). For a comparison

of this method with the one described above, the influx  $R_2$  is calculated at altitudes of 0.5, 1.5, 3, 5, and 8 km, i.e., in the centers of the layers under consideration. In the calculation of  $R_2$  the derivative transmission function with respect to altitude participates, which is calculated in the given case according to the formula

$$\frac{dD}{dz} = \rho_v \frac{\partial D}{\partial m_v} + \rho_u \frac{\partial D}{\partial m_u},$$

and in this case the transmission function is selected from [I.1].

TABLE 5

$z, \text{km}$	$F_{\text{sp}}$	$F_{\text{int}}$	$F_1$	Layer, km	$R_{\text{sp}}$	$R_{\text{int}}$	$R_1$
Model A							
0	0,150	0,152	0,138	0-1	0,040	0,030	0,026
1	0,190	0,182	0,164	1-2	0,027	0,025	0,21
2	0,217	0,207	0,185	2-4	0,19	0,15	0,14
4	0,255	0,238	0,214	4-6	0,16	0,14	0,12
6	0,286	0,207	0,237	6-10	0,12	0,12	0,03
10	0,334	0,314	0,249				
Model B							
0	0,114	0,118	0,089	0-1	0,49	0,39	0,41
1	0,163	0,157	0,130	1-2	0,33	0,28	0,27
2	0,196	0,184	0,157	2-4	0,21	0,17	0,14
4	0,236	0,217	0,184	4-6	0,15	0,14	0,09
6	0,268	0,246	0,202	6-10	0,14	0,11	0,00
10	0,312	0,288	0,203				
Model C							
0	0,161	0,170	0,169	0-1	0,18	0,16	0,18
1	0,179	0,186	0,187	1-2	0,15	0,13	0,12
2	0,194	0,199	0,199	2-4	0,11	0,10	0,07
4	0,217	0,219	0,213	4-6	0,09	0,09	0,06
6	0,235	0,237	0,221	6-10	0,05	0,06	0,04
10	0,256	0,261	0,240				

In Table 6 the magnitudes of  $R_2$  in  $\text{cal/m}^3 \text{ min}$  are compared with the spectral calculations. At an average error of 25-30% at individual altitudes the modulus of  $R_2$  is much greater than  $R_{\text{sp}}$  and  $R_{\text{int}}$ . This is apparently explained in the following manner. The densities  $\rho_v$  and  $\rho_u$  of the absorbing gases rapidly decrease with

altitude, while the transmission function of the layer lying above /31 the given level,  $D(m_v^* - m_v, m_u^* - m_u)$  rapidly increases. As a result in certain models

$$\frac{dD(m_v^* - m_v, m_u^* - m_u)}{dz}$$

has a local extremum, considerably exceeding the average value of this function. After  $dD/dz$ ,  $R_2$  also has an extremum.

TABLE 6

Layer	$R_{sp}$	$R_1$	$R_{sp}$	$R_1$	$R_{sp}$	$R_1$
	Model A		Model B		Model C	
0-1	0,40	0,36	0,49	0,34	0,18	0,16
1-2	0,27	0,23	0,33	0,26	0,15	0,12
2-4	0,19	0,18	0,21	0,25	0,11	0,08
4-8	0,16	0,23	0,15	0,18	0,09	0,06
6-10	0,12	0,08	0,14	0,16	0,05	0,14

For the investigation of the energy balance of the atmosphere, it is useful to know the general cooling of the troposphere. In Table 7 the total influx to the 0-10 km layer in cal/cm<sup>2</sup>/min is compared with that calculated by different methods. From this table it is apparent that the error of the approximations  $R_{int}$  and  $R_2$  amounts to about 10%, and  $R_1$  is of the order of 30%. Thus in spite of the characteristic indicated above, the approximation of  $R_2$  in the calculation of the cooling of the troposphere turns out to be more accurate than  $R_1$ .

TABLE 7

Model	Method			
	"sp"	"int"	"1"	"2"
A	-0.184	-0.162	-0.111	-0.173
B	-0.198	-0.170	-0.114	-0.210
C	-0.095	-0.090	-0.079	-0.109

In conclusion we note that all the comparisons are given only for "smooth" models of the atmosphere where there are no inversions of temperature and humidity. In real conditions the error of the approximate methods "1" and "2" may be larger. In problems of the general circulation of the atmosphere and other large-scale problems where simple methods of considering the radiant heat transfer are required, the local features of the profiles of temperature and humidity are not considered. We may hope that in such problems the application of approximate methods considered above will turn out to be entirely justified.

1. GARP Conference Report, Stockholm, July 1967.
2. Niylysk, Kh. Yu. and R. Yu. Noorma, "Spectral structure of the intensity and fluxes of thermal radiation in the free atmosphere", Collection: Issledovaniy Radiatsionnogo Rezhima Atmosfery (Collection of Research on Radiation Conditions in the Atmosphere), IFA AN ESSR, Tartu, 1967.
3. Niylysk, Kh. Yu. and R. Yu. Noorma, "Spectral structure of the intensity and fluxes of thermal radiation of the atmosphere in the far infrared region of the spectrum", Collection: Radiatsiya i Oblachnost' (Radiation and Cloudiness), Tartu, 1969.
4. Niylysk, Kh. Yu., "Certain problems of the refinement of theoretical calculations of the thermal radiation of the atmosphere", Collection: Issledovaniya Radiatsionnogo Rezhima Atmosfery (Collection of Research on the Radiation Conditions of the Atmosphere), IFA AN ESSR, Tartu, 1967.
5. Niylysk, Kh. Yu., "New radiation nomogram", Izv. AN ESSR, Seriya Fiz.-Matem. i Tekh. Nauk, 10, No. 4, 1961.



ESTIMATE OF THE ERROR IN CALCULATION  
OF FLUXES AND INFLUXES OF THERMAL RADIATION  
DUE TO ERRORS OF INITIAL METEOROLOGICAL PARAMETERS

Kh. Yu. Niylik

For calculation of the fluxes of atmospheric thermal radiation it is necessary to have data concerning the distributions of temperature, pressure, and the components absorbing the thermal radiation in the atmosphere with the specific synoptic situations under consideration [1]. Errors of the calculations of thermal radiation caused by errors of initial experimental data are estimated below.

At the present time sounding the atmosphere in the aerological network of the Soviet Union is performed basically by radiosondes. According to reports obtained from the Central Aerological Observatory and according to refs. [2,3], the errors of measurement of the temperature and pressure are located, respectively within limits of  $(0.4-1.1)^{\circ}$  and  $(3-8) \cdot 10^2$  newtons/m<sup>2</sup> (in the range of altitudes of 0-20 km). The errors of determination of the relative humidity to an altitude of 10 km amount to 4-10%, and they noticeably increase with altitude, and above 10-12 km data concerning the moisture content of the atmosphere are either lacking or are very unreliable.

In this work, in calculations of thermal radiation the errors in the values of the temperature and the relative humidity were assumed to be close to the magnitudes given above. Fluxes of descending and ascending radiation ( $F_{\downarrow}$  and  $F_{\uparrow}$ ) were calculated as well as radiation heat influxes ( $R$ ) for three spectral intervals (1600-1550, 1300-1250, and 940-900 cm<sup>-1</sup>), and also for the integral radiation (2975-25 cm<sup>-1</sup>) for eight models of the atmosphere in the interval of altitudes from 0 to 40 km. The standard model of the atmosphere served as the basic model [4]. The seven other models were obtained by variation of the deviations of the temperature ( $\Delta T$ ) and relative humidity ( $\Delta U$ ) from the corresponding characteristics of the basic model. In this case the maximum absolute error of the temperature was equal to  $2^{\circ}$ , and that of the relative humidity 10%. /33

In the calculations the spectral intervals were selected which make it possible to ascertain the characteristic features of the errors of radiation fluxes ( $\Delta F_{\downarrow}$  and  $\Delta F_{\uparrow}$ ) in various absorption conditions. We will note that the section of the spectrum in (1600-1550) cm<sup>-1</sup> is located in the center of the absorption band of water vapor, the section (1300-1250) cm<sup>-1</sup> on the side of

TABLE 1

$z, \text{ km}$	$i=0$ $\Delta T_0=0$ $\Delta U_0=0$	$i=2$ $\Delta T_2=0$ $\Delta U_2=5$	$i=3$ $\Delta T_3=1$ $\Delta U_3=0$	$i=4$ $\Delta T_4=2$ $\Delta U_4=10$	$i=6$ $\Delta T_6=1$ $\Delta U_6=\frac{U_0}{10}$	$i=2$ $\Delta T_2=0$ $\Delta U_2=5$	$i=3$ $\Delta T_3=1$ $\Delta U_3=0$	$i=4$ $\Delta T_4=2$ $\Delta U_4=10$	$i=6$ $\Delta T_6=1$ $\Delta U_6=\frac{U_0}{10}$
	$F_0 \downarrow (10^{-6} \text{ w} \cdot \text{cm}^{-2} \cdot \mu\text{m}^{-1})$	$\Delta F \downarrow = F_i \downarrow - F_0 \downarrow (10^{-6} \text{ w} \cdot \text{cm}^{-2} \cdot \mu\text{m}^{-1})$				$\overline{\Delta F \downarrow} = \frac{F_i \downarrow - F_0 \downarrow}{F_0 \downarrow}, \%$			
$\Delta \nu = 1600 - 1550 \text{ km}^{-1}$									
0	1371	0	38	77	38	0	3	6	3
10	38	85	4	136	6	223	10	357	16
40	22	280	2	382	3	1272	9	1736	14
$\Delta \nu = 1300 - 1250 \text{ km}^{-1}$									
0	1662	26	60	171	90	2	4	10	5
10	12	26	1	47	2	217	8	391	17
40	4	55	0,2	89	0,6	1375	5	2225	15
$\Delta \nu = 940 - 900 \text{ km}^{-1}$									
0	598	42	46	187	97	7	8	31	16
10	0.09	0.4	0.01	0.9	0.02	444	11	1000	22
40	0.002	0.3	0.0001	0.7	0.0004	15000	5	35000	20

$z, \text{ km}$	$F_0 \uparrow (10^{-6} \text{ watt w} \cdot \text{cm}^{-2} \cdot \mu\text{m}^{-2})$	$\Delta F \uparrow = F_i \uparrow - F_0 \uparrow (10^{-6} \text{ w} \cdot \text{cm}^{-2} \cdot \mu\text{m}^{-1})$				$\overline{\Delta F \uparrow} = \frac{F_i \uparrow - F_0 \uparrow}{F_0 \uparrow}, \%$			
$\Delta \nu = 1600 - 1550 \text{ km}^{-1}$									
0	1396	0	39	78	39	0	3	6	3
10	251	-4	5	2	0	-2	2	0.8	0
40	244	42	4	73	0	17	2	30	0
$\Delta \nu = 1300 - 1250 \text{ km}^{-1}$									
0	2172	0	49	98	49	0	2	5	2
10	1345	-20	13	-13	-10	-1	1	-1	-0.7
40	1333	-13	13	-4	-10	-1	1	-0.3	-0.8
$\Delta \nu = 940 - 900 \text{ km}^{-1}$									
0	2520	0	41	82	41	0	2	3	2
10	2395	-10	30	40	20	-0.4	1	2	0.8
40	2390	-10	30	38	18	-0.4	1	2	0.8

TABLE 2

z, km	$i=0$ $\Delta T_0=0$ $\Delta U_0=0$	$i=2$ $\Delta T_2=0$ $\Delta U_2=5$	$i=3$ $\Delta T_3=1$ $\Delta U_3=0$	$i=4$ $\Delta T_4=2$ $\Delta U_4=10$	$i=6$ $\Delta T_6=1$ $\Delta U_6=\frac{U_0}{10}$	$i=2$ $\Delta T_2=0$ $\Delta U_2=5$	$i=3$ $\Delta T_3=1$ $\Delta U_3=0$	$i=4$ $\Delta T_4=2$ $\Delta U_4=10$	$i=6$ $\Delta T_6=1$ $\Delta U_6=\frac{U_0}{10}$
	$F_0 \downarrow$ ( $10^{-4} \frac{F_0}{w} \cdot \text{c.u.}^{-2}$ )	$\Delta F \downarrow = F_i \downarrow - F_0 \downarrow$ ( $10^{-4} \frac{F_0}{w} \cdot \text{c.u.}^{-2}$ )				$\overline{\Delta F \downarrow} = \frac{F_i \downarrow - F_0 \downarrow}{F_0 \downarrow} (\%)$			
0	285	2.5	6.1	18	88	0.9	2.1	6.1	3.2
10	28	12	1.2	21	1.8	42	4.3	73	6.4
40	1.1	27	0.0	40	0.1	2445	0.0	3654	9.1

	$F_0 \uparrow$ ( $10^{-4} \frac{F_0}{w} \cdot \text{c.u.}^{-2}$ )	$\Delta F \uparrow = F_i \uparrow - F_0 \uparrow$ ( $10^{-4} \frac{F_0}{w} \cdot \text{c.u.}^{-2}$ )				$\overline{\Delta F \uparrow} = \frac{F_i \uparrow - F_0 \uparrow}{F_0 \uparrow} (\%)$			
0	391	-0.0	5.5	11.0	5.5	0.0	1.4	2.8	1.4
10	247	-1.4	2.3	1.8	0.7	-0.6	0.9	0.7	0.3
40	243	2.9	2.3	9.2	0.6	1.2	0.9	3.8	0.3

	$R_0$ ( $10^{-3} \frac{R_0}{w} \cdot \text{c.u.}^{-2}$ )	$\Delta R = R_i - R_0$ ( $10^{-3} \frac{R_0}{w} \cdot \text{c.u.}^{-2}$ )				$\overline{\Delta R} = \frac{R_i - R_0}{R_0} (\%)$			
1	-136	-0.6	-1.9	-6.2	-2.1	0.4	1.4	4.6	1.5
10	-36	43	-1.8	54.0	-2.9	-120.0	5.0	-149.0	8.1
40	-3.7	-9.8	-0.2	-14.0	-0.3	265.0	5.4	368.0	8.1

2\*

this band, and the interval  $(940-900) \text{ cm}^{-1}$  is one of the most "transparent" sections of the infrared region of the spectrum.

The results of these calculations are explained in detail in ref. [5]. Here we will give only the most characteristic data and the general conclusions.

In Table 1 the magnitudes and variability of the errors of fluxes of thermal radiation are presented for the spectral intervals considered, with averaging within the limits of each interval. In Table 2 are given analogous data for integral radiation, including, in addition, also errors of radiation influxes of heat. Here the following symbols are used:  $\Delta T$  is the absolute error of the temperature (in  $^{\circ}\text{C}$ );  $\Delta U$  is the absolute error of the relative humidity (in percentages);  $z$  is the altitude of the level for which the radiation is being considered (in km);  $\Delta \nu$  is the spectral interval (in  $\text{cm}^{-1}$ ); and  $i$  is the number of the model according to ref. [5].

It is apparent that the errors of the initial meteorological data may, in a number of cases, be the cause of quite serious errors in the calculations of the radiation fluxes. The maximum absolute errors of the spectral fluxes of counter-radiation ( $\Delta F_{\uparrow}$ ), originating as a consequence of errors of temperature, are observed in the central intervals of the absorption bands; they are especially great, apparently, in absorption bands located close to the maximum of the energy distribution curve of an absolutely black body (for example, absorption bands of carbon dioxide gas around 15 microns). The corresponding relative errors are little dependent upon the magnitudes of absorption (see  $\overline{\Delta F_{\uparrow}}$  at  $i = 3$  in Table 1). The maximum absolute errors of counter-radiation originating as a consequence of errors of humidity are observed at average magnitudes of the absorption function. We will remember that the absorption function has average values of about 0.3-0.7 in the central regions of the absorption bands at small magnitudes of the absorbing mass, at the edges of the absorption bands at large and average magnitudes of the absorbing mass, in the "atmospheric windows" at large magnitudes of the absorbing mass. Consequently, the altitude of the level where the maximum absolute errors of radiation are observed depends upon the vertical distribution of the absorbing substances in the atmosphere and upon the absorption function in the spectrum interval under consideration. The corresponding relative errors increase with an increase in the "transparency" of the spectral section (see  $\Delta F_{\uparrow}$  at  $i = 2$  in Table 1).

In considering the errors of the spectral fluxes of ascending thermal radiation, we see that  $\Delta F_{\uparrow}$  varies with altitude considerably less than  $\Delta F_{\downarrow}$ . Errors of humidity (even of the order of 10%)

in the lower troposphere have practically no effect on the magnitudes of  $F\uparrow$ . With altitude, the effect of  $\Delta U$  on  $\Delta F\uparrow$  increases somewhat. A comparison of the characteristic features of the variation of  $\Delta F\uparrow$  with altitude in various spectral intervals indicates that errors of temperature in the "atmospheric windows" and errors of humidity at the average values of absorption have the greatest effect on ascending radiation fluxes. Relative errors of the spectral fluxes of ascending radiation in the majority of cases do not exceed 5%.

In all the spectral intervals considered the errors of the radiant influx of heat in the lower troposphere are small—of the order of 1-5%. However, they rapidly increase with altitude, and above 9-10 km already relative errors of the spectral influx exceeding 100% are observed. In this case the magnitudes of  $\Delta R$  are basically determined by the error of the humidity and depend little upon the error of temperature.

The relative magnitudes and the nature of the distribution of the errors of integral fluxes of thermal radiation have a similarity with errors in the spectral interval with moderate absorption (for example, in the interval of 1300-1250  $\text{cm}^{-1}$ ). To an altitude of 6-7 km the magnitudes of  $\Delta F\downarrow$  and  $\Delta F\uparrow$  are comparatively small (even at  $\Delta T = 2^\circ$  and  $\Delta U = 10\%$  the values of  $\Delta F\downarrow$  do not exceed 10%). However, in the upper atmosphere in a number of cases very large values of the errors of integral counter-radiation are observed (see Table 2). In this case at altitudes  $z > 10$  km the effect of errors of temperature is negligible, and practically the only source of errors of  $\Delta F\downarrow$  are humidity errors. Errors in magnitudes of the ascending radiation are small and are almost independent of altitude.

We also note that the results given above agree well with the corresponding results of [6], where errors of the calculations of integral thermal radiation to an altitude of the order of 10 km were considered.

The values of integral radiant influxes of heat are very sensitive to errors of humidity. In models of the atmosphere where the magnitudes of  $\Delta U$  are considerable, the maximum of  $\Delta R$  around 10 km is observed, and in the lower troposphere and in the region of 20-30 km the values of the absolute errors of the influx are comparatively small; the corresponding magnitudes of relative errors ( $\Delta R$ ) in the upper troposphere and in the stratosphere exceed 100%. At small errors of humidity the magnitudes of  $\Delta R$  and  $\Delta F\downarrow$  are also small at all the altitudes in the atmosphere considered. <sup>37</sup>  
We should note that the relative errors of the integral influx are

considerably less than in the case of the individual spectral intervals considered in the given work.

The results of this work demonstrate that the accuracy of measurement of the atmospheric temperature that is obtainable at the present time (of the order of  $0.5-1.0^\circ$ ) is entirely satisfactory for the calculation of fluxes and influxes of the integral thermal radiation of the atmosphere. However, an increase in the accuracy of the measurement of the characteristics of humidity is necessary, especially in the upper atmosphere: while in the lower atmosphere the absolute error of the relative humidity,  $\Delta U = \pm 10\%$ , which makes it possible to obtain integral fluxes of radiation and radiant heat influxes with an accuracy of about 5-10%, above 8-10 km such an accuracy can be obtained in the radiation values only in a case when the relative error of the humidity  $\Delta U/U \leq 10\%$ . For determination of the spectral distribution of fluxes and influxes of radiation it is desirable to have initial meteorological data of even higher accuracy ( $\Delta T < 0.5^\circ \text{ C}$ ,  $\Delta U/U < 5\%$ ). Therefore, an increase in the reliability of the measurement of the content of water vapor and temperature in the atmosphere is one of the urgent problems of meteorology.

## REFERENCES

1. Kondrat'yev, K. Ya., *Aktinometriya (Actinometry)*, Leningrad, Gidrometeoizdat, 1965.
2. Marfenko, O.V., "Random errors of the RZ-049 radiosonde", *Trudy TsAO*. No. 22, 1957.
3. Marfenko, O. V., "Accuracy of temperature-wind sounding of the atmosphere", *Trudy Vses. nauchnogo meteorol. soveshchaniy (Proceedings of the All-Union Scientific Meteorological Conference)*, Vol. 9, Leningrad, 1963, pp. 118-124.
4. Kondrat'yev, K. Ya., Kh. Yu. Niylik, and R. Yu. Noorma, "On the spectral distribution of radiation influxes of heat in the free atmosphere", *Izv. AN SSSR, seriya FAO*, 11, No. 2, 1966.
5. Niylik, Kh. Yu., "On the dependence of the results of calculation of fluxes of thermal radiation of the atmosphere upon the errors of initial meteorological data", *Collection: Radiatsiya v atmosfere (Radiation in the Atmosphere)*, IFA AN ESSR, Tartu, 1969.
6. Kostyanoy, G.N. and Kh. Yu. Niylik, "Comparison of measured and calculated values of fluxes of long-wave radiation in the atmosphere," *Trudy TsAO*, No. 83, 1969.

Kh. Yu. Niylik

On the basis of refs. [1-3], below brief conclusions are given, obtained in the investigation of the possibilities of the calculation of fluxes of counter-radiation in broken cloud cover and the determination of magnitudes of thermal radiation of the atmosphere averaged throughout large territories. With this, an estimate of the accuracy of the proposed methodology of the calculations is given.

1. The effect of clouds on the counter-radiation of the atmosphere at the earth's surface depends considerably upon the moisture content and temperature of the atmosphere under the cloud. The appearance of clouds increases counter-radiation by 20-30%, on the average.

2. With a black model of the cloud, the thermal radiation of the lateral parts of the cloud, arriving at the earth's surface, may be calculated with a good accuracy as the radiation of their imaginary projection from the point of observation to the level of the lower boundary of the cloud at the temperature of this level. In other words, instead of a real cloud we may consider a plate, the dimensions of which depend upon the dimensions and upon the zenith angle of the cloud, and the radiation is equal to the radiation of a black body at the temperature at the level of the lower boundary of the cloud.

3. The closer the cloud zone to the horizon the less its effect on the magnitude of the counter-radiation of the atmosphere is felt. If the quantity of cloud cover  $n < 3$  and the cloud ring is located at the very horizon, the counter-radiation of the atmosphere shows practically no difference from the counter-radiation of a clear sky.

4. The linear dependence of fluxes of counter-radiation upon the degree of cloud cover occurs only in a case when the clouds are uniformly distributed with respect to the zenith angle. In the cloud cover located either at the horizon or near the zenith, the dependence of the counter-radiation upon  $n$  is nonlinear.

5. The variation of the altitude of the lower boundary of clouds, as a rule, affects the magnitudes of the ground counter-radiation of the atmosphere much less than seasonal variations of the meteorological characteristics of the atmosphere.



6. For calculations of counter-radiation for a given distribution of clouds in ring zones of the sky the following formula is recommended:

$$F \downarrow = \sum_{j=0}^k \left[ n_j \int_{\vartheta_j}^{\vartheta_{j+1}} J_n'(\vartheta) \sin \vartheta \cos \vartheta d\vartheta + \right. \\ \left. + (1 - n_j) \int_{\vartheta_j}^{\vartheta_{j+1}} J_0(\vartheta) \sin \vartheta \cos \vartheta d\vartheta \right]. \quad (1)$$

Here the sky is divided into  $k$  zones, the boundaries of which /39 are determined by the zenith angle of  $\vartheta_j$  and  $\vartheta_{j+1}$ . In each zone the degree of cloud cover must be known ( $10 n_j$ ) and the magnitudes of the radiations intensity for clear sky and entirely overcast sky (the values are  $J_0(\vartheta)$  and  $J_n(\vartheta)$ ). Thus in the given case very detailed initial data is required, and the corresponding calculations are quite cumbersome.

7. When  $k = 2$ , i.e., with consideration of the quantity of clouds individually in two zones (at intervals of the zenith angle  $\vartheta$  from  $0-60^\circ$  and from  $60-90^\circ$ ) the calculation error  $F \downarrow$  according to formula (1) is small—in the majority of cases it does not exceed 3% [1].

8. Finally, a simple formula

$$F \downarrow = n F_n \downarrow + (1 - n) F_0 \downarrow$$

makes it possible to calculate the counter-radiation of the atmosphere with a consideration of the quantity of clouds, regardless of their arrangement throughout the sky, with an error relative to the calculations according to formula (1) of the order of 5-10% (here  $F_n \downarrow$  is the counter-radiation with an entirely overcast sky,  $F_0 \downarrow$  is the counter-radiation with an entirely clear sky).

9. For the calculation of the averaged values of the counter-radiation  $\bar{F}_\Lambda \downarrow$  throughout the territory  $\Lambda$ , the following formula is proposed:

$$\bar{F}_\Lambda \downarrow = (1 - \bar{n}_\Lambda) F_0 \downarrow + \bar{n}_\Lambda F_n \downarrow, \quad (3)$$

where  $\bar{n}_\Lambda$  is the averaged quantity of relative cloud cover throughout the territory  $\Lambda$ . The calculation schemes for the determination of  $\bar{n}_\Lambda$  are given in refs. [4] and [III.25].

Formula (3) was derived under the assumption that over the territory  $\Lambda$  the meteorological characteristics of the atmosphere in a horizontal direction do not vary or vary only weakly. In the latter case the quantities  $F_0 \downarrow$  and  $F_n \downarrow$  are calculated on the basis of the average vertical distributions of temperature, pressure, and humidity for the given region.

10. At large gradients of the horizontal variation of the meteorological parameters it is advisable to divide the territory  $\Lambda$  into parts  $\Lambda_i$  and to determine the average value of the radiation flux for each of them [according to formula (3)]. The total averaged value of the counter-radiation is then calculated according to the formula

$$\bar{F}_{\Lambda} \downarrow = \frac{1}{\Lambda} \sum_i \bar{F}_i \downarrow \Lambda_i. \quad (4)$$

11. If data are lacking for calculation of the averaged values of the relative cloud cover then  $\bar{F} \downarrow$  are calculated according to formula (3) [or according to (3) and (4)] with the use of the corresponding magnitude of the absolute cloud cover  $n_0$  instead of  $\bar{n}_{\Lambda}$  [2]. Our estimates demonstrate that in calculation according to the approximate formula (3) with the use of  $\bar{n}_{\Lambda}$  we obtain somewhat exaggerated values of  $\bar{F}_{\Lambda} \downarrow$ , and with the use of  $n_0$ , somewhat understated values. We note that both variations give practically the same results at the following conditions: 1) the quantity of absolute cloud cover is greater than a scale of 6-8, 2) at any value of  $n_0$  if the vertical thickness of the clouds does not exceed 0.1-0.2 km and the dimensions of the clouds are not too small.

12. According to formulas (3) and (4) we may also determine the averaged magnitudes of the fluxes of ascending and effective thermal radiation, and on the basis of these results estimate the averaged values of the radiation influxes of heat. However, in the free atmosphere at the level of the clouds and above the clouds, where the effect of the horizontal heterogeneity of the atmosphere is already significant, the accuracy of the determination of the averaged magnitudes of thermal radiation according to formulas (3) and (4) is certainly less than near the earth's surface.

# REFERENCES

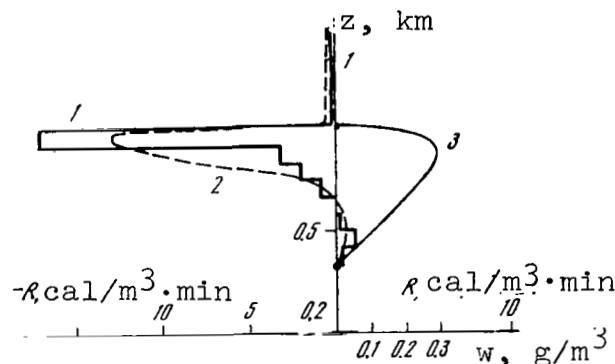
1. Niylik, Kh. Yu., "On calculations of thermal radiation of the atmosphere in conditions of partial cloud cover," Izv. AN SSSR, seriya FAO, 4, No. 4, 1968.
2. Niylik, Kh. Yu., "On the calculation of magnitudes of fluxes of counter-radiation of the atmosphere averaged throughout large territories," Izv. AN SSSR, Fizika atmosfery i okeana, 4, No. 5, 1968.
3. Avaste, O. A. and Kh. Yu. Niylik, "On the calculation of averaged magnitudes of short-wave and long wave fluxes and influxes of radiation in the real atmosphere," Trudy Vses. konferentsii po obshchey tsirkulyatsii atmosfery, Tbilisi, noyabr' 1968 (Proceedings of the Conference on the General Circulation of the Atmosphere, Tbilisi, November 1968), Izd. Mezhdunarodnogo geofizicheskogo komiteta pri Prezidiume AN SSSR, 1970.
4. Niylik, Kh. Yu., Yu. R. Mullamaa, and M. A. Sulev, "On the coverage of the sky with clouds," Collection: Radiatsiya i oblachnost' (Radiation and Cloudiness), IFA AN ESSR, Tartu, 1969.

VERTICAL PROFILES OF FLUXES OF LONG-WAVE RADIATION  
IN A CLOUDY ATMOSPHERE  
(Measurements and Calculations)

N. I. Goysa, V. D. Oppengeym, and Ye. M. Feygel'son

In the Southwest Ukraine region in the spring of 1967 a series of measurements of long-wave radiation fluxes and the effective radiation in cloud conditions during the day and the night was conducted. The measurements were conducted to an altitude of 3-4 km from an IL-14 aircraft by means of two independently calibrated instruments of different design: a Yanishevskiy balance gauge and radiation thermoelements (RTE) designed by B. P. Kozyrev. The RTE detectors made it possible to measure fluxes of incident  $F_{\downarrow}$  and ascending  $F_{\uparrow}$  long-wave radiation separately. In the free atmosphere actinometric measurements were conducted at intervals of  $\Delta z = 1000$  m and near the cloud boundaries and within the clouds at  $50 \text{ m} \leq \Delta z \leq 100 \text{ m}$ . Simultaneously, the altitude of the upper boundary of the cloud layer was determined, its thickness, the distribution of the absolute humidity within the cloud was measured, and also the distribution of the temperature and humidity with respect to altitude. The methodology of the measurements and the processing of the data are described in detail in refs. [1,2]. A comparison of the magnitudes of effective radiation, obtained by means of the Yanishevskiy balance gauge and the RTE demonstrated that no noticeable systematic differences are observed between the values of  $F$  obtained simultaneously by means of these instruments. The mean square deviation of the absolute magnitudes of the effective radiation, measured by the two instruments, amounts to  $\pm 0.022 \text{ cal per cm}^2 \text{ min}$  (with an average value of  $F = 0.15 \text{ cal/cm}^2 \text{ min}$ ), which agrees with the limits of accuracy of measurement of  $F$  of each of the instruments. Since the volume of experimental data is not great, this conclusion should be considered as preliminary. /41

On the basis of 25 vertical profiles of the effective radiation in one-layer St clouds, an experimental radiation model of the "average stratoformous cloud" was constructed. The method of construction and the basis parameters of this model are described in refs. [2,3]. The nature of the distribution of  $R$  in such an average cloud and above it is presented in the drawing, from which it is apparent that in the atmosphere above the cloud the radiation influx  $R$  of heat amounts to  $-0.3 \text{ cal/cm}^3 \text{ min}$  on the average, i.e., of the same order of magnitude as in a clear sky, somewhat exceeding the latter. Within the cloud the upper 50-meter layer is the most active. Here the radiation influx  $R_{v.g}$  amounts to  $-17.4 \text{ cal/m}^3 \text{ min}$  on the average. In the next 50-meter layer,  $R$  /42



Profiles of radiation cooling.

- 1- influx calculated according to average experimental data;
- 2- influx calculated according to average values of  $T$ ,  $\rho_v$ , and  $\rho_w$ ;
- 3- average profile of absolute humidity.

decreases to a fifth of its former figure, and amounts to  $-3.2 \text{ cal/cm}^3 \text{ min}$ . Then follows a layer of 150 m where  $R \approx 0$ . And, finally, at a depth of 300-350 m from the upper boundary of the cloud a radiation heating is observed, and the influx  $R_{n.g}$  here amounts to  $+0.4 \text{ cal/m}^3 \text{ min}$  on the average.

The radiation influx of heat to the "average cloud" as a whole amounts to  $-0.110 \text{ cal/cm}^3 \text{ min}$ , and 80% of the entire radiation cooling falls to the share of the upper 100 m.

Because of the complex of measurements described above, it turns out to be possible to perform calculations of the radiation fluxes and influxes according to a well-known methodology [4,5] by means of the integral transmission function of a cloudy atmosphere [6] and to compare the results of the calculations with data from measurements. The calculations of the influx according to average values of  $T$ ,  $\rho_v$ ,  $\rho_w$ , presented in the drawing turned out to be in good agreement with the average experimental model. A comparison of several individual examples of measurements and calculations demonstrated their good agreement for ascending fluxes at  $z \leq 3 \text{ km}$  and descending fluxes inside the cloud: the difference between the calculation and the measurements turned out to be of the order of 6%, on the average. The divergence in the magnitudes of the measured and calculated downflows reaches 15% at  $1 \text{ km} \leq z \leq 3 \text{ km}$ . Possible causes of this divergence are discussed in [2,7].

Influxes calculated according to the data from measurements given above and calculations near the upper boundary of the cloud ( $R_{v.g}$ ) and in the 1-3 km layer ( $R_{sl}$ ) are presented in the table.

$R_{sl}$	$R_m$ $R_{cal}$	10 Mar.	11 Mar.	12 March (by night)
		18.0 19.4	9 17.6	18.0 15.3
$R$	$R_m$	0.24	0.22	0.38
$1\text{ km} \leq z \leq 3\text{ km}$	$R_{cal}^m$	0.22	0.26	0.33

The table shows the good correspondence of  $R_m$  and  $R_{cal}$  in the layer above the cloud and the possibility of essential differences near the upper boundary. Nevertheless, even here the calculations correctly determine the order of  $R_{v.g}$  and make it possible to establish that in comparison with a cloudless atmosphere the influx at the upper boundary increases by two orders of magnitude.

The investigation performed demonstrates the possibility of the study of the radiation regime of stratoformous clouds and tropospheric layers with a thickness of 1-2 km by means of the individual units of actinometric instruments (Yanishevskiy balance gauges and RTE detectors).

1. Goysa, N. I., "Methodology of actinometric measurements from an IL-14 aircraft", Trudy Ukr. NIGMI, No. 55, 1966.
2. Goysa, N. I., V. D. Oppengeym, and Ye. M. Feygel'son, "Vertical profiles of fluxes of long-wave radiation in a cloudy atmosphere—measurements and calculations", Izv. AN SSSR, seriya FAO, No. 2, 1970.
3. Goysa, N. I., "An experimental model of the radiation regime of an 'average' stratoformous cloud", Trudy Ukr. NIGMI, in press.
4. Kondrat'yev, K. Ya., Aktinometriya (Actinometry), Leningrad, Gidrometeoizdat, 1965.
5. Feygel'son, Ye. M., "Influx of long-wave radiation in the cloudy conditions", Izv. AN SSSR, seriya FAO, No. 5, 1968.
6. Gradus, L. M., Kh. Yu. Niylik, and Ye. M. Feygel'son, "The integral transmission function for cloudy conditions", Izv. AN SSSR, seriya FAO, No. 4, 1968.
7. Kostyanoy, G. N. and Kh. Yu. Niylik, "Comparison of measured and calculated values of fluxes of long-wave radiation in the atmosphere", Trudy TsAO, No. 83, 1969.

## II. SHORT-WAVE RADIATION

### TRANSFER OF SOLAR RADIATION IN THE ATMOSPHERE

O. A. Avaste

In this article a survey is given of the basic results in the investigation of fluxes and influxes of solar radiation obtained by the author and described in more detail in refs. [1-6], [II.2].

In the statement of the problem, regions of visible and infrared radiation were considered separately, with a consideration of the factors considered in Table 1 in each specific case.

TABLE 1

Spectral region	Wavelength	Scattering considered	Absorption
visible	$0.3 < \lambda \leq 0.7 \mu$	multiple	not considered
near infrared	$0.7 < \lambda \leq 4 \mu$	one-time	spectral absorption by H <sub>2</sub> O and CO <sub>2</sub> gases considered

Absorption by ozone (the Chapuis bands) in the 20-60 km layer was considered by means of assigning the spectral "sub-zone" of the solar constant [1,7,8].

Scattering in molecules of air and in an aerosol was considered by assignment of the spectral optical thicknesses and the scattering indicatrix averaged for the entire column of the atmosphere [1].

In the near infrared region, absorption by water vapor and carbon dioxide gas plays an important part. In the work the spectral transmission functions of these gases were used.

A method was developed for calculating the spectral distribution of direct solar and scattered radiation, and also influxes at various altitudes [1-5]. The effect of the pressure varying in the beam path on the absorption function was considered by means of the parameter  $x_z$ , determined by the formula



$$r_z = \int_z^\infty [P(z) + l(z)]^n \rho(z) dz \left/ \left[ \int_z^\infty \rho(z) dz \right]^{1/2} \right. \quad (1)$$

Here  $\rho(z)$  (in  $\text{g/cm}^3$ ) is the concentration of the absorbing gas at the altitude  $z$ ;  $n$  is a constant;  $n(\text{H}_2\text{O}) = 0.3$ ;  $n(\text{CO}_2) = 0.4$ ;  $P$  (in mm Hg) is the atmospheric pressure;  $l$  (in mm Hg) is the partial pressure of the absorbing gas. /45

The absorption function  $A(x_z)$  for individual absorption bands of  $\text{H}_2\text{O}$  and  $\text{CO}_2$  gases is given in ref. [2].

The basic characteristics of the average standard model of the atmosphere used are: volumetric concentration of carbon dioxide gas constant (0.033% by volume), concentration of aerosol decreases exponentially as a function of altitude, total optical thickness (aerosol + air molecules)  $\tau^* = \tau(\lambda_0) = 0.3$  at  $\lambda_0 = 0.55$  microns, quantity of ozone 0.25 atm/cm, content of water vapor in the vertical column of the atmosphere  $m_v = \int_0^\infty \rho_v(z) dz = 2.1$ , in cm where  $\rho_v$  is the density of the water vapor.

Cloudless atmosphere. We will give certain results of [2-5]. The magnitude of the solar energy absorbed in the entire column of the atmosphere depends upon the general content of the water vapor, the altitude of the sun, and the optical thickness of the atmosphere, but is almost independent of the distribution of water vapor with altitude. In the calculation of the vertical distribution of the radiation heating of the air, it is necessary to consider the distribution of layers of water vapor as a function of altitude. At an average content of the water vapor in the atmosphere ( $w = 2.1$  cm) in the 0-20 km layer the absorbed direct solar radiation amounts to about 12% of the incident solar radiation from outside the atmosphere, with a variation of the zenith angle of the sun from 0 to 60 degrees. Radiation heating  $dT/dt$  for the average standard model at individual levels in the 0-20 km layer does not exceed 0.08 degree/hr. With a stratified distribution of the water vapor in the atmosphere, radiation heating may reach 3.0 degrees/hr in individual layers. In Fig. 1 the distribution of the quantity  $dT/dt$  for various contents of  $m_v$  and distributions of water vapor with altitude is given.

Absorption of scattered radiation  $\Delta D$  is small in comparison with absorption of direct solar radiation— $\Delta S'$  at a low albedo of

the earth's surface (for example, in the case of the sea). In Table 2 these quantities are compared at  $A = 6\%$ , which corresponds to the albedo of the sea for incident scattered radiation.

TABLE 2

$\vartheta$ , degrees	0	20	40	60	80
$\Delta S'$ , millical/cm <sup>2</sup> .min	234.7	224.2	192.9	140.0	95.9
$\Delta D$ , millical/cm <sup>2</sup> .min	9.2	9.0	7.9	8.7	9.0

The total flux  $Q_{ir}$  (direct solar + scattered radiation) in the near infrared region essentially depends upon the atmosphere of the mass. This dependence is represented in Fig. 2. The result of spectral calculations is designated by solid lines, and the magnitudes of  $Q_{ir}$  calculated according to the approximation formula recommended in [II.2] are designated by points, circles, and crosses.

/46

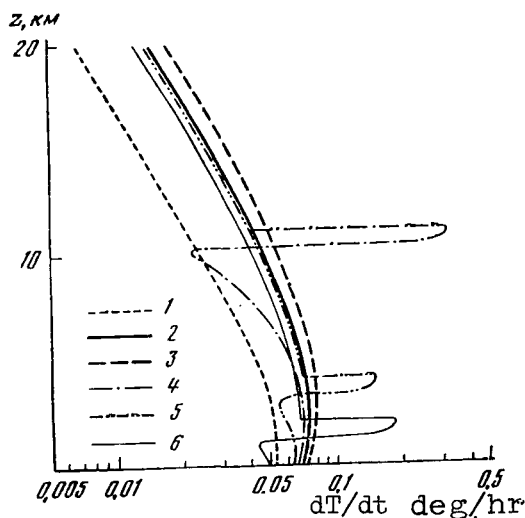


Fig. 1. Heating of the air due to absorption of direct solar radiation in the presence of layers of water vapor. 1-3) exponential decrease of the decrease of water vapor with altitude: 1)  $m_v = 0.5$  cm,  $\tau^* = 0.2$ ; 2)  $m_v = 2.1$  cm,  $\tau^* = 0.3$ ; 3)  $m_v = 3.0$ ,  $\tau^* = 0.5$ ; 4)  $\rho_v = 0.068 \cdot 10^{-5}$  g/cm<sup>3</sup>;  $10 < z < 11$  km; 5)  $\rho_v = 0.21 \cdot 10^{-5}$  g/cm<sup>3</sup>,  $3 < z < 4$  km; 6)  $\rho_v = 0.68 \cdot 10^{-5}$  g/cm<sup>3</sup>,  $1 < z < 2$  km; for the curves 4-6  $\tau^* = 0.3$ .

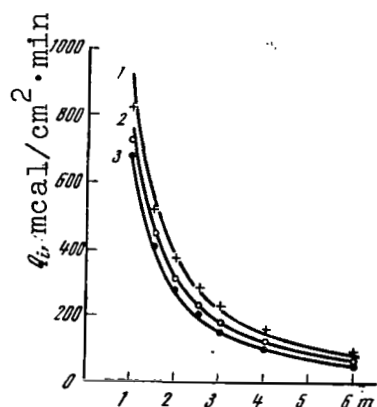


Fig. 2. Dependence of the total radiation flux in the near infra-red region upon the atmospheric mass. 1) optical thickness  $\tau^* = 0.2$ ;  $\lambda_0 = 0.55 \mu$ , content of water vapor  $m_v = 0.5$  cm; 2)  $\tau^* = 0.3$ ;  $m_v = 2.1$  cm; 3)  $\tau^* = 0.5$ ;  $m_v = 3.0$  cm; 3) quantities calculated according to approximation formula (3) of ref. [II.2] in cases 1, 2, 3, respectively.

The methods developed make it possible to calculate the daily sums of absorbed solar radiation in the atmosphere in a clear sky [3]. The isophotes of the direct solar radiation absorbed during the day (calories/cm<sup>2</sup> day) by seasons are given in Fig. 3.

The calculations given in ref. [5] demonstrated that in the use of the average value of the cosine of the zenith angle of the sun for a given calendar day determined by the equality

$$\overline{\cos \theta_0} = 1/\bar{m} = \frac{1}{t_n} \int_0^{t_n} \frac{dt}{m(t)},$$

we get values of  $\bar{Q}$  exceeding the magnitudes found by direct integration according to the formula

/48

$$Q = 2 \int_0^{t_n} \Delta S' [w, m(t)] dt. \quad (2)$$

Here  $t_n$  is the time of noon;  $\Delta S' [w, m, (t)]$  is the absorbed direct solar radiation for atmospheric mass  $m(t)$ . The ratio of the quantities  $\bar{Q}/Q$  for various values of the sun's declination  $\delta$  and the geographical latitude  $\phi$  is given in Table 3.

From Table 3 it is apparent that the use of the average value of  $\cos \theta_0$  leads to the greatest distortion of the quantity  $Q$  in winter in the high latitudes.

The diurnal sums of absorbed direct solar radiation in the atmosphere of the summer hemisphere amounts to about one-quarter

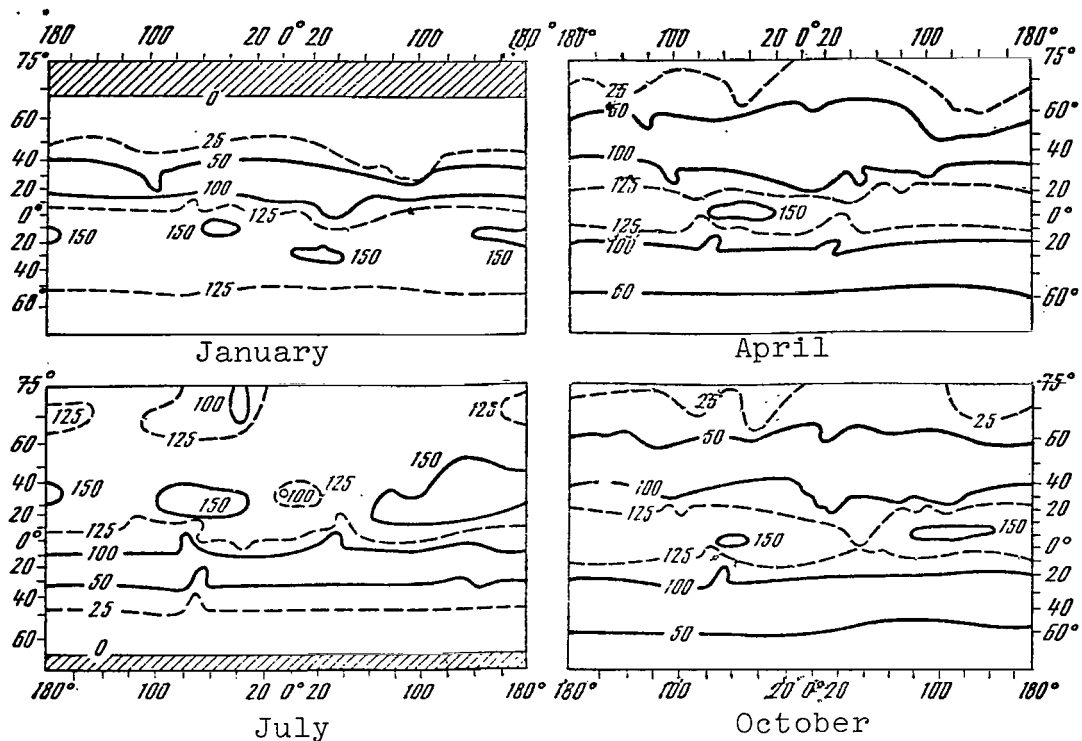


Fig. 3. Isolines of diurnal sums of absorbed direct solar radiation ( $\text{cal}/\text{cm}^2 \text{ day}$ ) in the atmosphere for four seasons (distribution of water vapor  $\rho_v$  taken from ref. [10]).

of the diurnal sums of the direct solar energy absorbed in the entire system consisting of the earth and the atmosphere; they are comparable with the diurnal sums of the radiation balance of the troposphere.

TABLE 3

$\delta$	$\alpha$ , degrees			$\delta$	$\alpha$ , degrees		
	15	45	75		15	45	75
$-23^\circ 27'$	1.16	1.35	—	$+10^\circ$	1.06	1.06	1.08
$-10^\circ$	1.08	1.11	1.6	$+23^\circ 27'$	1.03	0.99	0.99

In the winter hemisphere (in the spring and autumn) the absorption of direct solar radiation in the atmosphere decreases rapidly with an increase in latitude.

Cloudy conditions. Consideration of cloud layers leads to the necessity of introducing a number of additional parameters: the thickness of the layer, altitude of its lower boundary, spectral absorption and scattering factors, scattering indicatrices in the cloud, its optical thickness and others. In broken cloud cover we should consider also the quantity of clouds, on a scale of ten, and the structural parameters of the field of the clouds (for example, the distribution of the dimensions of the clouds and the distribution of the clouds throughout the sky).

In a case of cirrus clouds with a given albedo of the upper boundary of the clouds, the calculation of the flux and influx over the cloud is conducted in the same way as in a clear sky. In the calculation of these quantities under the cloud the following additional parameters are considered: 1) the brightness of the lower boundary of the cloud, 2) the spectral albedo of the underlying surface, 3) the optical thickness of the layer under the cloud, 4) the scattering indicatrix of the layer under the cloud, 5) the height of the lower boundary of the clouds, 6) the content of the water vapor in the layer under the cloud, 7) the distribution of water vapor in the layer under the cloud. /49

In the definition of spectral fluxes in the layer under the cloud at an altitude  $z$ , the following components of scattered radiation were considered: radiation emitted from the lower boundary of the clouds, respectively the flux  $D \downarrow^{(0)}(z)$ , reflected from the underlying surface,  $D \uparrow^{(0)}(z)$ ; scattered once downward,  $D \downarrow^{(1)}(z)$ ; reflected and scattered downward  $D \downarrow^{(*)}(z)$ ; reflected and scattered upward,  $D \uparrow^{(*)}(z)$ .

The total fluxes of descending and ascending radiation are equal to

$$\left. \begin{aligned} D \downarrow(z) &= D \downarrow^{(0)}(z) + D \downarrow^{(1)}(z) + D \downarrow^{(*)}(z), \\ D \uparrow(z) &= D \uparrow^{(0)}(z) + D \uparrow^{(1)}(z) + D \uparrow^{(*)}(z). \end{aligned} \right\} \quad (3)$$

The influxes to the layer  $(z, z_1)$  are calculated according to the formula

$$\Delta D(z, z_1) = D \downarrow(z) - D \downarrow(z_1) + D \uparrow(z_1) - D \uparrow(z). \quad (4)$$

The integral fluxes and influxes are obtained by the summation of the corresponding spectral quantities.

We will give certain results of the calculation of the transfer of radiation in a cloudy atmosphere.

1. For the brightness factor of the lower boundary of the clouds, the following formula is obtained [4]:

$$\delta(\delta_0, \theta, A) = 0.4 \delta(\delta_0, 0, 0) \{ (1 - 1.5 \cos \theta) [1 - f(A)] + 0.5 f(A) [4 + (3 - \kappa_1) \tau_0] \}, \quad (5)$$

where

$$f(A) = 4A [4 + (3 - \kappa_1) (1 - A) \tau_0]^{-1}. \quad (6)$$

Here  $\tau_0$  is the optical thickness of the clouds;  $\kappa_1$  is the elongation of the indicatrix [7];  $A$  is the albedo of the underlying surface;  $\delta(\delta_0, 0, 0)$  is the brightness of the cloud at the zenith;  $\delta_0$  is the spectral transmission function of the cloud, taken from monograph [8].

Calculations according to this formula made it possible to establish the following facts.

With a growth of the length of the scattering indicatrix in the cloud the brightness of the lower boundary of the cloud increases. At low albedos of the underlying surface, a strong decrease of the lower boundary of the clouds at the horizon is observed. With a growth of the albedo of the underlying surface, the brightness of the lower boundary of the clouds approaches the brightness of an orthotropic surface, i.e., it does not depend upon the sighting angle. In cirrus cloud cover fogginess of the layers outside the cloud has little effect on the magnitude of the flux of solar radiation arriving at the earth's surface.

Cloud cover has an appreciable effect on the distribution of the absorbed short-wave radiation in the atmosphere; a qualitative picture of the vertical distribution of the influx resembles the distribution in a clear sky in a case of a sharply expressed layer of water vapor (see Fig. 1). However, the radiation absorbed by the cloud exceeds the radiation absorbed by the layer of water vapor, due to an increase in the beam path by multiple scattering inside the cloud. /50

The reflection indicatrix of the clouds has a strong maximum in the direction of mirror reflection (a sun track). In radiation departing beyond the limits of the atmosphere, this maximum is smoother due to absorption and scattering by the layers of the atmosphere above the clouds, [9].

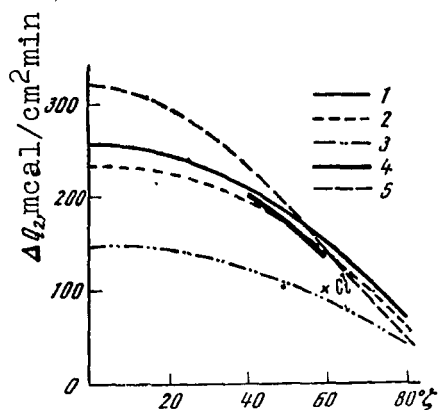


Fig. 4. Dependence of the solar radiation absorbed in the atmosphere upon the zenith angle of the sun. 1) cloudless atmosphere  $m_v=0.5$  cm,  $\tau^*=0.2$ ; 2) the same,  $m_v=2.1$  cm,  $\tau^*=0.3$ ; 3) the same,  $m_v=3.0$  cm,  $\tau^*=0.5$ ; 4) author's calculation, St clouds,  $\tau_0=30$ ,  $z_{n.g.}=1$  km,  $\Delta z=2$  km, spectral transmission according to ref. [8]; 5) according to [16], Cu clouds,  $\tau_0=20$ ,  $z_{n.g.}=1$  km,  $\Delta z=1$  km; cross indicates Ci clouds, albedo according to [12].

Cloud cover increases absorption in the layer above the clouds due to the strong reflection of radiation from the clouds. As a consequence of the great reflecting capability of the clouds, we should consider the effect upon non-orthotropic reflection of radiation in distinction from the case of reflection of the sea surface described above [9]. Absorption of the mirror component of solar radiation turns out to be considerable in high geographical latitudes, where the zenith angle of the sun is great.

The general concept of the dependence of the solar radiation absorbed in the atmosphere upon the zenith angle of the sun is given by Fig. 4. For low values of the zenith angles of the sun in the presence of clouds, the solar radiation absorbed exceeds the average absorption of a cloudless atmosphere by a factor of 1.2-1.5. At large zenith angles of the sun ( $\vartheta > 60^\circ$ ) in a cloudy atmosphere, less solar radiation is absorbed than in a cloudless atmosphere.

Certain data concerning the absorption of solar radiation in the column of the atmosphere, in  $\text{cal/cm}^2 \cdot \text{min}$ , are given in Table 4. Here  $z_{n.g.}$  is the altitude of the lower boundary of the clouds,  $\Delta z$  is the thickness of the cloud layer. In our calculations the

spectral transmission function and the albedo for St and As clouds were taken from monograph [8], and for Ci cloud from refs. [11,12].

TABLE 4

/51

$\vartheta_{\odot}$	$x = 2,1 \text{ cm}$ $\tau = 0,3 \text{ cm}$	From ref. [11]				Author's calculations		
		$z_{n,g} = 0,8 \text{ km}$ $\Delta z = 0,5 \text{ km}$	$z_{n,g} = 0,8 \text{ km}$ $\Delta z = 0,2 \text{ km}$	$z_{n,g} = 1 \text{ km}$ $\Delta z = 0,3 \text{ km}$	$z_{n,g} = 1 \text{ km}$ $\Delta z = 1 \text{ km}$	St. $\tau_0 = 30$	As. $\tau_0 = 6$	Ci. $\tau_0 = 6$
						$z_{n,g} = 1 \text{ km}$ $\Delta z = 2 \text{ km}$	$z_{n,g} = 2 \text{ km}$ $\Delta z = 1 \text{ km}$	$z_{n,g} = 6 \text{ km}$ $\Delta z = 0,5 \text{ km}$
40°	0,193	0,204	0,192	0,193	0,234	0,205	0,205	
60°	0,140	0,135	0,128	0,129	0,140	0,132	0,138	0,121

In the layer under the cloud considerably less solar radiation is absorbed than in the same layer in a clear sky ( $\Delta Q_{\text{clear}}$ ). The ratio of  $\Delta Q_{\text{cloud}}/\Delta Q_{\text{clear}}$  is given in Table 5. Here  $\Delta Q_{\text{cloud}}$  is absorption in clouds in the layer indicated.

TABLE 5

$\vartheta_{\odot}$ , degrees	40	60
$\tau_0 = 30$ , St, 1-3 km	1.85	1.21
Layer under cloud 0-1 km	0.32	0.18
$\tau_0 = 6$ , As, 2-3 km	2.47	3.90
Layer under cloud 0-2 km	0.59	0.17
$\tau_0 = 6$ , Ci, 6-6.5 km	-	11.88
Layer under cloud 0-6 km	-	0.20

The radiation absorbed in the layer under the cloud depends slightly upon the albedo of the underlying surface, since the contribution of reflected radiation to absorption under the clouds is small.

A more complex problem is the calculation of the flux and influx for broken cloud cover. In this case we must determine the averaged values of the flux and influx throughout the territory.



In the work two characteristics of cloud cover were used: relative cloud cover  $\bar{n}_\Lambda$  determined by means of projecting the clouds onto an imaginary hemisphere, the center of which is an observer on the earth's surface, and the absolute cloud cover  $n_0$ , determined by means of projecting the clouds onto a horizontal surface. The flux is created by three components: direct solar radiation  $S$ , radiation  $D_n$  scattered by the clouds, and radiation  $D_c$  scattered by the molecules of air and aerosols, and may be described by the formula

$$Q = SP(\vartheta_\odot) + \bar{n}_\Lambda D_n + (1 - \bar{n}_\Lambda) D_c. \quad (7)$$

Here  $P(\vartheta_\odot)$  is the probability of a free line of visibility in the /52 direction of the sun;  $\bar{n}_\Lambda$  is the averaged quantity of the relative cloud cover throughout the territory.

We note that the probability of a free line  $\Lambda$  of visibility averaged throughout the territory is associated with the relative cloud cover by the formula

$$\bar{n}_\Lambda = 1 - \int_{2\pi} \overline{P_\Lambda(w)} dw. \quad (8)$$

The quantities  $\bar{n}_\Lambda$  and  $\overline{P_\Lambda(w)}$  depend upon the structure of the cloud elements (i.e., upon the altitude and frequency of the distribution of the clouds in space).

The quantity of clouds determined from the earth's surface is greater than the quantity  $n_0$  determined from a satellite, since the terrestrial observer also sees the lateral parts of the cloud. In accordance with ref. [13] the values of the albedo of the system consisting of the earth and the atmosphere, obtained according to data from the "Nimbus-11" satellite in latitudes from  $50^\circ$  N to  $40^\circ$  S are smaller than the magnitudes calculated according to the climatic data concerning cloud cover. The estimates performed demonstrate that this divergence is explained by the different magnitudes of  $\bar{n}_\Lambda$  and  $n_0$ . With a cloud cover of 3-6 on a scale of 10, the divergences in the values of  $\bar{n}_\Lambda$  and  $n_0$  may reach 2-3 [14,15].

The average influx in broken cloud cover may be calculated according to the formula

$$\Delta Q(z, z_1, \theta_{\odot}) = P(\theta_{\odot}) \Delta Q_c(z, z_1) + [1 - P(\theta_{\odot})] \Delta Q_n(z, z_1), \quad (9)$$

where  $\Delta Q_c(z, z_1)$  and  $\Delta Q_n(z, z_1)$  are the vertical distributions of the influxes in a clear sky and in a cloudy sky.

# REFERENCES

1. Shifrin, K. S. and O. A. Avaste, "Fluxes of short-wave radiation in a cloudless atmosphere," Collection: Issledovaniya po fizike atmosfery (Research in Atmospheric Physics), No. 2, IFA AN ESSR, Tartu, 1960.
2. Shifrin, K. S. and O.A. Avaste, "The field of short-wave radiation in case of a clear sky," Geofisica Pura e Applicata, 53, 111, 101-110, 1962.
3. Avaste, O. A., "Influx of heat of solar radiation and total radiation flux on the surface of the sea," Collection: Issledovaniya radiatsionnogo rezhima atmosfery (Research on the Radiation Conditions of the Atmosphere), IFA AN ESSR, Tartu, 1967.
4. Avaste, O. A., "Influx of heat of short-wave radiation in a cloudless atmosphere," Collection: Aktinometriya i Atmosfer-naya Optika. Trudy Shestogo Mezhvedomstvennogo soveshchaniya po aktinometrii i optike atmosfery (Actinometry and Atmospheric Optics. Proceedings of the Sixth Interdepartmental Conference on Actinometry and Atmospheric Optics), June 1966, Tartu, Tallin, Izd-vo "Valgus," 1968.
5. Avaste, O. A., "Calculation of the direct solar radiation absorbed according to the measured distribution of the humidity of the atmosphere," Collection: Radiatsiya i oblachnost' (Radiation and Cloudiness), IFA AN ESSR, No. 12, 1969.
6. Avaste, O. A., "Spectral albedo of the basic types of underlying surfaces in the near infrared region of the spectrum," Collection: Issledovaniya po fizike atmosfery (Research on the Physics of the Atmosphere), No. 4, IFA AN ESSR, Tartu, 1963.
7. Sobolev, V. V., Perenos luchistoy energii v atmosferakh zvezd i planet (Transfer of radiant energy in the atmospheres of stars and planets), Moscow, Gos. izd-vo tekhn.-teor. literatura, 1956.
8. Felgel'son, Ye. M., Radiatsionnyye protsessy v sloistoobraznykh oblakakh (Radiation Processes in Stratoform Clouds), Izd-vo "Nauka," 1964.
9. Avaste, O. A., Yu. Mullamaa, and K. S. Shifrin, "The field of outgoing short-wave radiation in the visible and near infrared regions of the spectrum in a non-orthotropic underlying surface," Collection: Issledovaniya po Fizike Atmosfery (Research in the Physics of the Atmosphere), No. 6, IFA AN ESSR, Tartu, 1964.
10. Davis, P. A., "Tiros 3 radiation measurements and some adiabatic properties of the atmosphere," Mon. Wea. Rev., 93, No. 9, 535-545, 1965.

11. Blau, H. H. Jr., R. P. Espinola, and E. C. Reifenstein, "Near infrared scattering by sunlit clouds", Appl. Optics, 5, No. 4, 555-564, 1966.
12. McDonald, R. K., and R. W. Deltenre, "Cirrus infrared reflection measurements", J. Optical Soc. Amer., 53, No. 7, 860-868, 1963.
13. Raschke, E., "The radiation balance of the earth-atmosphere system from radiation measurements of the Nimbus II meteorological satellite", NASA Tech. Note TN D-4589, Washington, D.C., July, 1968.
14. Avaste, O. A., "Increase in cloud cover at the horizon in a case of ground observations", Collection: Radiatsiy i oblačnost' (Radiation and Cloudiness), IFA AN ESSR, Tartu, 1969.
15. Avaste, O. A., "Method of calculating the covering of the sky by the lateral parts of cloud elements", Collection: Radiatsiya v atmosfere (Radiation in the Atmosphere), IFA AN ESSR, No. 15, 17-37, 1969.
16. Korb, G., J. Michalowsky, and F. Möller, "Die Absorption der Sonnenstrahlung in der wolkenfreien und bewölkten Atmosphäre" (Absorption of Solar Radiation in the Cloudless and Cloudy Atmosphere), Beitr. Phys. Atm., 30, No. 1, 63-77, 1957.

# ON THE CALCULATION OF THE INTEGRAL FLUX AND INFLUX OF SOLAR RADIATION

O. A. Avaste, L. D. Krasnokotskaya,  
and Ye. M. Feygel'son

Simplified methods of calculating the total flux  $Q$  of solar radiation to the earth's surface and the influx  $\Delta B_S$  of direct solar radiation to the atmospheric layers are considered [1].

The effect of the turbidity of the atmosphere and absorption of solar radiation by atmospheric gases on the flux of solar radiation is investigated. The quantities  $Q$  and  $\Delta B_S$  are presented in a form of approximation formulas that are convenient for calculation.

Regions of visual radiation ( $0.4 < \lambda < 0.75$  micron) and infrared radiation ( $0.75 < \lambda \leq 3.0$  microns) are considered separately. The total radiation flux in the visible region,  $Q_v$ , may be expressed by the formula

$$Q_v = I_{0,v} \cos \vartheta_0 e^{-\tau_v \sec \vartheta_0} + D \downarrow_v, \quad (1)$$

where  $I_{0,v}$  is the extra-atmospheric intensity of solar radiation, integrated throughout the visible region of the spectrum;  $D \downarrow_v$  is the downflow of scattered radiation;  $\tau_v$  is the optical thickness in the visible region, satisfying the conditions  $\tau_v \approx \tau(\lambda_0)$  at  $\lambda_0 = 0.55$  micron [1];  $\vartheta_0$  is the zenith angle of the sun. The flux <sup>54</sup> of direct solar radiation,  $S_v$  [the first term in the righthand part of formula (1)] is easy to calculate. Calculation of the flux  $D \downarrow_v$  of scattered radiation required numerical solution of the transfer equations [1].

In Fig. 1 a quite weak dependence of  $Q_v$  upon  $\tau(\lambda_0)$  is observed which is explained by the opposite change of the fluxes  $S_v$  and  $D \downarrow_v$ , with a growth of  $\tau(\lambda_0)$ . Calculations at  $30^\circ < \vartheta_0 < 75^\circ$  demonstrated that  $Q_v$  varies by not more than 25% with a variation of  $\tau_v$  within limits of 0.2-0.6. The curve  $Q_v$  in Fig. 1 may be approximated by the following formula, proposed earlier for the entire summary

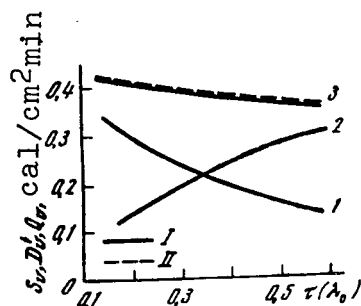


Fig. 1. Dependence of the direct radiation flux, scattered radiation flux, and total radiation flux in the visible range as a function of  $\tau(\lambda_0)$  at  $\vartheta_0 = 60^\circ$ .

1)  $S_v$ ; 2)  $D\downarrow_v$ ; 3)  $Q_v$ ; I) calculation of  $Q_v$  according to formula (1); II) calculation of  $Q_v$  according to (2).

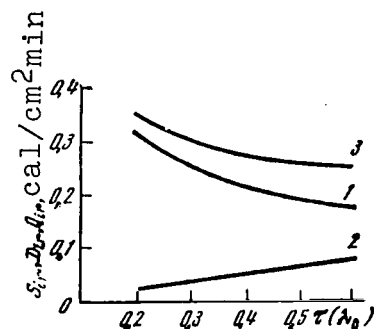


Fig. 2. Dependence of the direct radiation of flux, scattered radiation flux, and total radiation flux of the infrared range as a function of  $\tau(\lambda_0)$  at  $\vartheta_0 = 60^\circ$ .

1)  $S_{ir}$ ; 2)  $D\downarrow_{ir}$ ; 3)  $Q_{ir}$ .

radiation ( $0.3 < \lambda \leq 5$  microns) [2,3]:

$$Q_v = \frac{I_{0,v} \cos \vartheta_0}{1 + \varepsilon(\vartheta_0) \tau(\lambda_0) \sec \vartheta_0}. \quad (2)$$

If the parameter  $\varepsilon(\vartheta_0)$  is assigned in accordance with the table, formula (2) describes  $Q_v$  at  $0.2 < \tau(\lambda_0) < 0.6$  with an error less than 5%.

$\vartheta_0$	$30^\circ$	$60^\circ$	$75^\circ$
$\varepsilon(\vartheta_0)$	0.14	0.2	0.24

The results of the calculations of the direct radiation flux  $S_{ir}$ , scattered radiation flux  $D\downarrow_{ir}$ , and total radiation flux  $Q_{ir}$  in the near infrared region of the spectrum [4] are presented in Fig. 2. By comparing Figs. 1 and 2 we may see that the total flux in the infrared region depends upon the turbidity (air pollution)

more strongly than in the visible region. In this case the complex nature of the absorption spectra of the atmospheric gases make the calculation of  $Q_{ir}$  very laborious with respect to spectral data. /55

The following approximation formula, obtained according to data from spectral calculations [4], is recommended:

$$Q_{ir} = 0.8 [\tau(\lambda_0)]^{-0.24} x_0^{0.15} m^{-1.3} [\text{cal/cm}^2 \cdot \text{min}] \quad (3)$$

Here the parameter  $m$  is the atmospheric mass, and the parameter  $x_0 = x_z$  at  $z = 0$  is determined according to formula

$$x_0 = \int_0^\infty [P(z) + l(z)]^{0.3} \eta(z) dz \left/ \left[ \int_0^\infty \eta(z) dz \right]^{1.3} \right. \quad (4)$$

Here  $P$  (in mm Hg) is the atmospheric pressure,  $l$  (mm Hg) and  $\eta(z)$  ( $\text{g/cm}^3$ ) are the partial pressure and the density of the water vapor.

According to data from numerous calculations, the error of formula (3) does not go beyond limits of 5%.

The calculations have demonstrated that the magnitude of the total radiation,  $Q = Q_v + Q_{ir}$ , varies by 10-30% as a function of  $\vartheta_0$  with a variation of  $\tau(\lambda_0)$  within limits of 0.2-0.6, and by 5-15% in the variation of the total content of water vapor in the atmosphere within limits of 0.5-30 cm.

Formula (2) at  $\varepsilon \approx 0.1$ ;  $\tau = \tau_v + \tau_{ir}$  and  $I_0 = I_{0,v} + I_{0,ir}$  makes it possible to calculate  $Q = Q_v + Q_{ir}$  with an error of the order of 15%.

The influx of short-wave radiation to the layer ( $z_{k-1}, z_k$ ) also may be described by the approximation formula [5]:

$$\Delta B_s = 0.067 (x_{z_{k-1}} - x_{z_k}) \cdot x_{z_k}^{0.7} m^{-1} \text{ cal/cm}^2 \cdot \text{min} \quad (5)$$

In formula (5) only the absorption of direct solar radiation is considered, in comparison with which absorption by scattering is small.

The error of formula (5) does not exceed 5%.

The use of the parameter  $x_z$  in formulas (3) and (5) makes it possible to consider the effect of the variation of pressure in the path of a sun beam in the atmosphere on its absorption. This gives a certain advantage over the formulas of Kastrov and Muegge-Moeller [2,3], in which absorption of solar radiation is given only as a function of the general content of water vapor in the beam path.

In conclusion we note that the separate estimates made of the possible changes of the flux as a function of the variations of the turbidity and humidity of the atmosphere permitted by the climatic conditions demonstrated the larger role of the first of them.

Empirical formula (2) very accurately describes the dependence of the total radiation upon the turbidity of the atmosphere. This formula does not consider the change in humidity, which is insignificant at average values of the latter. Real oscillations of humidity may go far beyond the limits of the average values considered. In these cases, for calculation of the fluxes it is preferable to use formulas (1) and (3) at values of the fluxes  $D\downarrow_v$ , given in [1]. /56

Heating of the atmosphere due to absorption of direct solar radiation may be quite accurately and simply calculated by means of formula (5).



## REFERENCES

1. Avaste, O. A., L. D. Krasnokotskaya and Ye. M. Feygel'son, "Flux of solar radiation to the surface of the earth and influx to the atmosphere", Izv. AN SSR, seriya FAO, 1969.
2. Kondrat'yev, K. Ya., Aktinometriya (Actinometry), Gidrometeoizdat, 1965.
3. Sivkov, S. I., Metody rascheta kharakteristik solnechnoy radiatsii (Methods of Calculation of the Characteristics of Solar Radiation), Gidrometeoizdat, 1968.
4. Avaste, O. A., "Influx of the heat of solar radiation in the atmosphere and total radiation flux at the surface of the sea", Collection: Issledovaniya radiatsionnogo rezhima atmosfery (Research on the Radiation Conditions of the Atmosphere), IFA AN ESSR, Tartu, 1967.
5. Avaste, O. A., "Calculation of absorbed direct solar radiation according to the measured distribution of the humidity of the atmosphere", Collection: Radiatsiya i oblachnost' (Radiation and Cloudiness), IFA AN ESSR, Tartu, 1969.

# REFLECTION, TRANSMISSION, AND ABSORPTION OF RADIATION BY CLOUDS IN THE ABSORPTION BANDS OF WATER VAPOR

L. D. Krasnokotskaya and L. M. Romanova

The optical properties of clouds determine the quantity of radiation arriving at the surface of the earth and the heating of the atmosphere by radiant energy. Reflection, transmission, and absorption by clouds depend upon their absolute humidity, upon the dimensions of the droplets, upon the content of water vapor in the cloud, and upon the thickness and level of the cloud layer.

A survey of experimental data with respect to the albedos of clouds is contained in [1]. A survey of the theoretical data obtained by the beginning of the 1960's with respect to the optical properties of clouds is given [2]. To these data should be added the calculations [3], based on numerical solution of the transfer equation, calculations by the Monte-Carlo method [4,5], and calculation of fluxes from approximation transfer equations [6]. In [7,8] are given analytical expressions for calculation of the intensity of the radiation reflected and transmitted by a thick cloud layer.

In [2-8] the absorbing properties of atmospheric gases are described by the absorption factor  $\alpha_{\Delta\nu}$ . Actually, for finite spectral intervals of  $\Delta\nu$  the transmission functions  $\phi_{\Delta\nu}$  must be used, [57] which depend upon the mass  $m$  of the absorbing matter in the beam path. If the cloud is homogeneous, then this mass is proportional to the length  $l$  of the path in which the absorption occurs. Therefore, for determination of the radiation intensity  $I_{\Delta\nu}$  in a homogeneous cloud in the absorption band we must know the photon distribution  $J$  with respect to free paths  $l$  caused by scattering. Upon condition that in the interval  $\Delta\nu$  the scattering properties do not depend upon the wavelength, the intensity  $I_{\Delta\nu}$  is associated with the quantity  $J$  by the following relation [9,10]:

$$I_{\Delta\nu}(\tau_0, \omega, \omega_0) = I_{0, \Delta\nu} \int_0^\infty J(\lambda, \tau_0, \omega, \omega_0) \Phi_{\Delta\nu} \left( \rho \frac{\lambda}{\sigma} \right) d\lambda, \quad (1)$$

where  $\lambda = \sigma l$ ;  $\sigma$  is the scattering factor;  $I_{0, \Delta\nu}$  is the intensity of the radiation falling onto the upper boundary of the cloud;  $\rho$  is the density of the absorbing substance;  $\tau_0$  is the optical thickness of the cloud;  $\omega, \omega_0$  are the unit vectors in the direction of

the propagation of the scattered radiation and the radiation that is incident to the boundary of the cloud.

The transfer equation for the distribution with respect to runs, and certain solutions of it are contained in [9-11]. This distribution may also be obtained by the Monte-Carlo method [12]. Here for calculation of  $J$  we will use asymptotic formulas obtained in [13] for distribution with respect to free paths of photons reflected and transmitted by the layer of aturbid medium of great optical thickness. The results of this work must be somewhat refined: the limits of applicability of the formulas for layers of finite thickness have an upper boundary, since at values of  $\lambda$  greater than a certain value  $\lambda^*$ , the method of calculation of the integrals in [13] ceases to work. At rather large values of  $\lambda$  [14] the distribution with respect to free paths has the form of an exponential function. For the cases considered here, the asymptotic formulas [13] must be replaced by an exponential function at  $\lambda \sim 200$ .

In this work fluxes of reflected radiation  $A$ , absorbed radiation  $P$ , and transmitted radiation  $T$  of the sun, as reflected, absorbed, or transmitted by stratoform clouds, in the near infrared region of the spectrum, were calculated. The calculations were performed by means of graphic integration of the function

$J(\lambda) \Phi_{\Delta v}(\rho_v \frac{\lambda}{\sigma})$ , where  $\rho_v$  is the density of water vapor. Absorption in droplet water was not considered. In the calculations, transmission functions  $\Delta v$  were used [15], with subsequent processing [16].

A homogeneous cloud with an absolute humidity  $\rho_w = 0.2 \text{ g/m}^3$  was considered, as well as a monodispersed scattering indicatrix corresponding to  $\rho = 2\pi r/\lambda = 20$  and a scattering factor  $\sigma = 30 \text{ km}^{-1}$ . In the determination of the dependence of  $\Phi_{\Delta v}$  upon pressures [16] it was assumed that the altitude of the lower boundary of the cloud is equal to  $z_{n.g} = 0.5 \text{ km}$ .

In Table 1 the values of  $A$ ,  $T$ , and  $\Pi = 1 - A - T$  are given for each absorption band of water vapor in the near infrared region of the spectrum at different values of the optical thickness  $\tau_0$  of the cloud layer, and of the density  $\rho_v$  of water vapor. In the first column the values of  $A$  and  $T$  are given in the absence of absorption. /58

The error of calculation of the magnitudes of  $A$  and  $T$  due to approximate integration according to formula (1) amounts to  $\pm 3\%$ .

The data in Table 1 have only tentative value, since in the region 0.7-3.57 microns the scattering indicatrix and the most important characteristic for thick layers—the average cosine of the scattering angle in the droplets of water—vary considerably.

TABLE 1

$\tau_0$	Name of band	Interval of wave lengths, $\mu$	0,7	0,8	$\rho_{av}$	$\Phi$	$\Psi$	$\Omega$	$\bar{\chi}$	3,2
	Interval of wave lengths, $\mu$	Interval of wave lengths, $\mu$	0,70 0,71	0,79 0,84	0,85 0,99	1,03 1,23	1,25 1,54	1,70 2,10	2,27 3,0	3,0 3,57
$\rho_v = 1 \text{ g·m}^{-3}$										
$\infty$	$A_{\Delta v}$	1	0,99	0,99	0,96	0,96	0,78	0,78	0,61	0,84
	$\Pi_{\Delta v}$	—	—	—	0,04	0,04	0,22	0,22	0,39	0,16
30	$A_{\Delta v}$	0,81	0,81	0,81	0,79	0,79	0,66	0,65	0,53	0,71
	$T_{\Delta v}$	0,19	0,19	0,19	0,18	0,18	0,15	0,14	0,09	0,15
	$\Pi_{\Delta v}$	—	—	—	0,03	0,03	0,19	0,21	0,38	0,14
20	$A_{\Delta v}$	0,77	0,77	0,77	0,75	0,75	0,64	0,63	0,51	0,68
	$T_{\Delta v}$	0,23	0,23	0,23	0,22	0,22	0,19	0,18	0,12	0,20
	$\Pi_{\Delta v}$	—	—	—	0,03	0,03	0,17	0,19	0,37	0,12
$\rho_v = 5 \text{ g·m}^{-3}$										
30	$A_{\Delta v}$	0,81	0,81	0,81	0,79	0,77	0,55	0,54	0,39	0,56
	$T_{\Delta v}$	0,19	0,19	0,19	0,18	0,17	0,09	0,09	0,04	0,09
	$\Pi_{\Delta v}$	—	—	—	0,03	0,06	0,36	0,37	0,57	0,35
20	$A_{\Delta v}$	0,77	0,77	0,76	0,73	0,72	0,53	0,52	0,37	0,54
	$T_{\Delta v}$	0,23	0,23	0,23	0,22	0,22	0,15	0,14	0,08	0,15
	$\Pi_{\Delta v}$	—	—	0,01	0,05	0,06	0,32	0,34	0,55	0,31

From Table 1 it is apparent that at  $\tilde{\lambda} = 1/\nu \leq 1$  micron the albedo in the absorption bands of water vapor is close to the albedo outside the bands. Absorption here is small and does not go beyond the limits of the error of calculation. With an increase in the wavelength the albedo decreases with a corresponding increase of absorption in the cloud layer. With an increase in the density of the water vapor from  $1 \text{ g/m}^3$  to  $5 \text{ g/m}^3$  the absorption at  $\lambda \geq 1$  micron increases by approximately 50%, and the reflection decreases by 18-30%.

In Table 2 the values of the albedo  $A_{\text{int}}$ , transmission  $T_{\text{int}}$ , and absorption  $\Pi_{\text{int}}$  integrated throughout the interval of wavelengths of 0.7-3.6 microns are given.

TABLE 2

$\rho_v$	1 g/m <sup>3</sup>			5 g/m <sup>3</sup>	
$\tau_0$		30	20	30	20
$A$	0,92	0,76	0,73	0,72	0,68
$T$		0,18	0,21	0,16	0,23
$\Pi$	0,08	0,06	0,06	0,12	0,09

As is apparent from Table 2, the cloud absorbs 6-12% of the radiation falling on its upper boundary. This magnitude depends weakly upon the optical thickness of the cloud.

## REFERENCES

1. Goysa, N. I., "Vertical profiles of the short-wave albedo in the lower troposphere", Trudy Ukr. NIGMI, No. 82, 1969.
2. Feygel'son, Ye. M., Radiatsionnyye protsessy v sloistoobraznykh oblakakh, Izd-vo "Nauka", 1964.
3. Romanova, L. M., "The radiation fields in flat layers of a turbid medium with strongly anisotropic scattering", Optika i spektroskopiya, 14, No. 2, 1963.
4. Plass, G. N., and G. W. Kattawar, "Influence of single scattering albedo on reflected and transmitted light from clouds", Appl. Optics, 7, No. 2, 1968.
5. Plass, G. N. and G. W. Kattawar, "Monte Carlo calculations of light scattering from clouds", Appl. Optics, 7 No. 3, 1968.
6. Korb, G., and F. Möller, "Theoretical investigation on energy gain by absorption of solar radiation in clouds", Contract DA-91-591 EUC-1612, Germany, 1962.
7. Rozenberg, G. V., G. K. Il'ich, S. A. Makarevich, and Yu. R. Mullamaa, "On the brightness of clouds", Izv. AN SSSR, seriya FAO, 6, No. 4, 1970.
8. Sobolev, V. V., "Diffusion of radiation in a medium of large optical thickness in anisotropic scattering", Dokl. AN SSSR, 179, No. 1, 1968.
9. Irvine, W. M., "The formation of absorption bands and the distribution of photon optical paths in scattering atmospheres", Bull. Astron. Inst. Netherl., 17, No. 4, 1964.
10. Van de Hulst, H. C. and W. M. Irvine, "Scattering in model planetary atmospheres", Meteorol. Soc. Roy. Sci. Liege, ser. 5, 7, No. 1, 1963.
11. Romanova, L. M., "Distribution of photons with respect to free paths in a flat layer of a homogeneous turbid medium", Izv. AN SSSR, FAO, 1, No. 10, 1965.
12. Marchuk, G. I., G. A. Mikhaylov, M. A. Nazaraliyev, and R. A. Darbinyan, Resheniye pryamykh i nekotorykh obratnykh zadach atmosfernoy optiki metodom Monte-Karlo, VTs SO AN SSSR, Izd-vo "Nauka", Siberian Division, Novosibirsk, 1968.

13. Romanova, L. M., "Limiting cases of the distribution function /60 with respect to free paths of photons leaving a thick light-scattering layer", Izv. AN SSSR, seriya FAO, 1, No. 6, 1965.
14. Bowden, R. L. and C. D. Williams, "Solution of the initial value transport problem for monoenergetic neutrons in slab geometry", J. Math. Phys., 5, No. 11, 1964.
15. Howard, J. N., D. E. Burch, and C. D. Williams, "Infrared transmission of synthetic atmospheres", JOSA, 46, No. 3-6, 1956.
16. Shifrin, K. S. and O. A. Avaste, "Fluxes of short-wave radiation in a cloudless atmosphere", Collection: Issledovaniya po fizike atmosfery (Research in the Physics of the Atmosphere), IFA AN ESSR, No. 2, 1960.

EXPERIMENTAL INVESTIGATIONS OF FLUXES  
OF SOLAR RADIATION IN THE LOWER TROPOSPHERE  
IN St AND Sc CLOUDS

N. I. Goysa and V. M. Shoshin

The first measurements of radiation fluxes in a cloudy atmosphere were performed by W. Aldridge and M. Luckeish [2]. Similar measurements were renewed only 30 years later, at first by M. Neiburger [3] and then by Z. Fritz [4]. In the Soviet Union the first measurements of radiation characteristics of clouds were performed by N. I. Chel'tsov [5], whose work up to this time has not lost its acuteness and value. In subsequent years several works appeared [6-11] devoted to this problem. However, both with respect to volume and completeness of material and with respect to methodology they, at best, were only a repetition of the work of N. I. Chel'tsov mentioned above.

In 1963 experimental investigations of the radiation properties of clouds were begun in the Ukr. NIGMI.

The basic principles of the methodology of the measurement of radiation fluxes in a cloudy atmosphere were developed by V. G. Kastrov [12]. The methodology of the measurements being described is explained in detail in [13]. Together with radiation fluxes, the absolute humidity of the clouds, temperature, relative humidity and the pressure of the air were also determined, visual observations were made of the state of the cloud cover. For six years considerable experimental material was accumulated, the generalization of which was partially performed in [14-17].

We will first discuss the radiation characteristics of the cloud layer as a whole. The main problem is to ascertain the dependence of the radiation characteristics of the cloud (albedo  $A_k$ , transmissivity  $\psi$  and absorption capability  $b$ ) upon its initial parameters: the thickness  $H = z_{v.g.} - z_{n.g.}$  and the water supply  $m_w$ , and also upon the altitude of the sun  $h_\odot$ .

The problem indicated was considered in [1,3-11]. However, /61 there was inadequate experimental material concerning the radiation properties of cloud cover. Certain quantitative relationships such as, for example, the dependence of the radiation characteristics upon the water reserve in the cloud and the altitude of the sun were not considered in the works indicated, with the exception of [10].



The methodology of the processing of materials of measurements also requires refinement. Since a cloud, for short-wave radiation, is a semi-transparent medium, at the magnitudes of  $A_k$ ,  $\phi$ , and  $b$ , obtained as ratios

$$A_k = \frac{D_{(z_k, g)}^\dagger}{Q_{(z_v, g)}}; \quad \phi = \frac{D_{(z_k, g)}^\dagger}{Q_{(z_v, g)}}; \quad b = \frac{AB_k}{Q_{(z_v, g)}}, \quad (1)$$

the radiation reflected from the earth's surface must have an appreciable effect. This circumstance, although it was noted in a number of works [3,5,8], was not considered. Therefore, the magnitudes of  $A_k$  and  $\phi$  given in all the works cited above refer, naturally, not to the cloud itself but to the system consisting of the cloud, the layer under the cloud, and the earth's surface. This circumstance, at large differences in albedo  $A_z$  of the earth's surface, may cause an essential deterioration in the comparability of the results obtained.

In refs. [13,18] a somewhat different method of processing the results of the measurements was proposed, and in [14-16] it was applied. Its essence lies in the transition from the magnitudes of  $A_k$  and  $\phi$  determined from ratios (1) to their "true" values  $A_k^*$  and  $\phi^*$ , reflecting only the properties of the given cloud. Such a transition is accomplished by means of reducing the magnitudes of  $A$  and  $\phi$  corresponding to definite values of  $A_z$  to  $A_z = 0$  by means of the following formulas [13]:

$$A_k^* = \frac{A_k - \phi^2 \cdot A_3}{1 - \phi^2 \cdot A_3^2}; \quad \phi^* = \phi(1 - A_3 \cdot A_k). \quad (2)$$

In analogy with the "true" magnitudes of  $A_k^*$  and  $\phi^*$  we may introduce the concept of the "true" absorption capability  $b^*$ , which may be determined from the relation

$$A_k^* + \phi^* + b^* = 1. \quad (3)$$

However, as was demonstrated in [14,17] and as follows from [3,19] the quantities  $b$  and  $b^*$  are practically independent of such parameters of the cloud as  $H$  and  $m_w$ , and therefore they cannot be used as characteristics of the absorption capability. At this first glance paradoxical circumstance is explained by the

fact that the radiation  $\Delta B_k$  absorbed by the cloud is not determined so much by the flux  $Q_{(z_{v.g.})}$ , as by the radiation  $Q_{inp}$ . The latter, with an unchanged magnitude of  $Q_{(z_{v.g.})}$ , decreases with a growth of  $H$  and  $m_w$  [14] in connection with the increase in  $A_k^*$  and the decrease in  $\Phi^*$ . In this case the quantity  $\Delta B_k$  either does not change or even decreases. In connection with what was explained above, for the characteristics of the absorption capability of the cloud it is proposed to use the ratio  $b_{ef}^* = \Delta B_k / Q_{inp}$ , which may be called the effective absorption capability. The quantity  $Q_{inp}$  is determined according to the formula [14]:

$$Q_{inp} = Q_{(z_{v.g.})} (1 - A_k^*) \cdot \left( 1 + \frac{\Phi^* A_3}{1 - A_k^* A_3} \right). \quad (4)$$

In analogy with the concept of the "true" albedo and transmission capability of the cloud we may introduce the concept of the "true" effective absorption capability  $b_{ef}^*$ . It is easy to demonstrate that the quantity  $b_{ef}^*$  may be determined by means of the following equation:

$$b_{ef}^* = \frac{b^*}{1 - A_k^*}. \quad (5)$$

In Table 1 the average values of the basic parameters of St and Sc clouds are presented, and also the values of the quantities characterizing their radiation properties.

Aside from the parameters  $A_k^*$ ,  $\Phi^*$ ,  $b$ , and  $b_{ef}$  described above, here the average values of the rate of radiation heating due to short-wave radiation  $\theta_k$  and long-wave radiation  $\theta_d$  and their sum  $\theta$  are presented. These quantities, like the others given below, were obtained on the basis of data from 112 soundings of St and Sc. The sounding was performed primarily in the vicinity of the experimental test area of the Ukr. NIGMI (Krivoy Rog). Some flights were made over the airports of Khar'kov, Vinnitsa, Kiev, Odessa, Kirovograd, and Donetsk.

From Table 1 it is apparent that the forms of the clouds being investigated differ noticeably with respect to their parameters (the thickness, the position of the upper boundary, and water reserve supply).

TABLE 1

Form of cloud	No. of cases	Average values											
		z.	H	t	w, g/m <sup>3</sup>	m <sub>w</sub> , m <sup>2</sup>	A <sub>k</sub> , %	Φ, %	b, %	b <sub>ef</sub> , %	θ <sub>k</sub> , °/hr	θ <sub>d</sub> , °/hr	θ, °/hr
St	58	860	430	-2.5	0.20	85	73	21	6.2	25.3	0.17	-0.51	-0.34
Sc	54	980	350	-2.0	0.13	46	66	26	8.6	23.8	0.27	-0.71	-0.44

TABLE 2

Thickness m	A, %			Φ, %			k <sub>P</sub> , km <sup>-1</sup>	σ <sub>H</sub> , km <sup>-1</sup>	k <sub>P</sub> , H km <sup>-1</sup>	k <sub>P</sub> , H km <sup>-1</sup>	k <sub>P</sub> , H km <sup>-1</sup>
	av.	max.	min.	av.	max.	min.					
90-110	31.2	55.6	30.6	63.0	75.9	50.0	4.85	3.70	1.15	0.95	0.60
110-130	36.8	40.0	31.8	55.5	59.5	44.8	4.92	3.70	1.12	0.91	0.67
130-160	43.8	77.4	40.2	49.5	59.5	22.8	5.00	3.80	1.20	0.89	0.48
170-200	51.6	60.8	37.6	38.8	46.2	29.2	5.10	3.90	1.20	0.88	0.55
200-250	59.0	73.4	41.0	32.0	53.4	17.6	5.07	3.95	1.12	0.88	0.45
250-300	66.2	83.6	60.2	27.0	44.8	12.0	4.78	3.91	0.87	0.90	0.30
300-350	71.2	88.2	48.4	23.4	43.0	12.6	4.44	3.78	0.66	0.88	0.17
350-400	73.6	82.4	63.4	21.0	34.8	10.0	4.11	3.58	0.53	0.83	0.15
400-500	76.4	80.6	64.8	18.1	45.4	11.2	3.72	3.19	0.53	0.76	0.13
500-600	79.0	85.0	66.4	15.6	27.6	11.2	3.33	2.82	0.51	0.67	0.10
600-700	80.6	93.6	52.0	14.0	38.4	7.0	2.95	2.52	0.43	0.60	0.09
700-1000	82.1	89.4	62.2	12.4	38.3	5.5	2.35	2.00	0.35	0.50	0.07

This, in turn, served as the cause of the differences in the radiation characteristics, and also in the rate of radiation heating.

In Fig. 1 the dependence of the quantities  $A_k^*$  and  $\Phi_k^*$  upon the water reserve in the cloud is presented, and in Table 2, their dependence upon the thickness of the cloud layer. It is apparent that the radiation characteristics of the cloud undergo strong variations at small values of  $m_w$  (less than 50 g/m<sup>2</sup>) and  $H$  (less than 300 m). A further growth of these parameters leads to a relatively small variation of  $A_k^*$  and  $\Phi_k^*$ . We should note that the dependences considered are given without consideration of the effect of the altitude of the sun, which varied from case to case within limits of 6-52° at an average value of 25°. The dependence of  $A_k^*$  and  $\Phi_k^*$  upon the average specific humidity  $\bar{w}$  of the cloud turned out to be analogous to their dependence upon  $m_w$ .

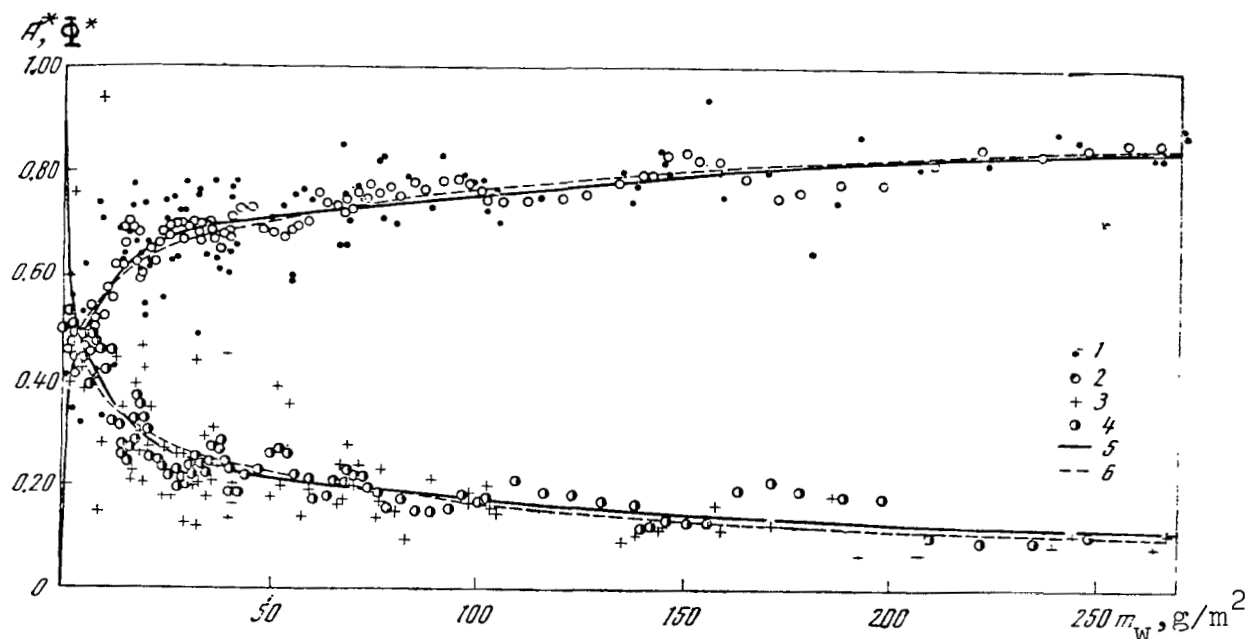


Fig. 1. Dependence of the "true" magnitudes of the albedo and the transmission of cirrus and cirrocumulus clouds upon their water reserve.

1 and 3- experimental points; 2 and 4- moving averages from five cases; 5- curve constructed according to experimental data; 6- the same, according to formulas (12).

It is interesting to establish the analytical connection of 65 the radiation characteristics with the parameters of the cloud. In certain works [8,18], it is assumed that the transmission function  $\Phi$  depends exponentially upon the optical thickness  $\tau_0$  of the cloud. If in this case we assume that  $\tau_0 = \sigma \cdot H$ , where  $\sigma$  is the scattering factor, we should expect an exponential dependence of  $A_k^*$  and  $\Phi^*$  upon  $H$ .

In Table 2 are given the scattering factors  $\sigma$ , attenuation factors  $k$ , and absorption factors  $k_p$ ,  $k'_p$ , and  $k''_p$ , calculated according to formulas:

$$A_k^* = 1 - e^{-kH}, \quad (6)$$

$$\Phi^* = e^{-kH} \quad (7)$$

$$h_{ef} = 1 - e^{-k_p \cdot H}, \quad (8)$$

$$h^* = 1 - e^{-k'_p \cdot H}, \quad (9)$$

$$k_p, \quad k = \sigma. \quad (10)$$

In Table 2 the dependence of the "true" magnitudes of the albedo, relative transmission, and attenuation factor  $k$ , scattering factor  $\sigma$ , and absorption factors  $k_p$ ,  $k'_p$ , and  $k''_p$  of short-wave radiation of stratoform clouds upon their thickness is presented. From Table 2 it follows that  $\sigma$  and  $k$  strongly depend upon  $H$ . This testifies to the unfitness of a linear connection between  $\tau_0$  and  $H$  for real clouds, which is also confirmed by earlier investigations. The dependence of  $A_k^*$  and  $\Phi^*$  upon  $H$  may also be expressed by the formulas:

$$A_k^* = \frac{H}{a + bH}; \quad \Phi^* = 1 - \frac{H}{a' + b'H}. \quad (11)$$

However, in these formulas the coefficients  $a$ ,  $a'$ ,  $b$ , and  $b'$  also depend upon  $H$ , although less so than  $\sigma$  and  $k$ . The values of the parameters in formula (11) for various thicknesses are given in [17].

The connection of the magnitudes of  $A_k^*$  and  $\phi$  with the water reserve  $w_m$  of the cloud may be presented in the form

$$A_k^* = 1 - e^{-0.46 \sqrt{w_m}}; \quad \phi^* = e^{-0.56 \sqrt{w_m}}. \quad (12)$$

As is apparent from Fig. 1, the curves constructed according to formulas (12) agree entirely satisfactorily with the data from the measurements.

A comparison of the data obtained concerning the dependence of  $A_k^*$  and  $\phi^*$  upon  $H$  with data from other authors [3,5,8,9,18] was performed in [14]. A satisfactory agreement is observed within the limits of accuracy of measurements and the spatial variability of the object being investigated. We should only note that in opposition to [5] we did not succeed in observing a systematic dependence of the radiation characteristics of St and Sc upon the parameters of these clouds,  $H$  and  $m_w$ .

One of the factors affecting  $\phi^*$  and  $A_k^*$  is the altitude of the sun,  $h_\odot$ . In spite of the comparatively small volume of materials from measurements, we succeeded in estimating this dependence tentatively (Table 3). For clouds of small thickness ( $H \approx 200$  m at  $h_\odot \geq 10^\circ$ ) the variation of the albedo of the upper boundary,  $\Delta A/\Delta h$  amounts to 0.4% per degree. With an increase in  $H$ , this effect attenuates and for thick clouds  $\Delta A/\Delta h = -0.15\%$  per degree. In this case the relative transmission decreases by approximately the same magnitude (a somewhat lesser magnitude).

In ref. [17] a tentative estimate is given of the dependence of the scattering factor and attenuation factor upon the altitude of the sun. It turned out that this dependence is close to linear.

The experimental data were compared with the calculations of Ye. M. Feygel'son [1], according to whom the albedo of St and Sc of average thickness (about 400 m) at  $h_\odot \approx 40^\circ$  is equal, respectively, to 63 and 72%. In this case  $\Delta A/\Delta h = -0.25\%$  per degree and  $-0.20\%$  per degree. The numbers indicated are close to our data.

According to the data in Table 3, we may judge the dependence of the quantities  $b^*$  and  $b_{ef}^*$  upon  $H$  and  $h_\odot$ . It is apparent that  $b^*$  is almost independent of  $H$  and  $h_\odot$ , while for  $b_{ef}^*$  this dependence

TABLE 3

Thick- ness, m	Symbols	Altitude of sun, degrees				
		10	20	30	40	50
175	$\Phi^*$	37,0	43,5	48,8	53,2	56,0
	$A^*$	59,5	52,4	47,0	43,6	41,0
	$b^*$	3,5	4,1	4,2	3,2	3,0
	$b_{ef}^*$	8,6	8,6	8,0	5,7	5,1
260	$\Phi^*$	23,2	27,8	31,0	34,5	37,2
	$A^*$	72,0	67,0	62,8	59,2	57,0
	$b^*$	4,8	5,2	6,2	6,3	5,8
	$b_{ef}^*$	17,2	15,7	16,6	15,4	13,5
350	$\Phi^*$	18,5	19,8	22,3	23,8	25,6
	$A^*$	75,5	73,2	70,8	68,8	67,4
	$b^*$	6,0	7,0	6,9	7,4	7,0
	$b_{ef}^*$	24,5	26,1	23,6	23,7	21,5
450	$\Phi^*$	14,5	16,0	17,5	19,0	20,5
	$A^*$	80,0	77,5	75,8	74,2	72,8
	$b^*$	5,5	6,5	6,7	6,8	6,7
	$b_{ef}^*$	27,5	28,8	27,6	26,4	24,6
610	$\Phi^*$	11,5	12,5	14,0	15,7	17,0
	$A^*$	83,6	81,2	79,7	78,2	77,0
	$b^*$	4,9	6,3	6,3	6,1	6,0
	$b_{ef}^*$	29,8	33,4	31,0	27,9	26,0
900	$\Phi^*$	10,0	11,0	11,7	12,3	13,0
	$A^*$	85,6	83,2	82,0	81,0	80,0
	$b^*$	4,4	5,8	6,3	6,7	7,0
	$b_{ef}^*$	30,5	34,5	35,0	35,2	35,0

is essential. From this it follows that the real variations of the absorption capability of the clouds may be characterized only by the quantities  $b_{ef}$  and  $b_{ef}^*$ .

In Fig. 2 the dependence of  $b_{ef}$  upon  $m_w$  and  $H$  is presented, constructed on the basis of data from direct measurements. In spite of the strong scattering of the points, the dependence is entirely clear, especially if we consider the averaged data. According to the scattering of the points, the accuracy of the determination of the radiation influx of heat to the cloud layer due to short-wave radiation was tentatively estimated. The mean square error turned out to be equal to 47% [14].

TABLE 4

z, km	Altitude of sun, degrees					
	10	20	30	40	50	60
0	0,460	0,405	0,650	0,870	1,050	1,205
0,2	0,173	0,425	0,673	0,893	1,080	1,220
0,5	0,186	0,446	0,697	0,919	1,110	1,244
1,0	0,202	0,469	0,722	0,950	1,145	1,280
2,0	0,228	0,495	0,749	0,989	1,185	1,330
3,0	0,249	0,520	0,781	1,031	1,225	1,365
4,0	0,256	0,539	0,809	1,066	1,256	1,400
6,0	0,283	0,569	0,842	1,101	1,294	1,430

TABLE 5

interval and ax. value of H, km	Symbols	Altitude of sun, degrees				
		10	20	30	40	50
0,09-0,22	$\Delta B_R^*$	0,007	0,019	0,030	0,034	0,034
0,175	$\theta_R^*$	0,08	0,22	0,35	0,36	0,39
0,2-0,3	$\Delta B_R^*$	0,010	0,024	0,045	0,060	0,066
0,26	$\theta_R^*$	0,08	0,19	0,35	0,47	0,52
0,3-0,4	$\Delta B_R^*$	0,012	0,033	0,050	0,070	0,079
0,35	$\theta_R^*$	0,07	0,19	0,29	0,40	0,46
0,4-0,5	$\Delta B_R^*$	0,011	0,031	0,048	0,068	0,076
0,45	$\theta_R^*$	0,05	0,14	0,22	0,26	0,34
0,5-0,7	$\Delta B_R^*$	0,010	0,030	0,046	0,058	0,068
0,61	$\theta_R^*$	0,03	0,10	0,15	0,19	0,23
0,7-1,2	$\Delta B_R^*$	0,009	0,027	0,046	0,064	0,079
0,9	$\theta_R^*$	0,02	0,06	0,10	0,14	0,18



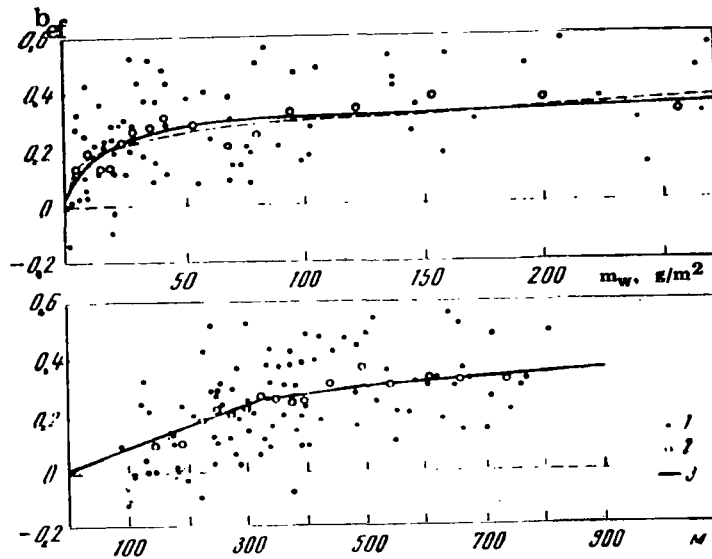


Fig. 2. Dependence of the effective absorption capability of cirrus and cirrocumulus clouds upon their water reserve and thickness.  
 1- experimental points; 2- averages from five cases;  
 3- curve constructed according to experimental data;  
 4- the same, according to formula (13).

The dependence of the absorption factor  $k_{p,m_w}$  ( $k_{p,m_w}$  is the absorption factor calculated per unit of water reserve  $m_w$ ) and the effective absorption capability  $b_{ef}$  upon the water supply in the cloud, in agreement with Fig. 2, may be presented by the following formulas: /69

$$k_{p,m_w} = 0.11 \sqrt[4]{m_w^{-3}}; \quad b_{ef} = 1 - e^{-0.11 \sqrt[4]{m_w}}. \quad (13)$$

It is interesting to note that in this case

$$k_{p,m_w} = k_{m_w} - \sigma_{m_w},$$

where  $k_{m_w}$  and  $\sigma_{m_w}$  were obtained from formulas (12).

If we know the magnitude of  $b^*$ , we may determine the radiation influx of heat to the cloud layer due to short-wave radiation. For

this we need information concerning the radiation arriving at the upper boundary of the cloud, as presented in Table 4. This table contains the averaged data from measurements of the fluxes  $Q$ , in  $\text{cal/cm}^2 \text{ min}$ , in a clear sky over an aircraft, and the quantities corresponding to  $z = 0$ , taken according to observations at Kiev in 1962-1964. Assuming that on the average the upper boundary of the clouds is located at a level of 1 km and using the data from Tables 3 and 4, it is easy to determine the radiation absorbed by clouds of different thickness  $H$  and the corresponding rate  $\theta_k^*$  of radiation heating as a function of  $h_0$ . These quantities are presented in Table 5.

TABLE 6

Latitude deg.	Month	Thickness, m					
		175	260	350	450	610	900
55	Oct.	1.8	1.7	1.6	1.2	0.8	0.5
	Nov.	0.8	0.7	0.7	0.5	0.3	0.2
	Dec.	0.5	0.4	0.4	0.3	0.2	0.1
	Jan.	0.6	0.6	0.5	0.4	0.2	0.1
	Feb.	1.3	1.2	1.1	0.8	0.6	0.4
	March	2.6	2.6	2.3	1.7	1.2	0.8
	April	3.6	4.1	3.5	2.6	1.7	1.2
50	Oct.	2.3	2.2	1.9	1.4	1.0	0.6
	Nov.	1.3	1.1	1.1	0.8	0.5	0.3
	Dec.	0.8	0.8	0.7	0.5	0.3	0.2
	Jan.	1.0	0.9	0.8	0.6	0.4	0.3
	Feb.	1.8	1.7	1.6	1.2	0.8	0.5
	March	2.8	3.0	2.6	1.9	1.3	0.9
	April	3.7	4.3	3.8	2.8	1.8	1.3
45	Oct.	2.6	2.8	2.4	1.8	1.2	0.8
	Nov.	1.7	1.6	1.5	1.1	0.7	0.5
	Dec.	1.2	1.1	1.0	0.8	0.5	0.3
	Jan.	1.4	1.3	1.2	0.9	0.6	0.4
	Feb.	2.3	2.2	1.9	1.4	1.0	0.7
	March	3.0	3.4	2.9	2.2	1.5	1.0
	April	3.8	4.5	3.9	2.9	2.0	1.4

One of the shortcomings of the majority of the work previously performed [10, 13, 17, and others] is the fact that in them information concerning the radiation heating of the clouds is given for individual moments of time. For many problems in the physics of the atmosphere, such data are needed for definite intervals of time (day, 24-hour period, etc.). Since  $\Delta B_k^*$  and  $\theta_k^*$ , as follows from Table 5, essentially depend upon  $h_0$ , the fragmentary information concerning these quantities given in the works indicated above describes the process of radiation heating of the cloud inadequately completely. The dependence of  $\Delta B_k^*$  upon  $h_0$  obtained can be used for determining the influx of radiation heat to the cloud in a 24-hour period, and then for calculating the diurnal magnitude of radiation heating. In Table 6 these quantities are given in degrees per 24 hour period for single-layer St and Sc clouds of various thickness in the cold season of the year. The data from this table are tentative. In spite of this, they can be used to judge the heating of low stratoform clouds by the sun in the cold season of the year in various geographical regions.

## REFERENCES

1. Feygel'son, Ye. M., Radiatsionnyye protsessy v sloistoobraznykh oblakakh (Radiation Processes in Stratoform Clouds), "Nauka" Press, 1964.
2. Luckiesh, M., "Aerial Photometry", Astrophys. J., 49, 1919.
3. Neiburger, M., "The reflection, absorption and transmission of insolation by stratus clouds", J. Meteorol. 6, No. 2, 1949.
4. Fritz, S., "Measurements of albedo of clouds", Bull. Amer. Meteorol. Soc., No. 1, 1950.
5. Chel'tsov, N. I., "Investigation of reflection, transmission, and absorption of solar radiation by clouds of certain forms", Trudy, TsAO, No. 8, 1952.
6. Belov, V. F., "The albedo of the underlying surface and certain forms of clouds in the vicinity of the Antarctic slope and Davis Sea", Trudy TsAO, No. 37, 1960.
7. Koptev, A. P., "Actinometric investigations from an aircraft in the Arctic", Nauch. soobshch. In-ta geol. i geogr. AN Lit. SSR, 13, 1962.
8. Koptev, A. P. and A. I. Voskresenskiy, "On the problem of the radiation properties of cloud cover", Trudy AANII, 239, No. 2, 1962.
9. Timofeyev, A. A., "Total radiation and albedo according to observations from an aircraft in the Arctic in 1963", Trudy AANII, 273, 1965.
10. Griggs, M., "Aircraft measurements of albedo and absorption of stratus clouds and surface albedos", J. Appl. Meteorol., 7, No. 6, 1968.
11. Robinson, L. D., "Some observations from aircraft surface albedo and absorption of cloud", Arch. Meteorol., Geophys. und Bioklimatol., Bd. 9, N. 1, 1958.
12. Kastrov, V. G., "Measurements of the absorption of solar radiation in the free atmosphere up to 3-5 km", Trudy TsAO, No. 8, 1952. /7
13. Goysa, N. I., "Methodology of actinometric measurements from an IL-14 aircraft", Trudy Ukr. NIGMI, No. 55, 1966.

14. Goysa, N. I., "Effect of the thickness and absolute humidity of stratoform clouds on reflection, transmission, and absorption of short-wave radiation". Trudy Ukr. NIGMI, no. 70. 1968.
15. Goysa, N. I. and V. M. Shoshin, "Vertical profiles of the short-wave albedo in the lower troposphere", Trudy Ukr. NIGMI, No. 82, 1969.
16. Goysa, N. I. and V. M. Shoshin, "An experimental model of the radiation regime of the 'average' stratoform cloud", Trudy Ukr. NIGMI, No. 82, 1969.
17. Goysa, N. I. and V. M. Shoshin, "Radiation balance of St and Sc cloud layers", Trudy Ukr. NIGMI, No. 86, 1970.
18. Goysa, N. I. and T. V. Zhekeznyakov, "Determination of the thickness and certain radiation characteristics of cirrus and cirrocumulus clouds according to the intensity of the total radiation at the surface of the earth", Trudy Ukr. NIGMI, No. 48, 1965.
19. Drasnokutskaya, L. D. and L. M. Romanova, "Reflection, transmission, and absorption of radiation by clouds in the absorption bands of water vapor", in this collection, page 56 [Russian text].

## AVERAGE VERTICAL STRUCTURE OF THE FIELD OF SHORT-WAVE RADIATION IN STRATIFORM St AND Sc CLOUD COVER

N. I. Goysa and V. M. Shoshin

Analysis of the material of radiation measurements demonstrates that even in the simplest cases of one-layer clouds the radiation field is variable to a considerable degree, especially within the cloud layer. In this case, random errors of measurement are superimposed upon the true vertical distribution of radiation fluxes, and especially that of influxes. In order to free ourselves from this, and also in order to ascertain the most characteristic features of the vertical structure of the radiation field, it is necessary to average the results of individual measurements. For this purpose, an experimental model of an "average" stratiform cloud was constructed according to 25 cases of actinometric sounding, in conditions of a clear sky, above a layer of St or Sc.

In the drawing the vertical profiles of various characteristics of the "average" cloud are given. Its basic parameters are:  $H = 400$  m,  $m_w = 72$  g/cm<sup>2</sup> [sic], average temperature  $-3.9^\circ\text{C}$ , position of upper boundary  $z_{v.g} = 830$  m above the earth's surface. The methodology of the construction of profiles of the temperature, the relative humidity of the air, and the water content (absolute humidity) in the "average" cloud is explained in [1].

In the construction of the profiles of short-wave fluxes, considerable difficulties arise associated with the necessity of the consideration of the effect of the altitude  $h_0$  of the sun and the albedo  $A_z$  of the underlying surface. The first may be avoided to a considerable degree if we do not operate with absolute values of the fluxes, but with their relative characteristics:  $\phi$ ,  $A_k$ ,  $b$ . Although these quantities, as demonstrated in [2], depend upon  $h_0$  to a certain degree, for  $h_0 > 15^\circ$  this dependence may be ignored in the first approximation.

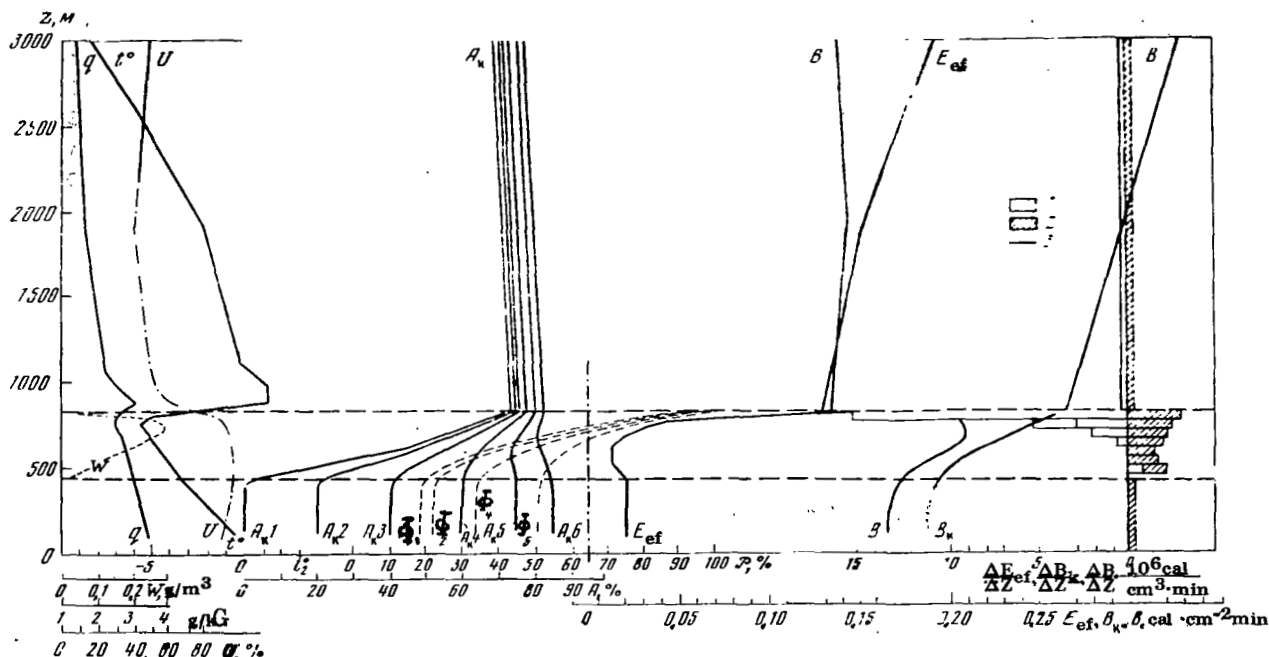
The effect of the albedo of the earth's surface may be excluded by using the "true" values of  $A_k^*$  and  $\phi^*$ . In [2] the methodology of their determination for the cloud as a whole is described, because of which expressions were obtained for the "true" values of the albedo and transmission for cloud layers ( $z_{n.g}$ ,  $z$ ) and ( $z$ ,  $z_{v.g}$ ) at  $z_{n.g} < z < z_{v.g}$ :

/73

$$A_{z, z_{n.g.}}^* = \frac{A_{z, z_{n.g.}} - \Phi_{z, z_{n.g.}}^2 \cdot A_{z, z_{n.g.}}^2}{1 - \Phi_{z, z_{n.g.}}^2 \cdot A_{z, z_{n.g.}}^2} \quad (1)$$

$$\Phi_{z, z_{n.g.}}^* = \Phi_{z, z_{n.g.}} \cdot \frac{1 - A_{z, z_{n.g.}} \cdot A_{z, z_{n.g.}}^*}{1 - A_{z, z_{n.g.}}^* \cdot A_{z, z_{n.g.}}^*} \quad (2)$$

$$A_{z, z_{n.g.}}^* = \frac{A_k - \Phi_{z, z_{n.g.}}^2 \cdot A_{z, z_{n.g.}}}{1 - \Phi_{z, z_{n.g.}}^2 \cdot A_{z, z_{n.g.}}^2} \quad (3)$$



Experimental model of the "average" stratoform cloud.

$t^\circ$  - the air temperature;  $U$  - the relative humidity;  $q$  - the specific humidity;  $\omega$  - the water content of the cloud;  $A_{k,i}$  and  $\Phi_i$  - the albedo and transparency or transmission of the cloud;  $i=1$  corresponds to  $A_z=0$ ;  $i=2$  corresponds to  $A_z=20\%$ ;  $i=3$  to  $A_z=40\%$ ;  $i=4$  to  $A_z=60\%$ ;  $i=5$  to  $A_z=75\%$ ;  $i=6$  to  $A_z=85\%$ ;  $B$  is the radiation balance;  $E_{ef}$  is the effective radiation;  $B_k$  is the balance of short-wave radiation;  $\Delta E_{ef}/\Delta z$ ,  $\Delta B_k/\Delta z$ , and  $\Delta B/\Delta z$  represent the radiation inputs of heat (1- long-wave; 2- short-wave; 3- total).

Here  $A_{z, z_{n.g}}$  and  $A_{z, z_{n.g}}^*$  are the measured and "true" values of the albedo of the cloud layer ( $z_{n.g}, z$ );  $\phi_{z_{v.g}, z}$  and  $\phi_{z_{v.g}, z}^*$  are the measured and "true" values of the relative transmission by the cloud layer ( $z, z_{v.g}$ );  $\phi_{z, z_{n.g}}$  is the relative transmission of the cloud layer ( $z_{n.g}, z$ ). We note that the ratio  $\phi_{z, z_{n.g}} = \phi / \phi_{z_{v.g}, z}$  occurs where  $\phi$  is the measured value of the relative transmission for the entire cloud;  $A_{z_{v.g}, z}^*$  is the "true" albedo of the cloud layer ( $z, z_{v.g}$ ).

Characteristics of the absorbing capability of the "average" cloud designated as  $b$  and  $b_{ef}$  were determined both for the entire cloud and for the layers ( $z_{v.g}, z$ ) = ( $b_{z_{v.g}, z}$  and  $b_{ef, z_{v.g}, z}$ ). For determination of the two latter quantities, the following formulas were used:

$$b_{z_{v.g}, z} = (1 - A_k) - \phi_{z_{v.g}, z} \cdot (1 - A_{z, z_{n.g}}), \quad (4)$$

$$b_{ef, z_{v.g}, z} = \frac{b_{z_{v.g}, z}}{(1 - A_k^*) \left( 1 + \frac{\phi_{z_{v.g}, z}^* \cdot A_{z, z_{n.g}}}{1 - A_k^* \cdot A_{z, z_{n.g}}} \right)} \quad (5)$$

The quantities  $A_{z, z_{n.g}}^*$  and  $\phi_{z_{v.g}, z}^*$ , obtained according to formulas (1) and (2) for each case of sounding, were then averaged by means of construction of the curves of their dependence upon the absolute humidity  $w$  of the corresponding layers of the cloud. The values of  $\overline{A_{z, z_{n.g}}^*}$  and  $\overline{\phi_{z_{v.g}, z}^*}$  for the "average" cloud were taken from this curve in accordance with the absolute humidity of the relative layers ( $z_{v.g}, z$ ) and ( $z, z_{n.g}$ ) 174

From Table 1, where the quantities  $\overline{A_{z, z_{n.g}}^*}$  and  $\overline{\phi_{z_{v.g}, z}^*}$  are given, it is apparent that the "average" stratoform cloud at  $A_3 = 0$  attenuates the flux falling on its upper boundary by 81%, and 41% falls to the share of the first 100-meter layer. The magnitudes of  $\phi_{z_{v.g}, z}^*$



in individual cases are subject to considerable oscillations, especially in thin layers. Such oscillations are explained by the variability of the absolute humidity and the microstructure of the cloud layers, and also by shortcomings in the methodology of the measurements.

According to the average values of the albedo and the transmission function, the magnitudes of  $b_{z.v.g.,z}$  and  $b_{ef,z.v.g.,z}$  were determined, which are also given in Table 1. It is apparent that the "average" cloud at  $A_z = 0$  absorbs 7.2% of the solar radiation falling on its upper boundary and 27.2% of the radiation entering the cloud. In the upper 100-meter layer 37.5% of the radiation is absorbed, out of that absorbed by the entire "average" cloud.

TABLE 1

z, m from upper boundary	$\Phi_{z.v.g.,z}^*$			$\Phi_{z.in.g.}$	$A_{z.in.g.}$	$A_{z.g.,z}$	$b_{z.v.g.,z}$	$b_{ef,z.v.g.,z}$
	av	max	min					
Upper boundary	1.00			0.19	0.74 (24)			
100	0.59 (50)	0.88	0.31	0.33	0.60 (24)	0.60	0.027	0.042
200	0.40 (46)	0.67	0.19	0.49	0.45 (38)	0.69	0.048	0.121
300	0.26 (37)	0.42	0.12	0.73	<del>0.28 (45)</del>	0.72	0.062	0.203
400	0.19 (24)	0.34	0.10			0.74	0.072	0.272

Note: The numbers in the parentheses signify the number of cases used in averaging.

For a description of the radiation regime of the layer over the cloud, an averaged profile of the albedo in this layer was constructed. From the drawing given it follows that over the "average" cloud the albedo decreases with altitude by 2%, on the average, for each kilometer of thickness in accordance with results of [2]. By using the data concerning the vertical profile of the albedo (see the drawing) and the data concerning the intensity of the downward flow of solar radiation [2], it is easy to determine the profile of the balance  $B_k$  and the absorbed  $\Delta B_k$  solar radiation (in  $\text{cal/cm}^2 \text{ min}$ ) in the layer over the cloud for various values of  $h_0$  and  $A_3 = 0$ . These data are presented in Table 2, from which it is apparent that in the layer above the

cloud the radiation influx depends strongly upon  $h_0$ , increasing with the rising of the sun over the horizon.

TABLE 2

175

Levels, m	Sym-bols	Altitude of sun					
		10	15	20	30	40	50
Above upper boundary	$B_R$	0,055	0,000	0,124	0,188	0,247	0,205
2000	$B_R$	0,064	0,402	0,139	0,211	0,276	0,333
3000	$B_R$	0,075	0,116	0,157	0,234	0,306	0,367
Upper boundary-2000	$\Delta B_R$	0,009	0,012	0,015	0,023	0,029	0,038
2000-3000	$\Delta B_R$	0,010	0,011	0,018	0,023	0,030	0,034
In the entire layer over the cloud	$\Delta B_R$	0,019	0,023	0,033	0,046	0,059	0,072

In the drawing, aside from the relative characteristics, vertical profiles of the magnitudes of  $B_k$ , effective radiation  $E_{ef}$ , radiation balance  $B$  and radiation influx due to short-wave radiation  $\Delta B_k$  and due to long-wave radiation  $\Delta B_d$  are presented, and also their sum  $B$ . These profiles were constructed under the assumption that  $Q(z_{v.g.}) = 1.00 \text{ cal/cm}^2 \text{ min}$  (which corresponds to  $h_0$  of about  $40^\circ$ ). These profiles demonstrate that the absorption of solar radiation occurs in the entire thickness of the cloud, and 14% of all the radiation absorbed by the cloud falls to the share of the lowest 100-meter layer.

The case of  $A_3 = 0$  was considered above.

The quantities  $\phi_{z_{v.g.}, z}$  and  $A_{z, z_{n.g.}}$  for real conditions ( $A_3 \neq 0$ ) may be determined according to their values at  $A_3 = 0$  by solving system of equations (1)-(3). In Table 3 the values of  $A_{z, z_{n.g.}}$  and  $\phi_{z_{v.g.}, z}$  are given for various values of  $z$  ( $z_{n.g.} < z < z_{v.g.}$ ) and, as a whole for the cloud, as a function of  $A_3$ . At  $Q(z_{v.g.}) = 1.00 \text{ cal/cm}^2 \text{ min}$ , with an increase in  $A_3$ ,  $A_{z, z_{n.g.}}$  increases, as

does  $\Phi_{z_{v.g}, z}$ . The albedo  $A_{300-n.g}$  of the lower layer increases most. The variation of  $A_z$  affects the magnitude of  $A_{v.g-n.g}$  considerably more weakly;  $\Phi_{v.g-n.g}$  undergo appreciable changes and  $\Phi_{z, z_{n.g}}$  lesser changes at  $z < z_{v.g}$ .

$A_3$  has an appreciable effect on the vertical distribution of  $\Phi_{z_{v.g}, z}$  and  $A_{z, z_{n.g}}$  (see the drawing). The vertical profile of  $\Phi_{z_{v.g}, z}$  does not change qualitatively in this variation, but the quantitative changes are very significant. The profile of the albedo varies even more. From the drawing it is apparent that at large values of  $A_3$  inside the cloud a decrease in  $A_{z, z_{n.g}}$  may be observed. The behavior of  $A_{z, z_{n.g}}$  at  $A_3 \neq 0$  agrees well with the data from specific measurements [3].

In real conditions ( $A_3 \neq 0$ ) the absorption by the "average" /77 cloud must increase as a consequence of the additional absorption of radiation reflected from the earth's surface. The ratio  $\Delta B_k / \Delta B_{k,0}$  may serve as a characteristic of additional absorption (the subscript "zero" corresponds to  $A_3 = 0$ ). The radiation characteristics of the layers ( $z_{n.g}, z$ ) and ( $z_{v.g}, z$ ) in the model of an average cloud at various values of  $A_3$  and at  $Q_{z_{v.g}} = 1.00$  cal per  $cm^2$  min are given in Table 3. From this table it follows that the cloud located over a surface with  $A_3 = 75\%$  (clean snow) must absorb approximately 30% more of the solar radiation than the same cloud located over a surface without snow ( $A_3 \sim 12-18\%$ ).

With an increase in  $A_3$  the contribution of the individual parts of the cloud to the total absorption also changes somewhat: the contribution of the lower half of the cloud, due to absorption of reflected radiation, increases somewhat (by 3-4%) and the contribution of the upper half decreases accordingly.

The absorption capability  $b$  increases from 0.072 ( $A_3 = 0$ ) to 0.105 ( $A_3 = 0.85$ ) with an increase of  $A_3$  (Table 3), although the properties of the clouds do not change. At the same time the

Table 3

z(below $z_{v.g.}$ ) in m	Quantities	Albedo of earth's surface					
		0,00	0,20	0,40	0,60	0,75	0,85
100	$A_{100, z_{n.g.}}$	0,595	0,616	0,652	0,703	0,756	0,804
	$P_{z_{v.g.}, 100}$	0,587	0,598	0,618	0,650	0,689	0,728
	$\Delta B_R$	0,027	0,028	0,030	0,032	0,034	0,037
	$\Delta B_R / \Delta B_{R, 0}$	1,00	1,035	1,11	1,18	1,26	1,37
	$\Delta B_R / \Delta B_{R, cloud}$	0,375	0,373	0,366	0,358	0,358	0,352
200	$A_{200, z_{n.g.}}$	0,454	0,505	0,571	0,660	0,745	0,810
	$P_{z_{v.g.}, 200}$	0,397	0,421	0,451	0,501	0,560	0,609
	$\Delta B_R$	0,021	0,021	0,022	0,023	0,025	0,029
	$\Delta B_R / \Delta B_{R, 0}$	1,00	1,00	1,05	1,09	1,19	1,38
	$\Delta B_R / \Delta B_{R, cloud}$	0,292	0,280	0,268	0,264	0,263	0,176
300	$A_{300, z_{n.g.}}$	0,232	0,346	0,471	0,611	0,740	0,830
	$P_{z_{v.g.}, 300}$	0,265	0,293	0,333	0,396	0,465	0,550
	$\Delta B_R$	0,014	0,015	0,017	0,019	0,022	0,023
	$\Delta B_R / \Delta B_{R, 0}$	1,00	1,07	1,21	1,36	1,57	1,64
	$\Delta B_R / \Delta B_{R, cloud}$	0,194	0,200	0,207	0,218	0,230	0,219
400	$\Delta B_R$	0,010	0,011	0,013	0,013	0,014	0,016
	$\Delta B_R / \Delta B_{R, 0}$	1,00	1,10	1,30	1,30	1,40	1,60
	$\Delta B_R / \Delta B_{R, cloud}$	0,139	0,147	0,159	0,150	0,149	0,153
Entire cloud	$A_R$	0,735	0,743	0,755	0,775	0,798	0,818
	$\Phi$	0,193	0,227	0,271	0,345	0,430	0,515
	$\Delta B_R$	0,072	0,075	0,082	0,087	0,095	0,105
	$\Delta B_R / \Delta B_{R, cloud}$	1,00	1,04	1,12	1,21	1,32	1,46
	$b$	0,072	0,075	0,082	0,087	0,094	0,105
	$b_{ef}$	0,272	0,274	0,272	0,271	0,271	0,273

magnitude of  $b_{ef}$  remains unchanged and equal to 27.2%. These quantities  $b$  and  $b_{ef}$  are close to the average values given in [2], and also to the data obtained by N. I. Chel'tsov [4] and by Neiburger [5].

## REFERENCES

1. Goysa, N. I. and V. M. Shoshin, "Experimental model of the radiation regime of a 'average' stratoform cloud", Trudy Ukr. NIGMI, No. 82, 1969.
2. Goysa, N. I. and V. M. Shoshin, "Experimental investigations of fluxes of solar radiation in the lower troposphere in St and Sc clouds", in this collection, page 60 [Russian text].
3. Goysa, N. I. and V. M. Shoshin, "Vertical profiles of the short-wave albedo in the lower troposphere", Trudy Ukr. NIGMI, No. 82, 1969.
4. Chel'tsov, N. I., "Investigation of reflection, transmission, and absorption of solar energy by clouds of certain forms", Trudy TsAO, No. 8, 1952.
5. Neiburger, M., "The reflection, absorption, and transmission of insolation by stratus clouds", J. Meteorol., 6, No. 2, 1949.

### III. TURBULENT AND RADIANT HEAT TRANSFER IN THE BOUNDARY LAYER OF THE ATMOSPHERE

#### ON THE CLOSING OF THE EQUATION OF HEAT INFLUX IN THE BOUNDARY LAYER OF THE ATMOSPHERE (According to Experimental Data)

L. R. Tsvang

The processes of heating and cooling of the boundary layer of the atmosphere are determined by a number of factors, playing a greater or lesser role in various synoptical situations, or over various types of underlying surface. In order to estimate the role of the various factors in these processes it is advisable to investigate the total equation of heat influx for the layer, which may be written in the following form: /78

$$C_p \rho \left( \frac{\partial T}{\partial t} + u \frac{\partial T}{\partial x} + v \frac{\partial T}{\partial y} + w \frac{\partial T}{\partial z} \right) = \frac{\partial B}{\partial z} + Q. \quad (1)$$

Here  $T$  is the potential temperature of the air;  $u$ ,  $v$ , and  $w$  are the longitudinal (along the  $x$  axis), transverse (along the  $y$  axis), and vertical (along the  $z$  axis) components of the wind velocity, respectively;  $B$  is the radiation balance;  $Q$  is the influx of heat in the layer due to the phase transitions;  $C_p$  is the specific heat content of the air at a constant pressure; and  $\rho$  is the density of the atmosphere.

Having presented the momentary values of the temperature and the components of the wind velocity as the sum of their average values and pulsations relative to this average and making the operation of averaging in equation (1), we obtain

$$\frac{\partial \bar{T}}{\partial t} + \bar{u} \frac{\partial \bar{T}}{\partial x} + \frac{\partial \bar{u}'T'}{\partial x} + \frac{\partial \bar{v}'T'}{\partial y} + \frac{\partial \bar{w}'T'}{\partial z} = \frac{1}{C_p \rho} \frac{\partial \bar{B}}{\partial z} + \frac{\bar{Q}}{C_p \rho}. \quad (2)$$

Here the bar over a symbol signifies the averaging in time (or in space) and the prime signs the pulsations of the corresponding components of the wind velocity or temperature relative to their average values. In the transition from (1) to (2), the following expressions were used:

$$\frac{\partial \bar{u}}{\partial x} + \frac{\partial \bar{v}}{\partial y} + \frac{\partial \bar{w}}{\partial z} = 0, \quad \bar{v} = \bar{w} = 0 \quad \text{and} \quad \bar{u}' = \bar{v}' = \bar{w}' = \bar{T}' = 0.$$

Simultaneous measurements of all the terms entering into equation (2) in the selected layer of the atmosphere make it possible to estimate the role of each of them in the heating of the given layer.

By investigating the transformation of the terms of the equation of influx of heat over various types of underlying surface as a function of altitude and under various synoptic conditions, we obtain data concerning the mechanism of heat transfer making it possible to check the theoretical models of this mechanism. A number of works have been devoted to this problem, which were performed in the Department of Atmospheric Turbulence of the IFA in recent years [1-3]. /79

In our measurements, not all the seven terms entering into equation (2) were determined. In the layer of air at altitudes from 1 to 500 m, where no phase transitions of the moisture occur, the last term in the righthand part of equation (2) may be ignored. We may also assume that the item  $\partial v' T' / \partial y$ , representing turbulent heat transfer in a direction perpendicular to the average transfer, will be equal to zero because of the symmetry of the motions of the air relative to the average wind direction. The term  $\partial u' T' / \partial x$ , determining the divergence of the horizontal turbulence of the heat flux, was not measured. We assumed that in any case it must be considerably less than the heat advection defined at  $\bar{u}(\partial \bar{T} / \partial x)$ . In the future, however, it is desirable to check this assumption experimentally.

Considering the assumptions expressed here, equation (2) may be written in the form

$$\frac{\partial \bar{T}}{\partial t} + \bar{u} \frac{\partial \bar{T}}{\partial x} + \frac{\partial \overline{w' T'}}{\partial z} = \frac{1}{C_p \rho} \frac{\partial \bar{B}}{\partial z} . \quad (3)$$

The measurements of three of the four terms entering into equation (3) (the advective heat influx was not measured) at first were performed in the surface layer of the atmosphere at altitudes of 1 and 4 m from the surface of the earth [1]. These measurements were conducted by means of an acoustic anemometer (vertical pulsations of the wind velocity  $w'$ ), a resistance thermometer (pulsations of the temperature  $T'$ ), and an electron multiplier making it possible to obtain the average values of the product  $w' T'$  in a period of 100 s directly in the process of measurements. The radiation balance was measured by means of the radiation thermoelements designed by B. P. Kozyrev.

The entire set of pickups was installed alternately at two altitudes, at each of which the measurements were performed for 10-15 min.

The results of the measurements demonstrated that in the majority of cases the balance with respect to the sum of the three items in equation (3) did not close. As a rule, an appreciable cooling of the 1-4 m layer due to turbulence was observed. An estimate was made of the possible role of the advective term. It turned out that at the average wind velocity observed during the measurements is sufficient to have horizontal temperature gradients  $\partial \bar{T} / \partial x$  of the order of  $0.1^\circ \text{ C} / 100 \text{ m}$ , in order to compensate for the role of turbulent heat transfer in (3) and to close the equation of heat influx. Gradients  $\partial \bar{T} / \partial x$  of such an order of magnitude or more were found by Rider and his associates and are described in [4]. The measurements of radiation heat influxes conducted simultaneously with measurements of turbulent influxes demonstrated that due to long-wave and short-wave components of radiation, the surface layer of the air in summer, in the daytime, was considerably heated. However, the inadequate accuracy of the measurements by means of radiation thermoelements did not make it possible to reach a reliable judgement of the relative role of radiation in heating of the surface layer of the air. /80

In 1966 measurements were made of the heat influx in the layer from 50-500 m from onboard an aircraft [2]. In these measurements all four terms in eq. (3) were determined. The apparatus and methodology of the measurements in [2] are analogous to those which were used in [1]. For consideration of the natural motions of the aircraft, corrections were introduced into the output signal of the acoustic anemometer directly in the process of measurement, and these corrections considered the vertical movements of the aircraft and the variations of its pitch angle. The measurements were conducted in summer in conditions of well-developed convection in flights over the steppe and over the sea.

Analysis of the results of the measurements demonstrated that in the conditions indicated, in the boundary layer of the atmosphere the turbulent, radiation, and advective heat influxes have the same order of magnitude.

In this case the necessity of increasing the accuracy of measurement of turbulent, radiation, and horizontal heat influxes from onboard an aircraft was ascertained. For this purpose, the following cycle of works was performed:

1. On measurements of the vertical turbulent heat flux.  
The vertical turbulent heat flux  $q_v$  is determined



by the relation

$$q_v = C_p \overline{\rho w' T'}. \quad (4)$$

Immediately questions arise concerning the necessary time (or distance) and concerning the averaging scale. The answer to these questions may be obtained by performing measurements of the spectra of the turbulent heat fluxes  $F_{wT}$ , which are the real part of the Fourier transform of the mutual correlation function  $R_{wT}(\tau)$ :

$$F_{wT}(\omega) = \frac{1}{2\pi} \int_{-\infty}^{\infty} R_{wT}(\tau) \cos \omega \tau d\tau, \quad (5)$$

where

$$R_{wT}(\tau) = \overline{w(t) T(t + \tau)}.$$

For measurements of the spectrum of heat fluxes a multi-channel magnetic recording apparatus and a system for reproduction and analog processing of the results of the measurements were developed [3].

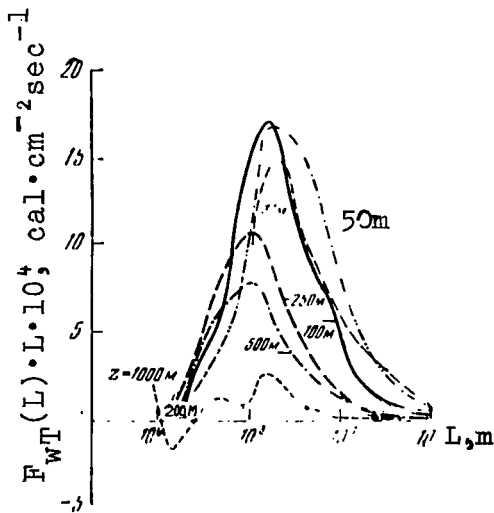


Fig. 1. Averaged spectra of turbulent heat fluxes for various altitudes.

$L$  - dimension of the heterogeneities, in m ( $L=u/f$ , where  $f$  is the frequency of the pulsations recorded,  $u$  is the speed of the aircraft); the digits at the curves designate the altitudes over the surface of the earth to which the data obtained refer.

The measurements of the spectra of heat fluxes were performed on a mast and on a tower at altitudes from 2.5 to 37 m in 1967 [5] and from onboard an aircraft at altitudes from 50 to 1000 m from the surface of the earth in 1967 and 1968 [3]. All the measurements were conducted in the summer season of the year, by day, in conditions of well-developed convection in the steppe regions of

the country. In Fig. 1 the spectra of the turbulent heat fluxes, averaged for various altitudes, on a scale  $F_{wT}(L) \times L$  are presented (along the abscissa axis the logarithms of  $L$  are plotted). Here  $L = 2\pi u/\omega$  ( $u$  is the speed of the aircraft) is the dimension of the turbulent heterogeneities, in meters. The presentation of the spectra of turbulent fluxes in such scales is clearest, since in this case the area under the curve determines the total quantity of heat transferred by the turbulent pulsations.

According to data from measurements it turned out to be possible to make the following conclusions: beginning from the surface layer up to altitudes of 500 m from the surface of the earth the spectra of turbulent heat fluxes have a clearly expressed maximum and drop practically to zero both in the region of large and in the region of small scales. Thus, the presentation of the total turbulent heat flux as the integral with respect to the spectrum  $F_{wT}(L)$

$$q = C_{p0} \int_0^{\infty} F_{wT}(L) dL = C_{p0} \int_0^{\infty} F_{wT}(L) L d \ln L \quad (6)$$

has a definite meaning, since the integral in (6) converges.

However, the behavior of the function  $F_{wT}(L) \times L$  in the region of scales greater than a few kilometers is unknown. Thus, in the spectrum measured at an altitude of 1 km at scales of heterogeneity greater than a few kilometers, values of  $F_{wT}(L) \times L$  are observed that differ from zero (Fig. 1). For purposes of identification of the results of the measurements conducted by various authors by means of apparatus that varied in characteristics, it is proposed (see [3]) to determine the turbulent heat flux as the flux created by pulsations with scales extending from the Kolmogorov microscale to scales corresponding to the break in the spectrum of  $F_{wT}(L) \times L$ . /82

For turbulent heat fluxes defined in such a manner, the boundary dimensions of the heterogeneities ( $L_{\min}$  and  $L_{\max}$ ) were found, within the limits of which the basic contribution to turbulent heat transfer is accomplished (90% of the general turbulent heat flux). These data, presented in Fig. 2, make it possible to determine the necessary frequency characteristics of the measuring apparatus and the averaging time in the measurement of turbulent heat fluxes at altitudes up to 500 m above the surface of the earth. We should emphasize that in direct measurements of the total heat fluxes [not determined from the spectra of  $F_{wT}$ , but in accordance with (4)]

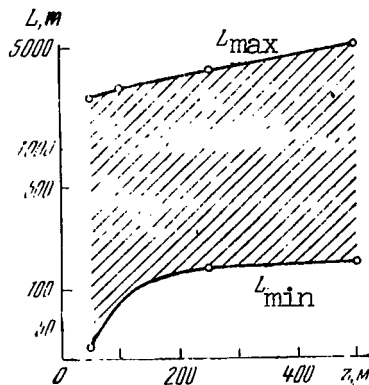


Fig. 2. Dependence of the dimensions of turbulent heterogeneities making the basic contribution to turbulent heat transfer upon altitude.

$L_{\min}$  and  $L_{\max}$  are the boundary dimensions of these heterogeneities, within the limits of which 90% of the energy of the turbulent heat flux is included.

it is necessary to limit the frequency range of the pulsations being measured in the low-frequency region by a magnitude close to  $\omega = (u \cdot 2\pi / L_{\max})$ . Otherwise, an indefinite error may be introduced into the results of the measurements due to random medium-scale fluctuations.

## 2. On measurements of the radiation heat influx.

For the purpose of increasing the accuracy of measurements of the radiation balance, at the Institute of the Physics of the Atmosphere, a modulation balance gauge was developed making it possible to measure the balance in two spectral regions: short-wave ( $\lambda = 0.3-3$  microns) and long-wave ( $\lambda = 3-40$  microns) [6].

/83

The modulation balance gauge successfully passed its test in field conditions in 1969.

## 3. On measurements of the horizontal heat influx.

It is determined both by the advective term  $\bar{u}(\partial T / \partial x)$ , and by the divergence of the horizontal turbulent heat flux,  $\partial \bar{u'T'}/\partial x$ . For measurement of the magnitude  $\bar{u'T'}$  an aircraft hot-wire anemometer was developed and tested, by means of which the first measurements of the spectra  $F_{uu}$  were conducted, i.e., pulsations of the horizontal component of the wind velocity, and the spectra  $F_{uw}$ , of the turbulent fluxes of momentum.

After completion of the works listed with respect to improvement of the methodology of measurements of the individual terms entering into equation (3), investigations of the heating mechanism of the boundary layer of the atmosphere and the closing of the equation of heat influx for this purposes will be continued.

## REFERENCES

1. Mordukhovich, M. I. and L. R. Tsvang, "Direct measurements of turbulent fluxes (of heat) at two altitudes in the surface layer of the atmosphere", *Izv. AN SSSR, seriya FAO*, No. 8, 1966.
2. Volkov, Yu. A., V. P. Kukharets, and L. R. Tsvang, "Turbulence in the boundary layer of the atmosphere over steppe and sea surfaces", *Izv. AN SSSR, seriya FAO*, No. 10, 1968.
3. Kukharets, V. P. and L. R. Tsvang, "Spectra of turbulent heat fluxes in the boundary layer of the atmosphere", *Izv. AN SSSR, seriya FAO*, No. 11, 1969.
4. Rider, N. E., I. R. Philip, and E. F. Bradley, "The horizontal transport of heat and moisture a micrometeorological study", *Quart. J. Roy. Meteorol. Soc.*, 89, N. 382, 1963.
5. Zubkovskiy, S. L. and B. M. Koprov, "Experimental investigation of the spectral turbulent heat fluxes and the momentum in the surface layer of the atmosphere", *Izv. AN SSSR, seriya FAO*, No. 4, 1969.
6. Sokolov, D. Yu., *Modulyatsionnyy balansomer (Modulation Balancer)*, Report of IFA, 1969.

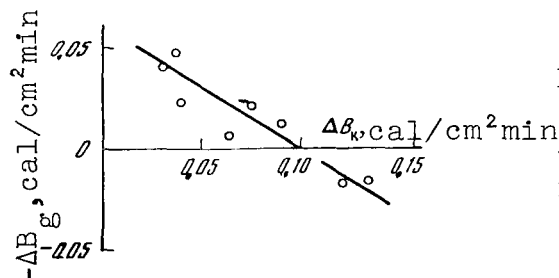
# DETERMINATION OF THE RADIATION HEAT FLUX IN THE BOUNDARY LAYER OF THE ATMOSPHERE

V. D. Oppengeym and G. P. Faraponova

In this work certain results of the measurements of fluxes of /84 short-wave and long-wave radiation in the boundary layer of the atmosphere (0.05-1.5 km) are given. Measurements of the fluxes were conducted by means of radiation thermoelements designed by V. P. Kozyrev (RTE) on an LI-2 aircraft in the summer period (July-August) in three regions of the Soviet Union: above the steppe in the vicinity of the city of Tsimlyansk and the city of Dnepropetrovsk and over the sea in the vicinity of the city of Gelendzhik. Actinometric measurements were made at altitudes of 50-70, 100-150, 250-300, 500, 750, 1000, and 1500 meters. For determination of the radiation heat influx, data obtained at hours near noon in cloudless weather were used (the presence of cloud cover of up to 2-3 on a scale of 10 on the sunlit side was assumed), and also by night.

The results of the work performed are described in detail in ref. [1].

According to the experimental data the vertical profiles of the short-wave radiation flux  $Q$ ,  $D\uparrow$  were constructed, as well as those of the long-wave radiation flux  $F\downarrow$ ,  $F\uparrow$ , and also profiles of the effective radiation  $F$ .



Dependence of the absorption of long-wave radiation,  $\Delta B_d$  upon the absorption  $\Delta B_k$  of short-wave radiation.

The radiation heat influx  $\Delta B$  in the layer  $(z_1; z_2)$  was determined as the sum of influxes of short-wave radiation,  $\Delta B_k = B_k(z_2) - B_k(z_1)$  and long-wave radiation,  $\Delta B_d = B_d(z_2) - B_d(z_1)$ . According to these data, the radiation variations of the temperature due to short-wave and long-wave radiation were calculated separately, and also the magnitudes of total radiation heating. The latter, in the

Steppe in vicinity of Tsimlyansk				Steppe in vicinity of Dnepropetrovsk				Black Sea near Gelendzhik			
Date	$\Delta B_K$	$\Delta B_d$	$\Delta B$	Date	$\Delta B_K$	$\Delta B_d$	$\Delta B$	Date	$\Delta B_K$	$\Delta B_d$	$\Delta B$
Day											
7/30/65	0,035	0,049	0,084	7/29/66	0,072	0,021	0,093	7/18/66	0,121	-0,017	0,104
8/01/65	0,030	0,042	0,072	7/30/66	0,061	0,006	0,067	7/21/66	0,137	-0,061	0,076
8/02/65	0,038	0,023	0,061	7/31/66	0,087	0,012	0,099	7/22/66	0,107	-0,035	0,072
Average measured	0,034	0,038	0,072	8/08/66	0,118	-0,016	0,102		0,122	-0,038	0,084
				8/14/66	0,131	-0,016	0,115				
					0,094	+0,001	0,095				
$\Delta B_K (H_2O) \text{ calc}$	0,022				0,019				0,030		
$\frac{\Delta B_K}{\Delta B_K (H_2O)}$	1,54				5,0				3,5		
Night											
8/4-5/65		-0,033		7/29/66		-0,046		7/23-24/66		-0,078	
8/05/65		-0,036									
Average measured		-0,034		8/14/66		-0,051		7/24/66		-0,127	
						-0,048				-0,102	

noontime hours over the steppe, according to data from the measurements, did not exceed 0.4 degree/hr, and radiation cooling in the nighttime hours was -0.1 to 0.2 degree/hr. Radiation heating over the sea (0.2-0.3 degree/hr) in the noontime hours with respect to absolute value, was close to the magnitude of total radiation cooling.

It was observed that above the steppe in the noontime hours at a small degree of turbidity (pollution) of the atmosphere, up to a level of 1-1.5 km, due to absorption of long-wave radiation, radiation heating of the air may be observed, the magnitude of which is comparable with heating due to short-wave radiation. In this case it was noted that at small values of  $\Delta B_k$  the influx  $\Delta B_d$  is positive (see drawing). With an increase in  $\Delta B_k$ , the magnitude of  $\Delta B_d$  decreased to zero, and then changed its sign. Apparently, the heating of the atmosphere due to absorption of long-wave radiation, which was observed at a small degree of pollution (a small value of  $\Delta B_k$ ) was caused by the strong superheating of the soil relative to the air, regulated by the content of aerosols in the atmosphere. By night cooling of the air was always observed. The data of the variations of the radiation balance in the 50-1000 m layer are given in the table, in calories per  $\text{cm}^2$  per minute. /86

According to F. Moeller's formula, the absorption of short-wave radiation by water vapor was calculated ( $\Delta B_{k(\text{H}_2\text{O})}$ ). It turned out that in all the cases considered  $\Delta B_k > \Delta B_{k(\text{H}_2\text{O})}$ , and the ratio  $\Delta B_k / \Delta B_{k(\text{H}_2\text{O})}$  varied within limits from 1.5 to 5.0, increasing with an increase in the pollution of the atmosphere in the region being investigated. The results obtained indicate the considerable role of the atmospheric aerosol in the process of absorption of short-wave radiation.

In estimation of the results we should bear in mind the fact that the observed variations of  $\Delta B_k$  in a number of cases turned out to be comparable with instrumental and methodological errors of measurement, which indicates the necessity of the continuation of these works with more accurate measurements of the radiation fluxes.

#### REFERENCE

1. Faraponova, G. P., V. D. Oppengeym, V. I. Kolesnikova, A. K. Mayorov, and M. A. Kuznetsova, "Determination of the radiation heat influx in the lower layers of the atmosphere", Izv. AN SSSR, seriya FAO, 4, No. 9, 1968.



#### IV. STATISTICAL STRUCTURE OF RADIATION FIELDS IN CLOUDS

##### SOME PROBLEMS OF THE METHODOLOGY OF MEASUREMENT OF AVERAGE FLUXES OF SHORT-WAVE RADIATION IN CLOUD COVER

Yu. R. Mullamaa, V. K. Pyldmaa, and M. A. Sulev

The majority of the phenomena of nature should be considered /87 as random in space and in time. For investigation of any sort of characteristics of these processes or their interrelationships, the accumulation of an enormous amount of experimental material is required. But, on the other hand, if we note certain characteristics of the phenomenon in advance or have made certain assumptions concerning them, we may, by depending on the laws of mathematical statistics, set up experiments in a more reasoned manner, save time and funds necessary for obtaining the information of interest, and also estimate the accuracy and reliability of the results obtained. It is precisely from this standpoint that in this article certain problems of the methodology of measurement of average fluxes of short-wave radiation (in terms of mathematical statistics, estimates of mathematical expectation) are considered. All the ratios explained below are general and applicable for any random process if we assume that it is steady-state [1]. For an example, and for purposes of obtaining certain quantitative estimates, specific results of ground and aircraft measurements of the variability of the field of short-wave radiation were used [3], [IV.17; IV.19; IV.22].

In measurements of natural processes, one report taken separately is random in nature; to obtain reliable information, a certain averaging is required. Obtaining an accurate average (mathematical expectation) of a random function is practically impossible, and therefore, instead of it, an estimate of it is used, which, with a specific method of processing the material, is calculated according to the formula

$$\bar{\Phi} = \frac{\sum_{i=1}^M \varphi_i}{M}, \quad (1)$$

where  $\bar{\Phi}$  is the average radiation flux;  $\varphi_i$  is the magnitude of the flux in the  $i$ -th reading;  $M$  is the number of successive readings used to obtain the average. The dispersion of the average, with /88  $M$  successive readings, as is well-known [1,2], is determined by

$$\sigma_{\Phi_M}^2 = \frac{\sigma^2}{M^2} \left[ M + 2 \sum_{k=1}^{M-1} (M-k) r(k\Delta) \right], \quad (2)$$

where  $\sigma^2$  is the dispersion of the total series  $\varphi_1$ ;  $\Delta$  is the interval between adjacent readings;  $r(k\Delta)$  is the standardized autocorrelation function. In Fig. 1 examples of the variation of the square root of the dispersion of the average radiation flux,  $\sigma_\Phi$  as a function of the averaging scale are presented. The quantities entering into formula (2) were taken from specific measurements and the autocorrelation functions were approximated by an exponential function of the form  $r(k\Delta) = e^{-\alpha k\Delta}$ . In Fig. 2 the fluctuation of the variability factor  $V_\Phi = \sigma_\Phi / \Phi$  of the average for the same cases is given.

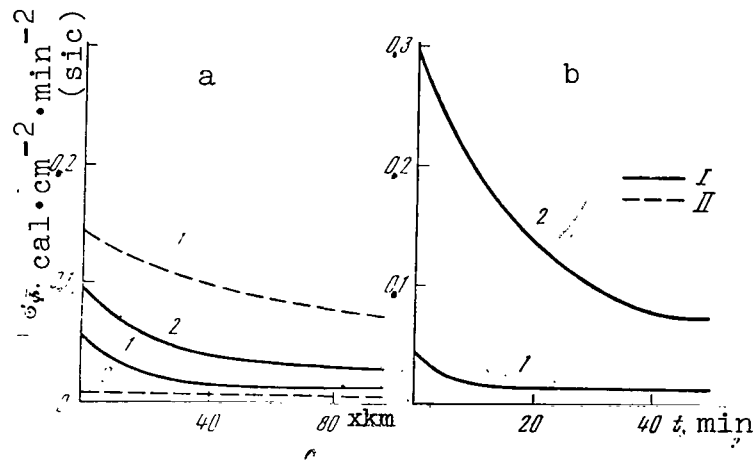


Fig. 1. Mean square deviations  $\sigma_\Phi$  of average fluxes as a function of the averaging scale.  
a- averaging with respect to space (aircraft measurements);  
1- flight over clouds 8-10 Sc; 2- flight under clouds 10 Cu fr. Sc; I- descending fluxes; II- ascending fluxes;  
b- averaging with respect to time (ground measurements);  
1- 10 St fr.; 2- 9 Cu.

Frequently in the statement of the experiment it is required that we determine the necessary averaging scale to obtain an average with the assigned accuracy. In this case, it is advisable to use the concept of the confidence interval

$$[\bar{\Phi}_M - \delta \bar{\Phi}_M; \bar{\Phi}_M + \delta \bar{\Phi}_M].$$

As is well known, the interval where with a probability  $\beta$  the unknown parameter, such as  $\bar{\Phi}$ , for example, is found, is called the confidence interval. In the first approximation, considering the distribution of the deviations of the estimates of the average  $\bar{\Phi}_M$  from the true  $\bar{\Phi}$  to be normal, we obtain [1] /89

$$\delta\bar{\Phi}_M(\beta) = \sigma\bar{\Phi}_M \arg \operatorname{erf} \beta, \quad (3)$$

where  $\arg \operatorname{erf} \beta$  is such a value of the argument of the integral of probability at which the latter is equal to  $\beta$ . Having assumed the maximum permissible error of the average flux  $\sigma\bar{\Phi}_M$  and the probability  $\beta$  with which the result of the averaging must have an error less than  $\sigma\bar{\Phi}_M$ , we may determine the necessary averaging scale for performance of (3) with respect to the variation of  $\sigma\bar{\Phi}_M$  with an averaging scale  $M$ .

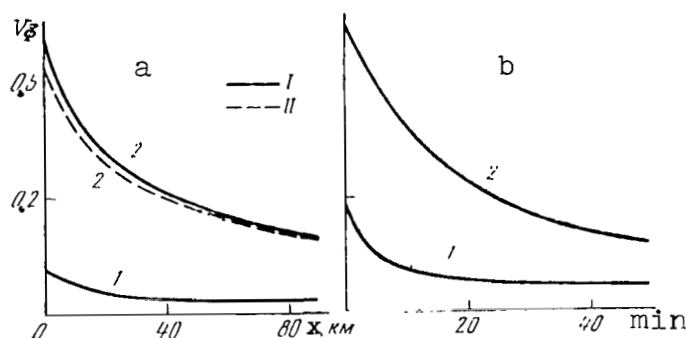


Fig. 2. Variability factors  $V_{\bar{\Phi}}$  of the average fluxes as a function of the averaging scale.  
a- averaging with respect to space: 1- flight over clouds 8-10 Sc; 2- flight under clouds 10 Cu fr. Sc; I- descending fluxes; II- ascending fluxes; b- averaging with respect to time: 1- 10 St fr.; 2- 9 Cu.

For the quantitative estimates of the effect of the averaging scale on the accuracy of the results, we may use the so-called efficiency index, representing the ratio of the dispersion of the average to the dispersion of the random function under consideration,  $k_e = \sigma_{\bar{\Phi}}^2 / \sigma_{\Phi}^2$ . The quantity which is the reciprocal of it,  $N_e = 1/k_e$  is called the effective number of measurements and demonstrates how many specific independent measurements are needed to

achieve the same accuracy as in the mean arithmetical method of processing. The condition of independence requires that the interval between adjacent measurements with respect to time or in space be greater than the argument of the autocorrelation function at which the latter becomes practically equal to zero. In Fig. 3 the efficiency index  $k_e$  is represented, with a scale of the effective number of measurements corresponding to the averaging scale indicated on the abscissa axis.

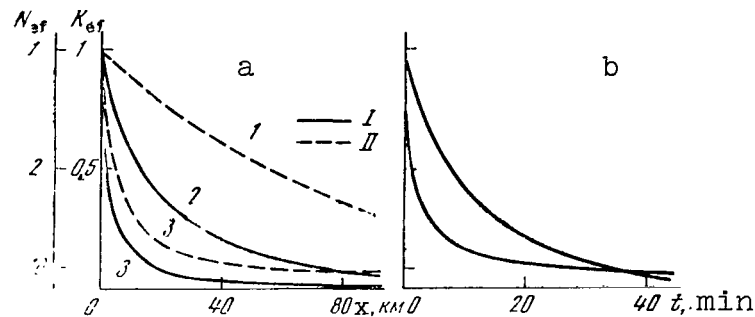


Fig. 3. Efficiency index  $k_e$  with the scale of the effective number of measurements,  $N_e$  and the averaging scale corresponding to it.

a- averaging with respect to space; 1- flight over clouds 8-10 Sc; 2- flight under clouds 10 Cu fr. Sc; 3- flight through summit of Ac layer; I- descending flows; II- ascending flows; b- averaging with respect to time: 1- 10 St fr; 2- 9 Cu.

At a given averaging scale the efficiency of the estimate of the average depends upon the interval between readings or upon the number of readings in an averaging segment. With an increase in the number of readings the accuracy of averaging at first increases rapidly, and then slower and slower, and finally becomes almost constant. Therefore, to facilitate the processing of numerous measurements it is advisable to determine the so-called optimum step, i.e., the interval between readings, a further decrease of which does not lead to a noticeable increase in the accuracy of results. Its value,  $\Delta_{opt}$ , may be determined in approximation according to [1] from the relation

$$\frac{4}{3} r \left( \frac{\Delta_{opt}}{2} \right) - \frac{5}{6} r (\Delta_{opt}) = \frac{1}{2}. \quad (4)$$

In statistical analysis, aside from the average value of radiation fluxes, a determination of dispersion and correlation function is required, and also an estimate of the accuracy of their averaging. In the practical processing of recordings of radiation fluxes the dispersion estimates  $\sigma_{\Phi}^2$  and the autocorrelation function  $r(\Delta k)$  are calculated according to the following formulas [1]:

$$\sigma_{\Phi}^2 = \frac{1}{M(1-k_e)} \sum_{i=1}^M (\varphi_i - \bar{\Phi})^2, \quad (5)$$

$$r(k\Delta) = \frac{1}{\sigma_{\Phi}^2(M-k)} \sum_{i=1}^{M-k} (\varphi_i - \bar{\Phi})(\varphi_{i+k} - \bar{\Phi}). \quad (6)$$

To ascertain the accuracy of the estimates of the dispersion and the autocorrelation function we must determine their dispersions  $\sigma_{\sigma_{\Phi}^2}^2$  and  $\sigma_{r(k\Delta)}^2$ , respectively. We succeed in this only for a normal /91  
steady-state random sequence of the magnitudes  $\varphi_i$ . In this case, following [1], we obtain

$$\sigma_{\sigma_{\Phi}^2}^2 = \frac{2\sigma_{\Phi}^4}{M} \left[ 1 + 2 \sum_{i=1}^{M-1} \left( 1 - \frac{i}{M} r^2(i\Delta) \right) \right] \quad (7)$$

and

$$\sigma_{r(k\Delta)}^2 = \frac{\sigma_{R(k\Delta)}^2 [1 - r^2(k\Delta)]^2}{\sigma_{\Phi}^4}, \quad (8)$$

where

$$\sigma_{R(k\Delta)}^2 = \frac{\sigma_{\Phi}^4}{(M-k)^2} \sum_{i=-(M-k)}^{M-k} [(M-k-|i|) r_i^2 + r_{i+k} r_{i-k}] \quad (9)$$

is the dispersion of the unstandardized autocorrelation function. For two specific cases, in Fig. 4 the standardized autocorrelation functions  $r(\Delta k)$  are given, the square roots of their dispersion, and the variability factors  $V_{r(\Delta k)} = \sigma_{r(\Delta k)} / r(\Delta k)$ . As we should have expected, the correlation function as the second moment is determined with a much lower accuracy than the average fluxes. Usually at  $r_{\Phi} \leq 0.1$  the error of its determination becomes greater than 100% and further consideration of the correlation function does not make any sense.

At the present time, a considerable amount of experimental material has been accumulated with respect to the variability of fluxes of short-wave radiation in space and time in cloud cover, as in refs. [3], [IV.17]; [IV.19]; [IV.22], which makes it possible to formulate the following conclusions.

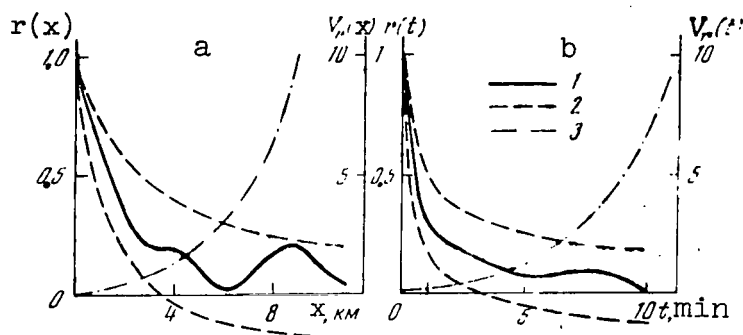


Fig. 4. Autocorrelation function  $r(x)$  (1) with mean square deviation  $\sigma_r$  (2) for the total radiation flux and its variability factor  $V_r$  (3).

a- according to aircraft measurements; b- according to ground measurements.

1. At the measured fluxes of short-wave radiation in a cloudy atmosphere to obtain a reliable average a considerable averaging is required. For aircraft measurements, the necessary averaging scale with respect to space amounts to 25-100 km, depending upon the type of radiation and the state of the cloud cover, and for ground measurements averaging with respect to time within limits from several minutes to several hours is required, depending upon the form and quantity of the clouds. In the majority of cases, such an accuracy of the average flux may be obtained with 5-10 independent measurements. We must note that these independent measurements may be accomplished by two methods. In the first place, they may be performed from one observation point at a certain interval of time, and the minimum possible interval is determined by the condition of independence  $\Delta t \geq t_{r \rightarrow 0}$ , where  $t_{r \rightarrow 0}$  is the value of the argument of the autocorrelation function in which the latter approaches zero. In the second place, independent measurements may be simultaneous, but performed at different points, the distance between which is  $\Delta x \geq x_{r \rightarrow 0}$ . The maximum possible interval between the independent

measurements is determined by the requirement that all the measurements be located within the limits of the steady-state random process being investigated.

2. In the processing of recordings for purposes of obtaining average magnitudes of fluxes, it is always useful to consider the optimum step (taking the ordinates and readings), since this makes it possible to save time and labor in data processing considerably. Usually the optimum spatial step in aircraft measurements of fluxes of short-wave radiation lies within limits of 0.4-7.0 km, and the time step in ground measurements is not less than 1 minute.

3. Averaging in space or in time, or averaging according to independent measurements, makes it possible to decrease the dispersion of the average radiation flux by an order of magnitude in comparison with one momentary measurement. For a further decrease in the error, a considerable increase in the averaging scale is required, which is usually practically impossible, since in nature steady-state situations (fields of clouds) of adequate length are rarely encountered. From this follows the necessity of revision of methods of experimental determination of radiation fluxes, their vertical profiles and radiation heat influxes in the atmosphere. In measurements in natural conditions we should bear in mind the fact that the accuracy of the result obtained is determined not only by the accuracy of the instruments, but primarily by the nature of the variability of the quantity being measured.

## REFERENCES

1. Vilenkin, S. Ya., Statisticheskiye metody issledovaniya sistem avtomaticheskogo regulirovaniya (Statistical Method of Study of the Systems of Automatic Regulation), Moscow, "Sov. Radio," 1967.
2. Lamli, Dzh. L. and G. A. Panovskiy, Struktura atmosfernoyn turbulentnost' (Structure of Atmospheric Turbulence), Izd-vo "Mir," 1966.
3. Mulamaa, Yu. R., M. Sulev and V. Pyldmaa, "Space and time structure of fluxes of short-wave radiation and the problem of measuring the average fluxes," Collection: Radiatsiy i oblachnost' (Radiation and Cloudiness), IFA AN ESSR, Tartu, 1969.



# ON THE ACCURACY OF THE AVERAGING OF TOTAL RADIATION FLUXES

V. K. Pyldmaa

The measurement of fluxes of solar radiation not infrequently is associated with their averaging in a certain interval of time. While in a cloudless sky averaging does not present any special difficulties, in clouds, especially broken clouds, because of the essential variability of the radiation field, the problem of the accuracy that can be achieved unavoidably arises. Since the nature of the variability of the radiation field in time depends upon the form and quantity of the clouds [IV.19], the accuracy of the determination of the average fluxes also must depend upon the parameters of the cloud field. /93

By using the data concerning the variability of the radiation field from experiment [IV.19], we will consider what the possible accuracy of the averaging of total radiation fluxes in certain specific conditions of cloud cover may be. We will select the relative mean square error of the estimate of the average flux as the index of the accuracy of averaging:

$$\gamma_{\bar{Q}} = \frac{\sigma_{\bar{Q}}^2}{\bar{Q}^2}. \quad (1)$$

Here  $\bar{Q}$  is the average flux of relative total radiation [IV.19],  $\sigma_{\bar{Q}}^2$  is the dispersion of the estimate of the average, determined from the relation (see [2])

$$\sigma_{\bar{Q}}^2 = \frac{\sigma^2}{M} \left[ M + \sum_{k=1}^{M-1} (M-k) r(k\Delta t) \right], \quad (2)$$

where  $r$  is the standardized autocorrelation function;  $\sigma^2$  is the dispersion of the random process under consideration;  $\Delta t$  is the time interval between adjacent readings; and  $M$  is the number of readings. As is apparent from formulas (1) and (2), the averaging accuracy that can be achieved is determined on the one hand by the nature of the variability of the process being investigated, and, on the other hand, by the selected step between the reading and the averaging scale.

As the dispersions  $\sigma^2$  entering into formulas (1) and (2), and the average flux  $\bar{Q}$ , we will use their averaged values, obtained from measurements [IV.19]. The autocorrelation functions necessary for the calculation of  $\gamma_{\bar{Q}}$  were obtained according to

measurements at Tyraver and were averaged according to several realizations (Fig. 1). The dependence of  $r(t)$  upon the quantity of cumulus clouds presented in Fig. 1 testifies to the equal value of time correlation connections with a considerable amount of cover of the sky by clouds and the presence of extensive regions of cloudless sky. At the same time  $r(t)$  at  $n = 10$  points for various forms of clouds (10 Ci or Cs, 10 Sc, 10 St, 10 Cu) practically coincide. It is possible that the essential dependence of  $r(t)$  upon the form of clouds appears at  $n < 10$ , where the joint effect of the characteristics of the structure of the cloud cover and the characteristic angular velocity of its motion is noticeably felt.

194

In problems connected with the averaging of radiation fluxes in time, the average flux is either determined for a certain given interval of time (such as, for example, the average per hour) or is given the necessary accuracy of the result, and the averaging scale in this case is not strictly limited. We will consider the possibilities of averaging in these cases.

For random processes, as is known [2], an optimum interval  $\Delta t_0$  between specific readings exists, a further decrease of which does not lead to an increase in the accuracy of averaging. The optimum step  $\Delta t_0$ , determined from the relation [1]

$$\frac{4}{3} r\left(\frac{\Delta t_0}{2}\right) - \frac{5}{6} r(\Delta t_0) = \frac{1}{2}, \quad (3)$$

is presented in Fig. 2, as a function of the quantity of cumulus clouds. Since  $\Delta t_0$  is determined only according to the form of the autocorrelation functions, its value for 10 Cu is applicable also for 10 points for the other forms of clouds that have been considered.

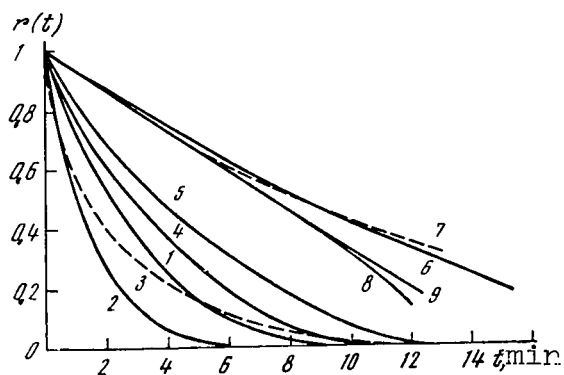


Fig. 1. Averaged autocorrelation functions of the total radiation flux for various conditions of cloud cover.

- 1) 2 Cu; 2) 3-4 Cu; 3) 4-5 Cu;  
4) 6 Cu; 5) 7-8 Cu; 6) 9-10 Cu,  
(Cb); 7) 10 Ci, Cs; 8) 10 Sc;  
9) 10 St.

The essential dependence of  $\Delta t_0$  upon the quantity of cumulus clouds /95 testifies to the fact that it is impossible to formulate single rules for selection of the interval between readings for measurement of radiation fluxes with one and the same efficiency in various conditions of cloud cover.

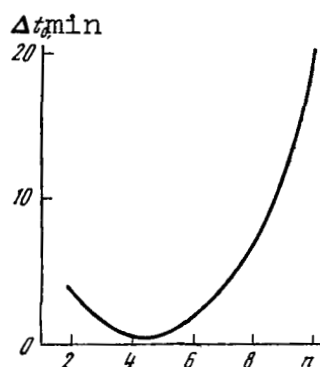


Fig. 2. Dependence of the optimum interval between adjacent readings upon the quantity of cumulus clouds for averaging of total radiation fluxes.

By using the values of the optimum step  $\Delta t_0$  presented in Fig. 2 we will consider with what accuracy we may determine the average total radiation fluxes per hour in various conditions of cloud cover. In Fig. 3 the corresponding values of  $\gamma_{\bar{Q}}^*$  as a function of the quantity of cumulus clouds, and also as a function of various forms of clouds when  $n = 10$  points, as calculated according to formulas (1) and (2). As is apparent from the dependences presented, the average flux in cumulus clouds is determined with the greatest relative error. In this case the relative mean square error of the estimate of the average increases with a growth of the cover of the sky by

clouds. If at  $2Cu$   $\gamma_{\bar{Q}}^* = 0.06-0.07$ , then at  $9-\overline{10}$  Cu it reaches a value of 0.20.

Up to this time for recording of radiation fluxes, galvanographs of type MShch have been widely used. The printing frequency [2] recommended for them amounts to 10-20 points per hour. In Fig. 3 the corresponding values of  $\gamma_{\bar{Q}}^*$  at  $\Delta t = 3$  and 6 minutes (curves 2 and 3) are given. The small difference in the fluctuation of the curves testifies to the relative proximity of the measurement regime recommended in [2] (for determination of the average total radiation flux in an hour) to the optimum value.

We will further consider how the accuracy of the determination of average fluxes changes with an increase in the averaging scale at an unchanged value of the interval between regions. For this the optimum step  $\Delta t = \Delta t_0$  is used, and we will calculate  $\gamma_{\bar{Q}}^*$  according to ratios (1) and (2) for various values of  $M$ . The dependence of  $\gamma_{\bar{Q}}^*$  upon the averaging scale for various degrees of the

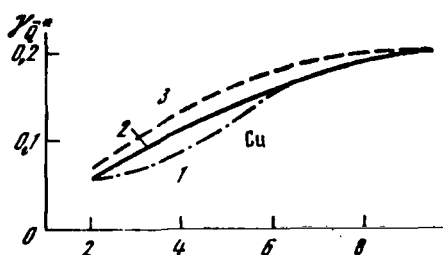


Fig. 3. Relative mean square error of the average of the total radiation flux per hour in different measurement regimes and under various conditions of cloud cover. 1- cumulus clouds,  $\Delta t = \Delta t_0$ , St, Sc, Ci, Cs; 2- cumulus clouds,  $\Delta t = 3$  min; 3- cumulus clouds,  $t = 6$  min.

cover of the sky by cumulus clouds as obtained is presented in Fig. 4. It is apparent that the necessary averaging scale to obtain a result with a definite given accuracy essentially depends upon the cloud cover. For example, to achieve values of  $\gamma_{\bar{Q}}^* \leq 0.20$  the period of measurements at 9-10 Cu must be not less than 1 hour. At the same time, such an accuracy is already achieved at 2 Cu by a single /96 randomly selected reading.

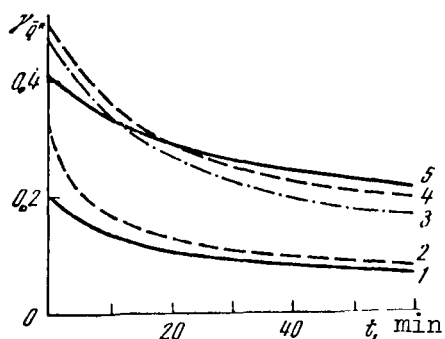


Fig. 4. Dependence of the mean square error of averaging of total radiation fluxes in cumulus clouds upon the averaging scale.

$\Delta t = \Delta t_0$ ; 1) 2 Cu; 2) 3-4 Cu; 3) 6 Cu; 4) 7-8 Cu; 5) 9-10 Cu, (Cb).

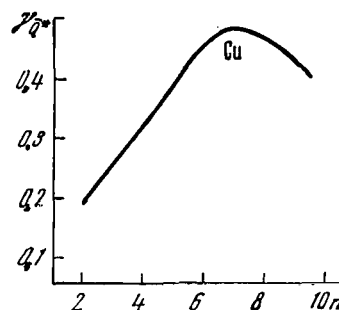


Fig. 5. Mean square error of estimation of the average total radiation flux at  $\Delta t = 0.5$  min and  $M = 3$ .

In the network of actinometric stations the solar radiation fluxes according to the so-called "urgent observations" are determined on the basis of a small number of specific readings with an insignificant time interval in each period. We will assume that the averaging is performed on the basis of three readings determined with a time interval  $\Delta t = 0.5$  minutes. The dependence of

$\gamma_{\bar{Q}}^*$  upon the quantity of cumulus clouds in such a regime of measurement is presented in Fig. 5. The relative mean square error increases with an increase in the quantity of the clouds and at  $7 \geq n \geq 5$  reaches a magnitude of 0.4-0.5, which is obviously intolerable. At 10 points of cover by other forms of clouds (St, Sc, Ci, Cs) the error is considerably less, although also at 10 St and Sc  $\gamma_{\bar{Q}}^* > 0.2$ .

## REFERENCES

1. Vilenkin, S. Ya., Statisticheskiye metody issledovaniya statsionarnykh protsessov i sistem avtomaticheskogo upravleniya (Statistical Method of Study of the Stationary Processes and Systems of Automatic Control), Moscow, "Sov. radio," 1967.
2. Rukovdstvo gidrometeorologicheskim stantsiyam po registratsii radiatsii (Manual of Hydrometeorological Stations for the Registration of Radiation), Leningrad, Gidrometeoizdat, 1961.

ON THE METHODOLOGY OF THE STUDY OF THE  
STATISTICAL STRUCTURE OF GROUND FLUXES OF  
SOLAR RADIATION IN CLOUDY CONDITIONS

R. G. Timanovskaya and Ye. M. Feygel'son

In the study of the variability of total radiation fluxes arriving at the earth's surface in cloudy conditions, a correlation analysis of individual time realizations was performed which is validated for steady-state random processes. /97

Some estimates of the steady-state nature and optimum period of observation in cumulus and continuous cloud cover are given below.

Cumulus clouds. Realizations with a duration of 2-6 hours for a check of the steady-state nature of the process were divided into successive parts with a duration of not less than one hour each. The statistical characteristics calculated for each part of the realization and for the entire realization as a whole were compared with each other.

Altogether, 20 comparisons were made, examples of which are presented in the table. The symbols used are explained in [IV.21].

From a comparison of the partial and total realizations it was ascertained that with the preservation of the value of the cloud cover the average value of the flux varies but little in comparison with the mean square deviations  $\sigma_{Q*}$ . The dispersions of the flux and other parameters of the statistical structure vary by not more than 20%. Correlation radii  $t_2$  and probabilities of the second mode of the distribution function turn out to be most variable.

If in the extent of a total realization the cloud cover changes, then variations of the average value of the flux become comparable with the mean square deviations, and the variability of the other parameters also increases.

Apparently a necessary condition of a steady-state nature of the process of variation of fluxes in cumulus clouds in time is the preservation of the degree of cloud cover over the extent of the period of observation. This condition determines the upper limit of the duration of observation  $T_{\max}$ .

For determination of the lower limit  $T_{\min}$  the time of establishment of dispersions was considered.

Date	Duration of realization, hrs.	Degree of cloud cover, %	$\bar{q}$	$\sigma_q$	$t_1$ , sec	$t_2$ , sec	Parameters of distribution functions					
							$Q_{min}$	$Q_{max}$	modes		probability	
									$Q_1$	$Q_2$	of first mode, $p_1$	of 2nd mode, $p_2$
3/25/67	2,3 I	8,0	0,624	0,071	82	206	0,30	1,08	0,30	0,96	0,20	0,40
	2,3 II	8,0	0,670	0,074	82	274	0,30	1,14	0,36	0,96	0,17	0,14
	4,6 I + II	8,0	0,647	0,072	82	246	0,30	1,14	0,36	0,96	0,17	0,12
6/25/67	1,2 I	5,0	0,730	0,094	55	219	0,18	1,08	0,24	1,02	0,13	0,19
	1,2 II	5,0	0,715	0,101	82	206	0,18	1,14	0,30	0,96	0,15	0,29
	2,4 I + II	5,0	0,722	0,097	68	206	0,18	1,14	0,30	0,96	0,13	0,24
7/15/68	2,2 I	4,5	0,789	0,086	63	277	0,12	1,02	0,12	0,90	0,12	0,31
	2,2 II	4,4	0,784	0,122	76	302	0,12	1,14	0,18	0,96	0,10	0,31
	4,4 I + II	4,5	0,786	0,104	70	289	0,12	1,14	0,18	0,96	0,08	0,31
7/3/67	1,2 I	8,0	0,650	0,109	41	219	0,24	1,14	0,24	1,02	0,25	0,22
	1,2 II	6,0	0,808	0,122	82	205	0,18	1,14	0,24	1,08	0,13	0,37
	1,2 III	5,0	0,730	0,102	68	205	0,18	1,14	0,24	1,02	0,12	0,19
	2,4 I + II	7,0	0,730	0,119	71	219	0,18	1,14	0,24	1,08	0,19	0,23
	2,4 II + III	5,5	0,770	0,112	68	205	0,18	1,14	0,24	1,08	0,13	0,25
5/27/68	2,2 I	9,0	0,361	0,070	277	504	0,12	1,20	0,18	1,08	0,26	0,03
	2,2 II	6,0	0,733	0,122	315	630	0,24	1,14	0,30	1,08	0,15	0,16



Let us assume that a realization of the process  $Q(t)$  with a duration  $T$  at a dispersion equal to  $\sigma^2$  has been given. We will consider the particular intervals of time  $\Delta_n^{(i)}T = \left| \frac{(i-1)T}{n}; \frac{iT}{n} \right|$ , ( $i = 1, 2, 3, \dots, n$ ), in each of which  $m$  points of measurement are contained:  $Q_j$ ,  $j = 1, 2, \dots, m$ .

We will calculate the particular dispersions

$$\sigma_i^2 = \frac{1}{m-1} \sum_{j=1}^m (Q_j^{(i)} - \bar{Q}_i)^2,$$

where

$$\bar{Q}_i = \frac{1}{m} \sum_{j=1}^m Q_j^{(i)},$$

/99

and then the average dispersion  $\sigma_n^2$ , determined according to the formula

$$\sigma_n^2 = \frac{1}{n} \sum_{i=1}^n \sigma_i^2.$$

We will determine the maximum value of  $n$  at which with a given error the following equality is fulfilled:

$$\sigma_n^2 = \sigma^2.$$

The corresponding interval  $2\Delta_nT = T_{\min}$  determines the minimum length of the realization. The optimum period of observation must apparently satisfy the condition:

$$T_{\min} \leq T_{\text{opt}} \leq T_{\max}$$

and

$$T_{\text{opt}} \geq 10t_2, [1].$$

In Fig. 1 for several realizations of the magnitude of  $Q$  in cumulus clouds the dependence of the parameter  $\sigma_n^2/\sigma^2$  upon the length  $\Delta_nT$  of the interval is presented. From these and other similar data (altogether 25 cases were considered) it was ascertained that the period of establishment of the dispersion,  $T_{\min}$  varies within limits of 20-60 minutes, with an average value of 40 minutes.

/100

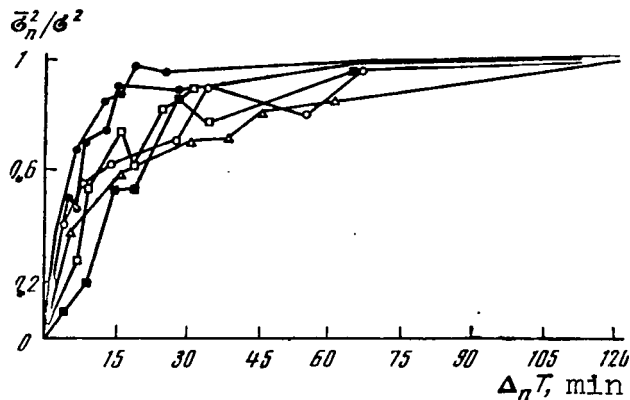


Fig. 1. Dependence of the parameter  $\tilde{\sigma}_n^2/\sigma^2$  upon the length  $\Delta_n T$  of the interval in cumulus cloud cover.

The correlation radius  $t_2$  in cumulus clouds is approximately equal to 5-10 minutes. According to data in [2], one point of cumulus cloud cover in summer is usually preserved at a constant value for 1-2 hours. Thus, the optimum period of ground observations of radiant fluxes in cumulus cover turns out to be of the order of 1-2 hours.

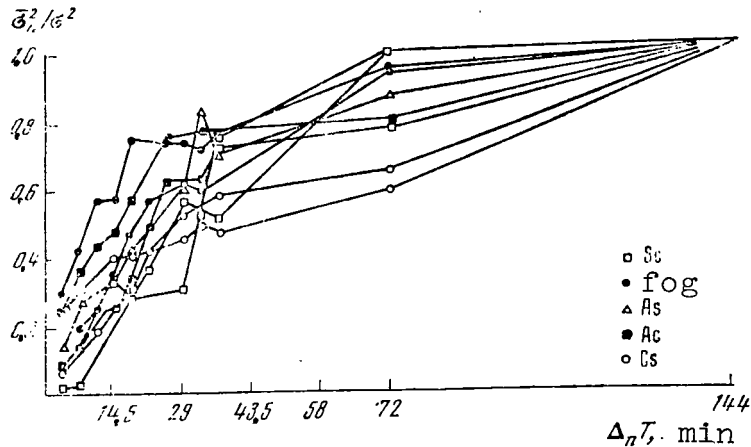


Fig. 2. Dependence of the parameter  $\tilde{\sigma}_n^2/\sigma^2$  upon the length  $\Delta_n T$  of the interval in continuous cloud cover of various forms.

Continuous cloud cover (overcast). In Fig. 2 individual examples of the process of establishment of a dispersion in continuous clouds of various forms are given. It is apparent that the

period  $T_{\min}$  in this case considerably exceeds the time of establishment of a dispersion in cumulus clouds. An increase in  $T_{\min}$  is noted in the transition from low continuous cover (fog, Ns, Sc) to clouds of the middle level (Ac, opaque, As) and then to continuous clouds of the upper level (Cs).

The necessary averaging period amounts to not less than 1 hour in a case of clouds of the lower level, not less than 1.5-2 hours for the middle level, and more than 2 hours for the upper levels.

The correlation radius  $t_2$  in continuous cloud cover of various forms varies within limits of 10-60 minutes [IV.19].

From this it follows that the duration of realizations in continuous cloud cover must be of the order of 2-10 hours. In this case the properties of the cloud cover must be preserved, which in the case under consideration, are not characterized by the points on a scale of ten.

The necessity of such a prolonged period of observation  $T_{\text{opt}} \approx$  /101  
 $\approx 2-10$  hours makes the possibility of studying the statistical structure of the total radiation flux in continuous clouds according to data from ground actinometric measurements doubtful. In this case only the average values of the fluxes and their dispersions can be determined reliably.

#### REFERENCES

1. Ariel', P. Z. and E. K. Byutner, "Distortions and errors originating in calculations of statistical characteristics according to experimental data", Trudy GGO, No. 187, 1966.
2. Sonechkin, D. M. and I. S. Trayapitsyna, "Some results of an investigation of the statistical structure of cloud cover", Trudy GMTs, No. 11, 1967.

# TOTAL RADIATION AT THE SURFACE OF THE EARTH IN VARIOUS CONDITIONS OF CLOUD COVER

V. K. Pyldmaa and R. G. Timanovskaya

The total radiation  $Q$  is an important component of the heat balance of the atmosphere. In cloud conditions it is basically determined by cloud cover and is subject, together with the latter, to considerable variations. For purposes of investigating the variability of solar radiation at the surface of the earth in time in various forms and degrees of cloud cover in March 1967 at two points in Dnepropetrovskaya Oblast' (Zhovtnevoye and Dnepropetrovsk), located at a distance of about 110 km from each other, continuous recording of the total radiation fluxes was performed. In autumn 1966 these measurements were conducted at the Zvenigorod Scientific Station of the IFA AN SSSR and since May 1967 at the Institute of Physics and Astronomy of the AN ESSR at Tyraver.

Yanishevskiy pyranometers served as radiation detectors, and automatic potentiometers as recorders. The quantity and form of the clouds during the measurements at Zvenigorod were determined according to photographs of the sky taken at an interval of 30 minutes and at Tyraver the quantity of cloud cover was determined visually.

The measurements were conducted only with clouds of one form, when the cloud cover varied by not more than 1 point.

The duration of the time series caused by this requirement varied from 1 to 5 hours. The processing of the data in the form of specific readings taken from a continuous recording tape with an interval of 9 or 12 seconds was performed on a Minsk electronic digital computer. For approximate exclusion of the diurnal fluctuation of the total radiation, the following dimensionless quantity was subjected to analysis:

$$Q^* = \frac{Q}{Q_0} \quad (1)$$

where  $Q_0$  determines the average diurnal fluctuation of the possible total radiation of a cloudless sky for the given geographical point and calendar day [1]:

$$Q_0 = I_0 \cos \vartheta_0 [1 + g \sec \vartheta_0]^{-1}. \quad (2)$$

Here  $g$  is a coefficient characterizing the optical thickness of the atmosphere and the albedo of the underlying surface.

For  $Q^*$  the following statistical characteristics were calculated: average fluxes  $\bar{Q}^*$ , dispersions  $\sigma_{Q^*}^2$ , variability factors  $V_{Q^*}$ , distribution density  $p(Q^*)$ , standardized autocorrelation functions  $r(t)$ , and intercorrelation functions  $r^*(t)$  with observation at two points.

TABLE I

Cloud cover	No. of realizations	$\bar{Q}^*$		$\sigma_{Q^*}^2$		$V_{Q^*}$	
		ave.	Limits of variability	ave.	Limits of variability	ave.	Limits of variability
<u>10</u> Ci	2	0.72	0.71—0.74	0.012	0.008—0.017	0.15	0.12—0.18
10 Cs	3	0.65	0.64—0.67	0.027	0.012—0.040	0.18	0.10—0.28
10 As	4	0.48	0.43—0.50	0.010	0.003—0.026	0.19	0.11—0.33
<u>10</u> Ac	4	0.71	0.70—0.74	0.030	0.030	0.25	0.23—0.26
10 Sc	7	0.31	0.14—0.55	0.004	0.002—0.012	0.21	0.13—0.37
10 St	6	0.21	0.11—0.40	0.002	0.001—0.004	0.30	0.06—0.50
fog	3	0.31	0.30—0.32	0.003	0.002—0.004	0.18	0.14—0.21
10 Ns	4	0.24	0.21—0.26	0.003	0.001—0.005	0.20	0.13—0.27
<u>10</u> Cu, (Cb)	2	0.48	0.34—0.61	0.039	0.030—0.048	0.44	0.36—0.51

In Table 1, where the average values and boundaries of variability of certain statistical characteristics obtained for various cloud conditions are given, it follows that even in conditions of low continuous cloud cover (fog, Ns, St, Sc) the total radiation fluctuates noticeably. In the transition from low continuous cloud cover (fog, Ns, St) to continuous cloud cover of the middle level (As, Ac) and then to cumulus cloud cover (Cu) the intensity of the fluctuation increases noticeably.

As a rule, the average flux  $\bar{Q}^*$  increases from clouds of the lower levels to clouds of the middle and upper levels. Usually in continuous stratoform cloud cover of the lower level  $\bar{Q}^* < 0.5$ . /103

The statistical characteristics of the field  $Q^*$  in cumulus cloud cover have been considered in more detail. In Fig. 1 the

dependence of the magnitude of the average flux  $\bar{Q}^*$  upon the quantity of Cu is given. We may, in the first approximation, describe the clearly expressed linear dependence in the range  $n = 2-10$  by the formula

$$\bar{Q}^* = 1.20 - 0.08 n.$$

The mean square deviations  $\sigma_{Q^*}^2$  acquire the maximum value at  $n = 5-6$  (Fig. 2); the region of greatest values of the variability factors  $V_{Q^*}$  is shifted in the direction of greater coverage of the sky, and, precisely,  $V_{Q^*, \max}$  is observed at  $n = 7-8$  points (Fig. 3).

TABLE 2

Cloud cover	$Q_{\min}$	$Q_{\max}$	Mode	Prob. of mode	Median
10 Ns	0.12	0.36	0.24	0.42	0.24
10 St	0.12—0.31	0.30—0.88	0.21—0.36	0.30—0.55	0.21—0.40
9 St fr	0.43—0.48	1.17—1.21	0.63	0.12—0.17	0.63—0.65
fog	0.18—0.20	0.42—0.60	0.30—0.36	0.25—0.44	0.30—0.38
10 As	0.24—0.35	0.72—0.74	0.36—0.45	0.24—0.34	0.42—0.48
[10] Sc	0.39—0.51	0.90	0.50—0.65	0.12—0.18	0.59—0.65
[10] Ac	0.42	0.96	0.54	0.13	0.66
9 Ac	0.52	1.20	0.98	0.16	0.94
5 Cu fr	0.43	1.20	0.45 & 0.94	0.07 & 0.22	0.95
7 Cu	0.42	1.20	0.48 & 1.08	0.16 & 0.14	0.72
9 Cu	0.29	1.34	0.50 & 0.98	0.13 & 0.05	0.54

For the segments of time realizations considered by us the distribution densities of the flux,  $Q^*$ , were determined. In Fig. 4 examples of the distributions obtained are presented, and in Table 2 some of their numerical parameters. As a rule, at 10 points of strataform cloud cover the distribution has a monomodal form with values of the mode and the median being very close. However, with a decrease in the quantity of clouds and, consequently, with an increase in the role of direct radiation of the sun in the total radiation flux, the difference between the values of the mode and the median is increased. The greatest distinction is observed in cumulus cloud cover at which the distribution has a bimodal form.

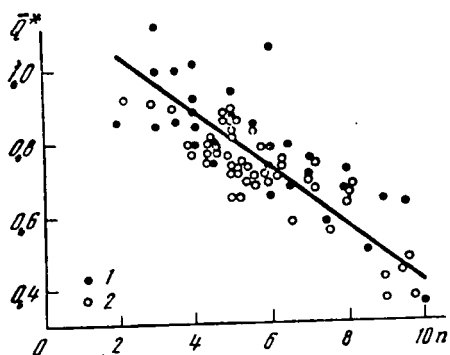


Fig. 1. Dependence of the average flux  $Q^*$  upon the quantity of Cu. /104  
1- according to measurements at Tyraver;  
2- according to measurements at Zvenigorod.

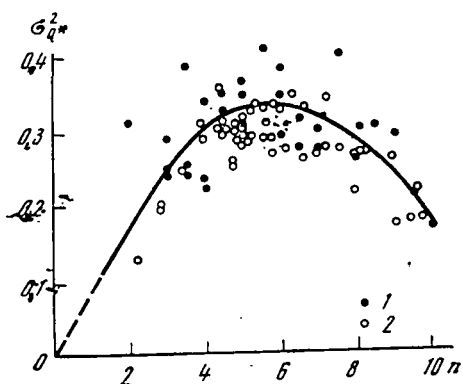


Fig. 2. Dependence of the mean square deviation of the flux  $Q^*$  upon the quantity of Cu.  
1- according to measurements at Tyraver;  
2- according to measurements at Zvenigorod.

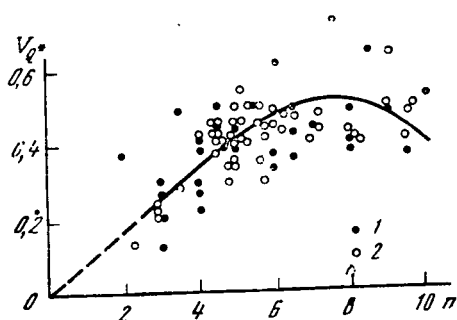


Fig. 3. Dependence of the variability factor of the flux  $Q^*$  upon the quantity of Cu.  
1- according to measurements at Tyraver;  
2- according to measurements at Zvenigorod.

The first mode, corresponding to small values of  $Q^*$ , characterizes the radiation flux when the sun is covered by clouds. The second mode corresponds to conditions when the total radiation flux is determined by direct and scattered radiation. In cumulus cloud cover the scattering of direct radiation of the sun by the lateral /105



surfaces of the clouds also plays a notable role, as a result of which the range of variability of  $Q^*$  widens, and a value of  $Q^* > 1$  is observed.

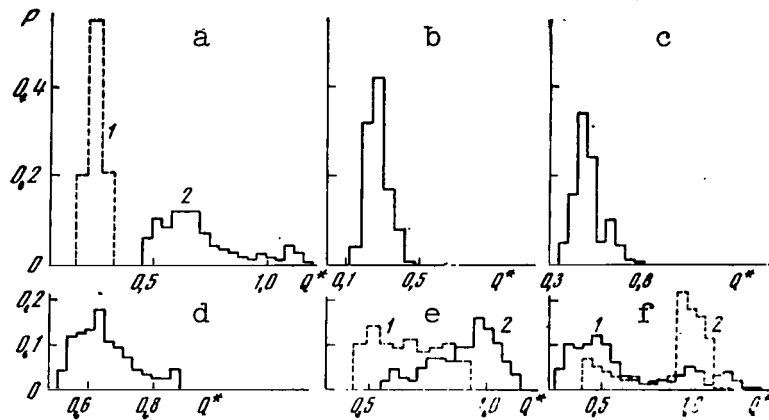


Fig. 4. Distribution densities of fluxes  $Q^*$   
a-1) 10 St; 2) 9 St; b) 10 Ns;  
c) 10 As; d) 10 Sc; e-1) 9 Cu;  
2) 5 Cu fr.

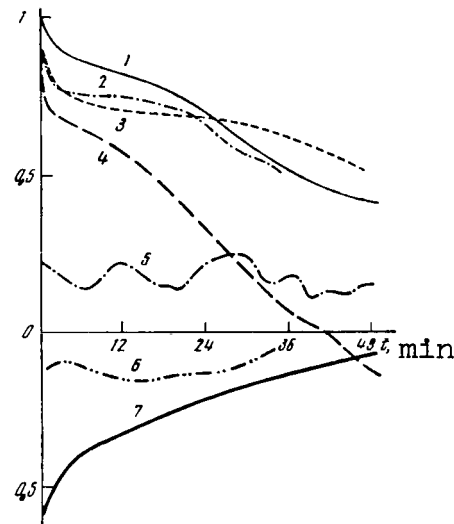


Fig. 5. Standardized autocorrelation functions.  
1-4) primarily continuous cloud cover (16, 9, 29, 31 March);  
5) cumulus cloud cover (25 March);  
6,7) various cloud cover (15, 23 March).

For cases of simultaneous recording of total radiation fluxes with a duration from 5 to 8 hours at the Zhovtnevoye and Dnepropetrovsk points, the average fluxes  $\bar{Q}^*$  and their dispersions  $\sigma_{Q^*}^2$  were calculated (Table 3), and also the intercorrelation functions  $r^*(t)$ , which are given in Fig. 5.

If, according to the visually estimated state of the cloud cover approximately the same situations are observed at both points

then the total radiation fluxes turn out to be close to each other, and the magnitudes of  $r^*(t)$  are positive, and the correlation function is smooth. In this case the intercorrelation may be reliable or weak. Sufficiently reliable correlation is characteristic for cases when at both points it is primarily continuous cloud cover of the lower or middle levels that were noted (Fig. 5, curves 1-4). In broken cloud cover of the lower level (Cu, Sc) the magnitudes of  $Q^*$  correlate only weakly with each other (Fig. 5, curve 5).

Table 3

Date (March)	Zhovtnevoye			Dnepropetrovsk		
	$\bar{Q}^*$	$\sigma_{Q^*}^2$	Cloud cover	$\bar{Q}^*$	$\sigma_{Q^*}^2$	Cloud cover
9	0,290	0,055	fog	0,160	0,034	fog
16	0,630	0,323	[10] Ac	0,744	0,250	9 Ac
24	0,470	0,182	[10] As, Ac	0,520	0,175	10 As, Ac
29	0,508	0,248	[10] Ac	0,874	0,208	8-10 Ac
31	0,290	0,125	[10] Sc	0,530	—	10 Ac
20	0,626	0,207	10 St, Cl, Ac	0,645	0,163	9-10 Sc
25	0,645	0,323	7 Cu	0,560	0,314	7 Cu
19	9,588	—	fog, 10 St	0,737	—	fog, 9 St fr
15	0,487	0,173	As, St fr	0,171	0,088	10 St
23	0,917	0,350	As, cloud-less	0,300	0,087	fog, St

If the meteorological conditions at the measurement points were different then the correlation between the fluxes either was lacking or was replaced by an anti-correlation (Fig. 5, curves 6, 7).

## REFERENCE

1. Kondrat'yev, K. Ya., Aktinometriya (Actinometry), Leningrad, Gidrometeoizdat, 1965.

# SOME PARAMETERS OF CUMULUS CLOUDS OBSERVED BY PHOTOGRAPHS OF THE SKY AND FROM GROUND ACTINOMETRIC MEASUREMENTS

R. G. Timanovskaya and Ye. M. Feygel'son

The complex of measurements described in [IV.21] made it possible to obtain certain information concerning cumulus clouds in their distribution throughout the sky. For this, photographs of the sky were used, continuous recordings of the readings of an actinometer, and also measurements of the wind velocity at the level of the clouds. The device for photographing the sky and the methodology of calculating the quantity of clouds were described in [1].

The recurrence of the general quantity of clouds involved,  $n$ , obtained from 385 photographs in conditions when the magnitude of  $n$  varied within limits of  $1 \leq n \leq 9$  is presented in Table 1.

Table 1

n, Points	1	2	3	4	5	6	7	8	9	Total
no. of cases	13	46	58	79	56	55	36	23	19	385
%	3.4	11.9	15.0	20.5	14.5	14.3	9.4	6.0	4.9	100

In Table 2 the distribution of the average zonal number of points of cloud cover,  $n_\varphi$ , with respect to angular zones ( $\Delta\varphi = 10^\circ$ ) is given for various general relative quantities of the clouds. In the next to the last column in Table 2 the average values of the general relative quantity of clouds within the limits of each gradation are given. The general value of the ball number is calculated according to the formula

$$n = \frac{1}{2\pi} \sum_{i=1}^m n_{\varphi_i} S_{\varphi_i} \quad (1)$$

at given values of  $n^\varphi$ . Here  $S_{\varphi_i}$  is the relative area of the angular zone  $\Delta\varphi_i$ ;  $m$  is the number of zones.

The data in Table 2 are presented in Fig. 1, together with the theoretical curves from [2]. The average data of the observations agree excellently well with the calculation at  $3 \leq n \leq 6$ , which confirms the correct selection of the Gaussian statistical model of the distribution of cumulus clouds throughout the sky in [2]. However, if there are few clouds ( $n \leq 2$ ) or if there are many of them ( $n \approx 7$ ), the photographic number of points of cloud cover essentially differs from the calculated value. Probably in these conditions the distribution of cloud cover throughout the sky for ground observations ceases to be statistically homogeneous and Gauss's law turns out to be inapplicable. /108

TABLE 2

n	$\Delta\theta$								Gen. rel. points, n	Number of cases
	0-10	10-20	20-30	30-40	40-50	50-60	60-70	70-80		
1,5	0	0,1	0,3	0,4	0,5	1,2	1,6	1,7	0,7	13
1,5-2,5	0,8	0,9	1,2	1,6	2,0	2,3	2,8	3,0	2,0	46
2,5-3,5	1,8	2,0	2,0	2,2	2,4	3,0	4,0	4,3	2,9	58
3,5-4,5	2,7	2,7	3,0	3,3	3,4	3,6	4,6	5,2	3,9	79
4,5-5,5	3,9	3,9	4,0	4,0	4,2	4,4	5,1	6,5	4,9	56
5,5-6,5	4,8	4,9	5,0	5,2	5,3	5,3	5,9	7,4	6,0	55
6,5-7,5	7,2	6,8	6,4	6,3	6,1	6,4	7,0	7,7	7,1	36
7,5-8,5	8,6	8,2	8,4	8,0	7,7	7,2	7,4	7,9	7,9	23
8,5-9,5	9,6	9,2	9,2	8,8	8,5	8,6	9,0	9,0	9,0	19

Aside from the direct data described above, the authors attempted to extract information relative to cloud cover from actinometric measurements. Such a possibility, justified by the high sensitivity of fluxes of solar radiation to the appearance of clouds, is discussed, for example, in [3].

The relative duration of sunshine  $s_0$  may be defined as the fraction of the period of observation corresponding to the condition  $S > \epsilon$ , where  $S$  is the momentary flux of solar radiation measured by the actinometer,  $\epsilon$  is the threshold flux estimated below. This fraction may be found if the function of the probability distribution relative to the magnitudes of direct solar radiation is known similar to the function presented in [IV.21].

It is apparent that the probability of the second mode  $S_2$  of the distribution curve makes the basic contribution to the quantity

$s_{\odot}$ . Together with this, the curves indicate that the recurrence of rather large fluxes of solar radiation,  $S_1$  where  $S_1 \ll S_1 < S_2$  ( $S_1$  is the first mode) is adequately great. Apparently the fluxes  $S_1$  are determined by the probability of "semi-transparent" states of the sky originating in the covering of the sun by optically thin clouds or in partial covering of the sun by clouds. These also include conditions of fictitious transparency, originating because of the inertia of the actinometer and the possible entry of light reflected by the edges of the clouds into the instrument. In the consideration of the fluxes  $S_1$  the magnitude of  $s_{\odot}$  is determined according to the formula

$$s_{\odot} = \sum_{i=0}^k p_{2-i}. \quad (2)$$

Here  $p_{2-i}$  is the probability of the  $i$ -gradation of  $S_{2-i}$  on the probability distribution curve preceding the second mode. The number  $k$  of gradations considered in formula (2) was determined according to the maximum value of the linear correlation factor  $r$  between the magnitudes of  $s_{\odot}$  and  $\bar{S}^*$ , and also  $s_{\odot}$  and  $\bar{Q}^*$ , where  $\bar{S}^*$  and  $\bar{Q}^*$  are the average relative direct radiation fluxes and total radiation fluxes for each period of observation. Corresponding regression curves at different values of the parameter  $k$  are presented in Fig. 2. /109

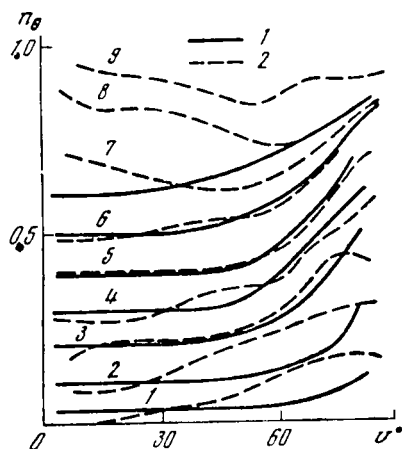


Fig. 1. Distribution of the zonal point number of cumulus cloud cover.  
1) calculated data;  
2) average data from observations.

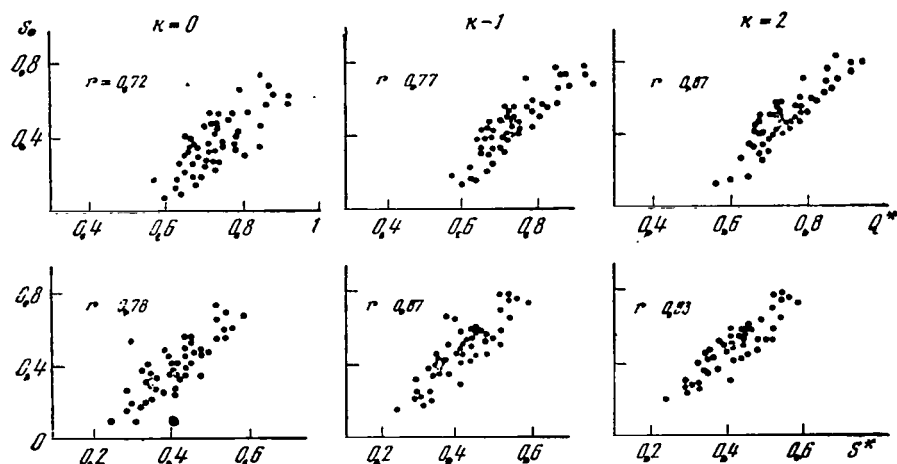


Fig. 2. Connection between duration of sunlight  $s_{\odot}$  and average relative fluxes of total radiation,  $\bar{Q}^*$ , and between  $s_{\odot}$  and the average relative fluxes of direct radiation  $\bar{S}^*$  (b).

It is apparent that the essential scattering of the points at  $k = 0$  with a growth of  $k$  is replaced by a more regular dependence of  $\bar{S}^*$  and  $\bar{Q}^*$  upon  $s_{\odot}$ , and the coefficient  $r$  increases simultaneously. Our experience has demonstrated that we may always find the optimum number  $k = k_0$  in formula (1) from the conditions /110

$$\left. \frac{dr}{dk} \right|_{k=k_0} = 0; \quad \left. \frac{dr}{dk} \right|_{k > k_0} < 0.$$

Since the second mode of the distribution function is more variable than the first, in practice it turned out to be more convenient to determine the duration of sunlight according to the formula

$$s_{\odot} = 1 - \sum_{i=0}^{k_1} p_{1+i}, \quad (3)$$

where  $p_{1+i}$  is the probability of the  $i$ -th gradation following the first mode. In this case usually  $k_1 \approx 7$  occurs at a step with respect to  $\bar{S}^*$  equal to 0.06. It turns out that the average fluxes of direct radiation and total radiation are basically formed in conditions when the random values of direct solar radiation satisfy

the inequality  $S \geq 0.72 - 0.44 \text{ cal/cm}^2 \text{ min}$  at  $35^\circ \leq \varphi_\odot \leq 50^\circ$ . The time interval corresponding to these conditions determines the duration of sunshine.

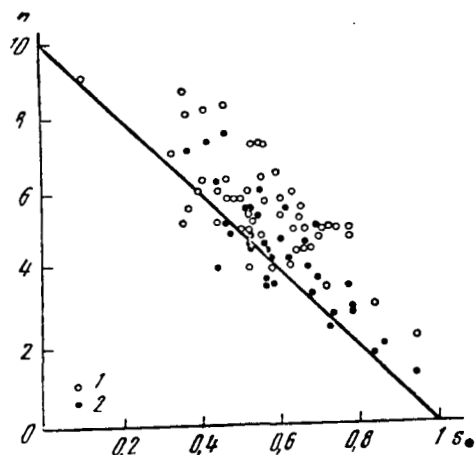


Fig. 3. Connection of the duration of sunshine with the general point number  $n$  (1) and with the zonal number  $n_\odot$  (2) in the direction to the sun.

The proposed method of determination of the duration of sunshine according to the actinometer is quantitative. As was indicated in [4], the use of an actinometer for determination of  $s_\odot$  has a number of advantages in comparison with the use of a heliograph for this purpose, in particular in the possibility of automation of processing [5].

In Fig. 3 the connection of the duration of sunshine with the general point number of cloud cover is presented. Usually we assume that between these parameters the following relation holds

$$s_\odot = 1 - n \quad (4)$$

( $n$  is in fractions of a unit), which is natural in the assumption /111 that the clouds are absolutely opaque. With consideration of the effect of semi-transparency, equality (3) must be replaced by the inequality

$$s_\odot > 1 - n,$$

which is also observed in Fig. 3.

Each point in this drawing corresponds to the average point number of the cloud cover in periods of time that are not less than 2 hours and to the relative duration of sunshine for the same period. The scattering of points in Fig. 3 is very great, but nevertheless the validity of inequality (4) is obvious.

In this same drawing the connection between the quantities  $s_\odot$  and  $n_\odot$  (the zonal point number in the direction of the sun) is presented. The following relation holds



$$0 < |s_{\odot} - (1 - n_c)| < |s_{\odot} - (1 - n)|, \quad (5)$$

which testifies to the closer connection of the duration of sunshine with the zonal point number in the direction of the sun than with the general point number. Together with this it is apparent that the duration of sunshine is not determined entirely by the zonal point number either. It is apparent that there are real states of "semi-transparency", considered in the determination of  $s_{\odot}$ .

It was observed that the scattering of the points in Fig. 3, if not entirely explained by the considerable dependence of the quantity  $s_{\odot}$  upon the linear dimensions of the cloud,  $\ell$ , determined according to autocorrelation functions [IV.21], is partially explained by this fact. This dependence, as presented in Fig. 4, in turn is probably caused by the increase in the number of clouds in the sky with a decrease in  $\ell$  at  $n = \text{const}$  and an increase in the area of their peripheral semi-transparent parts.

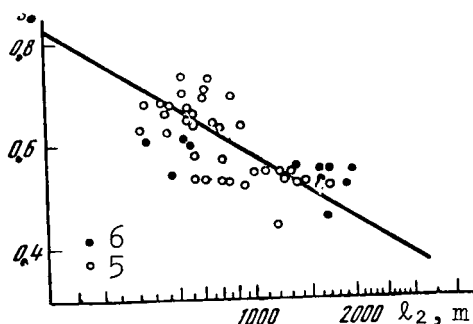


Fig. 4. Dependence of the duration of sunshine upon the dimensions of cloud formations.

The characteristic of cloud cover  $s_{\odot}$  proposed for reducing the fluxes to parameters has a physical nature closely connected with the effective transparency of the clouds (in distinction from the purely geometrical parameter  $n$ ). Therefore, the less the optical density of the clouds, the more significant must be the difference between the parameters  $n$  and  $s_{\odot}$ . We may hope that the parameter  $s_{\odot}$  makes it possible to classify fluxes without additional information relative to the form of cloud cover. The advantages of this parameter in conditions of continuous cloud cover are obvious—frequently the continuous cloud cover is not too dense optically (C1, Ac) and causes appreciable fluctuations of the radiation fluxes [IV.19]. The determination of this parameter is performed within the framework of actinometric measurements and does not require additional observations. /112

All these considerations are tentative and require more complete validation and checking. It is necessary primarily to ascertain to what degree the readings of the actinometer are in agreement with the true transparency of the clouds.

However, regardless of the answer to this question, we may affirm that the parameter  $s_{\odot}$  is more closely connected with fluxes of direct solar radiation and total solar radiation than the point number of the cloud cover. This affirmation is based on a comparison of the dependences of various statistical characteristics of fluxes upon  $s_{\odot}$  and  $n$ .

## REFERENCES

1. Bibikova, G. N., "Experience in observation of clouds by the photographic method by means of a spherical mirror," Vestn. Mosk. un-ta, No. 2, 1960.
2. Mullamaa, Yu. R., "Coverage of the sky by cumulus clouds," Collection: Radiatsiya i Oblachnost' (Radiation and Cloudiness), AN ESSR, 1969 (in the press).
3. Wörner, H., "On the problem of the automization of the Cloudiness Data by means of radiation measurements," Abhandlungen des Meteorol. Diensts Republik, N. 82, (V. XI), 1967.
4. Perren de Brishambo, Solnechnoye izlucheniye i radiatsionnyy obmen v atmosfere (Solar radiation and radiation interchange in the atmosphere), Izd-vo "Mir," 1968.
5. Laýsk, A. A., "Statistical analyzer for bioactinometric measurements," Vestn. "Voprosy radiatsionnogo rezhima rastitel'nogo pokrova," Tartu, 1965.

# FLUXES OF SOLAR RADIATION AT THE SURFACE OF THE EARTH IN CUMULUS CLOUD COVER

R. G. Timanovskaya and Ye. M. Feygel'son

For a description of the variability in time of fluxes of solar radiation, as a function of the state of cumulus cloud cover, at the Zvenigorod Scientific Base of the IFA since autumn 1966 a complex of measurements has been conducted.

In the hours near noon fluxes of direct radiation and total radiation were recorded continuously (for 2-5 hours), measured by an actinometer and a pyranometer designed by Yu. D. Yanishevskiy. Simultaneously, not less frequently than every half hour, the sky was photographed and the zonal and general relative number of points of the cloud coverage were calculated. Every hour, by means of weather balloons, the wind velocity  $v$  at the level of the clouds was measured. The methodology of the actinometric measurements, calculation of the quantity of clouds, and statistical processing of the data were explained in [1,2] and [IV.19].

/113

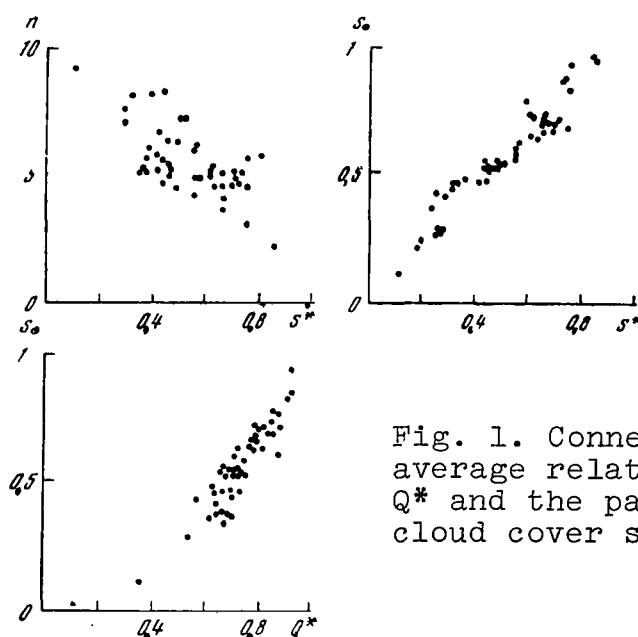


Fig. 1. Connection between the average relative fluxes  $\bar{S}^*$  and  $Q^*$  and the parameters of the cloud cover  $s_0$  and  $n$ .

The relative fluxes of direct solar radiation and total solar radiation were considered, as determined according to the formulas

$$S^* = \frac{S}{S_0}, \quad Q^* = \frac{Q}{Q_0}.$$

The average values of the relative fluxes  $\bar{S}^*$ ,  $\bar{Q}^*$ ; their dispersions  $\sigma_{S^*}^2$ ,  $\sigma_{Q^*}^2$ ; variability factors  $V_{S^*}$ ,  $V_{Q^*}$ ; the differential and integral distribution functions,  $p(S^*)$ ,  $p(Q^*)$ , and  $P(S^*)$ ,  $P(Q^*)$ ; and also the standardized autocorrelation functions  $r(t)$ . These characteristics were calculated according to individual time realizations, which is quite lawful for random steady-state processes [IV.18]. Realizations with a duration of about 2.2 hours at 1000 specific readings in each case were selected. Altogether, 60 such realizations were considered.

In Table 1 the average statistical characteristics of fluxes  $S^*$  and  $Q^*$  are given for the four gradations of the parameter  $s_\odot$ , where  $s_\odot$  is the duration of sunshine, determined according to the actinometer [IV.20].

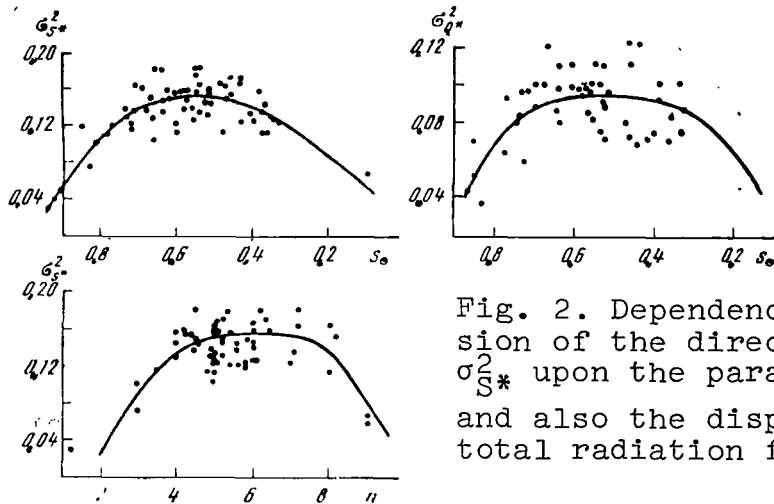


Fig. 2. Dependence of the dispersion of the direct radiation flux  $\sigma_{S^*}^2$  upon the parameters  $s_\odot$  and  $n$ , and also the dispersion of the total radiation flux  $\sigma_{Q^*}^2$  upon  $s_\odot$ .

The connection between the average values of fluxes  $S^*$  and  $Q^*$  and the quantities  $n$  and  $s_\odot$ , presented in ref. [1] and in Fig. 1, is described by equations of linear regression of the form

$$\bar{Q}^* = 0.70s_\odot + 0.32 \quad (r = 0.91), \quad (1)$$

$$\bar{S}^* = 1.00s_\odot - 0.04 \quad (r = 0.96), \quad (2)$$

$$\bar{Q}^* = 1.24 - 0.09n \quad (r = 0.85), \quad (3)$$

$$\bar{S}^* = 1.42 - 0.16n \quad (r = 0.72), \quad (4)$$

where  $r$  is the linear correlation factor.

TABLE 1

Form of clouds	Gradations of relative duration of sunshine, $s_{\odot}$	No. of cases	Average value of $s_{\odot}$	Average points of cloud cov., $n$	Av. wind velocity $v$ , m/s	$Q^*$	$Q_2^*$	$v_{Q^*}$	$S^*$	$S_2^*$	$v_{S^*}$	$t_1^1$ sec	$l_1^1, m$	$t_2^1$ sec	$l_2^1, m$
Cu	<0.2	6	0.06	10	12	0.410	0.050	0.55	—	—	—	221	2650	420	5040
Cu	0.3—0.5	23	0.40	7	12	0.650	0.085	0.45	0.420	0.148	0.90	101	1200	307	3700
Cu	0.6—0.8	27	0.69	5	10	0.820	0.095	0.38	0.633	0.147	0.60	88	880	280	2800
Cu	>0.8	4	0.87	4	12	0.910	0.050	0.25	0.810	0.071	0.34	60	720	180	2200

$t_1^1$  and  $t_2^1$  are correlation radii determined from the conditions  $r(t)=0.5$ ;  $r(t_2)=0.1$ ;  $l_1=vt_1$ ;  $l_2=vt_2$ .

TABLE 2

Grada- tions of $s_{\odot}$	Flux $Q^*$							Flux $S^*$							no. of cases
	$Q^*$ min.	$Q^*$ max.	Mode		prob. of mode		med- ian	$s^*$ min.	$s^*$ max.	Mode		prob. of mode		med- ian	
			$Q_1^*$	$Q_2^*$	$p_1$	$p_2$				$s_1^*$	$s_2^*$	$p_1$	$p_2$		
<0.2	0.06	1.08	0.3	—	0.21	—	0.3	—	—	—	—	—	—	—	6
0.3—0.5	0.12	1.20	0.3	0.9	0.14	0.10	0.54	0.0	1.02	0.0	0.90	0.37	0.14	0.24	23
0.6—0.8	0.06	1.14	0.18	0.9	0.08	0.24	0.84	0.0	1.02	0.0	0.84	0.22	0.18	0.84	27
>0.8	0.12	1.14	0.18	0.84	0.03	0.31	0.84	0.0	0.96	0.06	0.78	0.05	0.29	0.84	4

Formulas (1) and (3), and also (2) and (4), lead to different values of the fluxes  $\bar{S}^*$  and  $\bar{Q}^*$  in cases of a clear sky ( $s_{\odot} = 1$ ,  $n = 0$ ) and continuous dense cloud cover ( $s_{\odot} = 0$ ,  $n = 10$ ). This apparently is explained by the difference of correlation (see the numbers in parentheses) between the fluxes and the number of points of cloud cover and between the fluxes and the duration of sunshine. Incidentally, it is possible that the divergences observed are caused by the inadequate number of data at  $s_{\odot} = 0$ ,  $n = 10$  and  $s_{\odot} = 1$ ,  $n = 0$ , used for calculation of the coefficients of expressions (1)-(4).

Fig. 2 shows the dependence of the statistical parameters  $\sigma_{S^*}^2$ ,  $\sigma_{Q^*}^2$  upon the parameters of the cloud cover,  $n$  and  $s_{\odot}$ . This dependence turned out to be nonlinear; the dispersions are at the maximum at  $0.3 < s_{\odot} \leq 0.7$  ( $4 \leq n \leq 8$ ), decreasing in an almost clear sky or an almost overcast sky. The variability factor  $V_{S^*}$ , presented in Fig. 3, is connected linearly with the quantities  $n$  and  $s_{\odot}$ , in distinction from the coefficient  $V_{Q^*}$  (also see [1]) and in the latter case an equalization is observed and, possibly, a decrease in  $V_{Q^*}$  with a decrease in  $s_{\odot}$ .

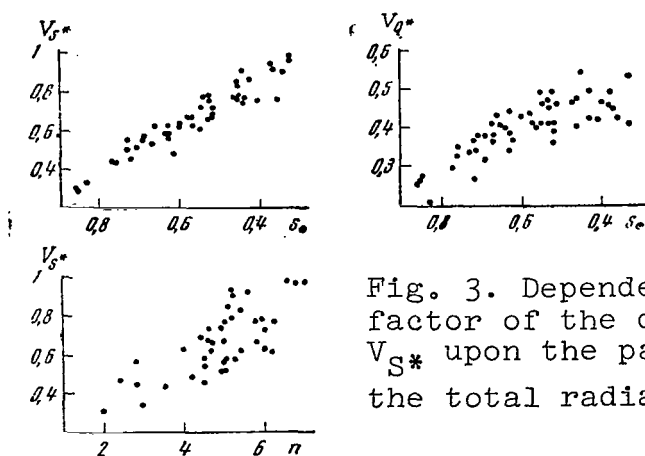


Fig. 3. Dependence of the variability factor of the direct radiation flux  $V_{S^*}$  upon the parameters  $s_{\odot}$  and  $n$  and the total radiation flux  $V_{Q^*}$  upon  $s_{\odot}$ .

In Fig. 4 the average integral distribution functions of the quantities  $S^*$  and  $Q^*$  with respect to 50 realizations at  $0.4 < s_{\odot} < 0.8$  are given. It is apparent that in cumulus clouds with a probability  $\geq 50\%$  the relative total radiation fluxes exceed the values of 0.8 ( $Q_{\text{obs}} > 1.4 \text{ cal/cm}^2 \text{ min}$  at  $\odot = 45^\circ$ ) and the direct

radiation fluxes, 0.5 (0.8 cal/cm<sup>2</sup> min at  $\vartheta_{\odot} = 45^{\circ}$ ). These fluxes are 25-30% formed with the sun covered with clouds, 50% with an open sun, and 20-25% due to semi-transparent situations. /117

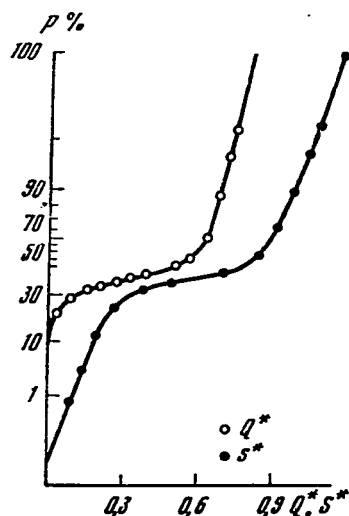


Fig. 4. Average integral distribution functions of the probabilities of relative fluxes of direct radiation and total radiation (on a probability scale).

The differential distribution functions of the probabilities of fluxes  $S^*$  and  $Q^*$  are presented in Fig. 5 and in Table 2 their parameters are given. In a case of total radiation  $Q_1^* > 0$  occurs and  $Q_{\max}^* > 1$ , where  $Q_1^*$  is the value of the first mode of the distribution curve  $Q_{\max}^*$  is the maximum measured value of the flux.

The difference of the first mode from zero testifies to the essential role of the scattered radiation in the formation of the total flux. The contribution of scattered radiation becomes basic according to Fig. 5 at  $s_{\odot} < 0.4$ .

We will consider a section of the distribution curve of the probabilities of the flux  $Q^*$  at  $Q^* > 1$ . The appearance of such values of  $Q^*$ , as was noted in [3], is characteristic for cumulus clouds and is caused by the reflection of direct solar radiation by the lateral surfaces of the set of clouds. The curves in Fig. 5 make it possible to estimate this effect quantitatively. For example, at  $s_{\odot} \approx 0.4$  about 10% of the time  $Q^* > 1$  is observed. The contribution of such values of  $Q^*$  to the average flux  $\bar{Q}^*$  is close to 10%. /118

The dependences of certain parameters of the distribution functions upon  $s_{\odot}$  and  $n$ , presented in Figs. 6 and 7 demonstrate that the recurrence of the first and second modes of the distribution functions of fluxes  $S^*$  and  $Q^*$ , and also the median of these distributions depends linearly upon the parameters  $s_{\odot}$  and  $n$ . In this case, as before, a closer connection with the quantity  $s_{\odot}$  than with  $n$  is noticeable. /119

In Fig. 8 the characteristic examples of standardized autocorrelation functions are presented— $r(t)$  almost the same for total



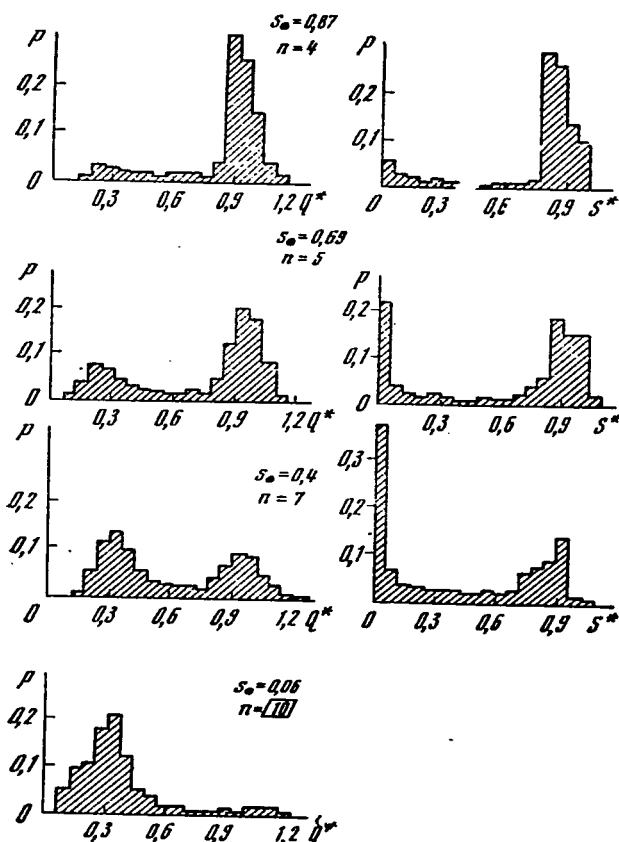


Fig. 5. Average differential distribution functions of the probabilities of relative fluxes of direct radiation and total radiation.

radiation fluxes and direct radiation fluxes. Calculations of  $r(t)$  were performed for the time interval  $(0, 0.1\Delta T)$ , where  $\Delta T$  is the duration of the realization. The quantities  $\left. \frac{dr(t)}{dt} \right|_{t \approx t_0}$ , where  $0 < t_0 < t_1$ , in cumulus clouds, essentially differ from those corresponding to a case of any other cloud cover (see [IV.19] and Table 1): in the first case the derivative is the greatest and the correlation radius is the least, which corresponds to comparatively small horizontal dimensions of the cumulus clouds.

Fig. 8 demonstrates that in the interval  $t_2 < t < 0.1\Delta T$  the function  $r(t)$  may be both periodic and monotonic at one and the same values of the parameters  $n$  and  $s_0$ . In averaging according

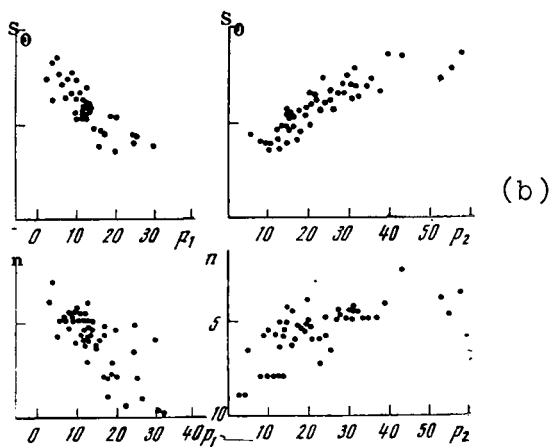
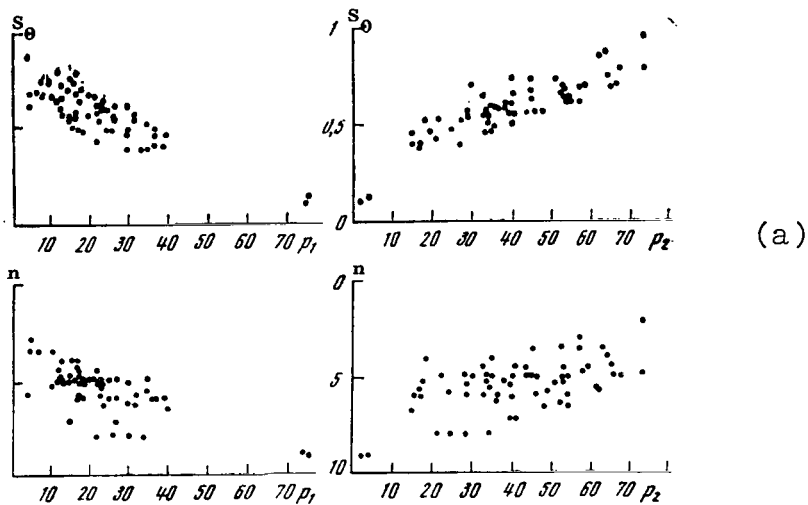


Fig. 6. Dependence of the probabilities of the first ( $p_1$ ) and second ( $p_2$ ) modes of the distribution functions of direct radiation (a) and total radiation (b) upon the parameters  $s_0$  and  $n$ .

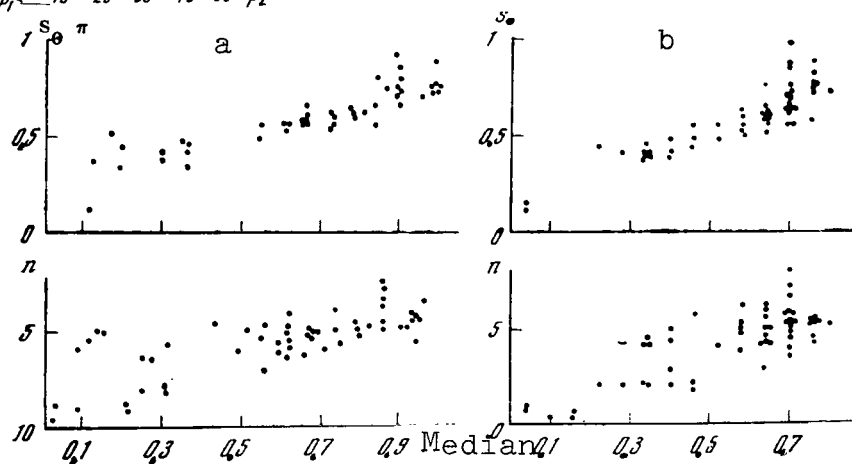


Fig. 7. Dependence of the median of the distribution functions of probabilities of direct radiation (a) and total radiation (b) upon the parameters  $s_0$  and  $n$ .

to 47 realizations, corresponding to the average point number of cumulus cloud cover,  $n_0 \approx 5$ , no periodicity is manifested (Fig. 9), but nevertheless, it is real, and characteristic for rapidly passing clouds, i.e., either at adequately small dimensions of the cloud heterogeneities or at adequately large wind velocities.

As is apparent from Table 1 and Fig. 10, the correlation radii increase with the growth of the point number of cloud cover. Since the wind velocity varied but little, we may think that an increase in the point number of cumulus clouds occurs not only due to an increase in the number of cloud heterogeneities but also due to their enlargement.

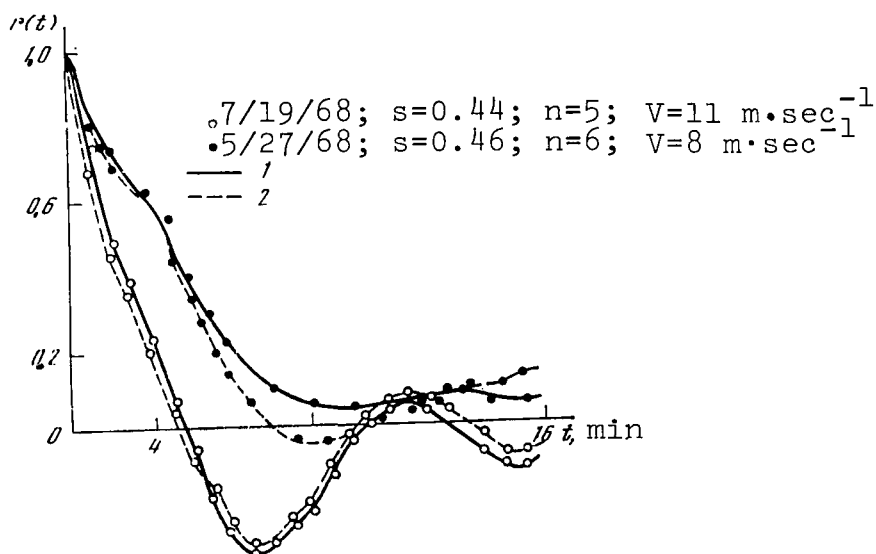


Fig. 8. Standardized autocorrelation functions of the total radiation fluxes (1) and direct radiation fluxes (2).

The dimensions of the cloud heterogeneities determining the structure of fluxes of direct radiation and total radiation, according to Table 1, amount to 180-420 sec or 2200-2000 m. Although the material of the observations is still not great, the analysis performed demonstrates that a close connection exists between the average values of fluxes of solar radiation and the totality of their statistical characteristics on the one hand and such parameters of the

/121

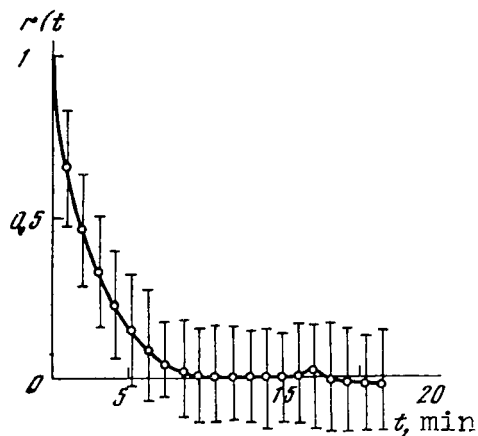


Fig. 9. Averaged standardized autocorrelation function of fluxes of direct (and total) radiation. Vertical segments designate the scattering of correlation functions used in averaging.

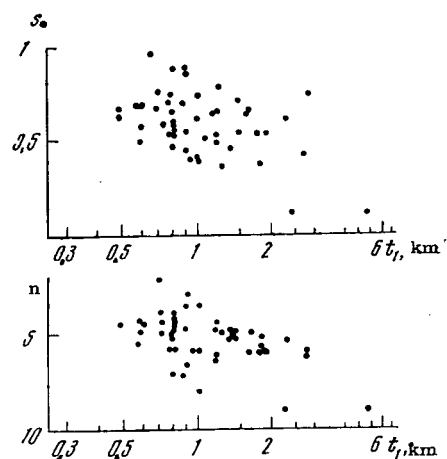


Fig. 10. Dependence of the parameter  $t_1$  for direct radiation and total radiation upon  $s_0$  and  $n$ .

clouds as the point number of the cloud cover or the duration of sunshine on the other. A successive comparison of the connection of the statistical parameters of the fluxes with each of these parameters of the clouds forces us to give preference to the second.

The statistical characteristics of the fluxes calculated make it possible to estimate their variability and to penetrate into the physical structure: to determine the role in the formation of fluxes of direct, scattered, and reflected light; to ascertain the effect of clear, semi-transparent, and cloudy sections of the sky, and large and small cloud formations.

#### REFERENCES

1. Pyldmaa, V. K. and R. G. Timanovskaya, "Certain statistical characteristics of the total radiation in cloudy conditions", Izv. AN SSSR, seriya FAO, No. 5, 1969.
2. Timanovskaya, R. G. and Ye. M. Feygel'son, "Fluxes of solar radiation at the surface of the earth in cumulus cloud cover", Meteorologiya i gidrologiya, No. 11, 1970.
3. Kondrat'yev, K. Ya. Aktinometriya (Actinometry), Leningrad, Gidrometeoizdat, 1965.

# SPATIAL STRUCTURE OF THE FIELD OF SHORT-WAVE RADIATION IN STRATOCUMULUS AND CUMULUS CLOUD COVER

M. A. Sulev

In 1967-1969 at the IFA AN ESSR, together with the Ukr. NIGMI, aircraft investigation of the spatial variability of fields of short-wave radiation and cloud cover was conducted. In this article the results of investigations in 1967 and 1968 are considered. In the spring of 1967 we succeeded in obtaining adequate material only for stratocumulus clouds, in the summer of 1968 the field of intra-mass cumulus cloud cover was investigated.

In horizontal flights, the fluxes of total and reflected short-wave radiation were recorded continuously, and beginning in 1968, also the presence of clouds in the direction of the zenith (or nadir) on the flight path. The fluxes were measured by M80 standard pyranometers as recorders for which the eKVT/1 automatic potentiometers served. The presence of clouds was determined by a special narrow-angle detector (the angle of view was of the order of  $1^\circ$ ), operating in a narrow spectral range of about 0.85 micron. The output signal of this detector, after amplification, was recorded on a K-4-51 loop oscillograph. The length of one flight varied from 100 to 600 km, amounting to 300 km on the average. The ordinates were taken from the tapes of the automatic recorders with an interval from 0.5 to 6 sec (from 0.035 to 0.4 km, respectively), depending upon the form of the curves. Certain results of the investigations indicated are given below. /122

Stratocumulus cloud cover. In stratocumulus cloud cover the flights were conducted over and under the layer, and in certain cases also inside the layer, at a distance of approximately 100 m from the upper boundary. All the results obtained at 8, 9, 10, and 10 Sc coincided quite well. Certain average statistical characteristics of the fluxes of short-wave radiation are given in the table.

As is apparent from the table, the variability factor of all the quantities measured varies from 0.15 to 0.5, the correlation radius  $x_{0.5}$  takes the greatest value for a flux of reflected radiation over the clouds, and the least inside the layer. We should emphasize that the averaging scales necessary to obtain an average value with a reliability of  $\beta = 0.95$  are much greater than those usually assumed at measurements of the vertical profile of the radiation fluxes (of the order of 10 km). From this it becomes obvious why to obtain plausible results averaging according to a considerable number of profiles is required.

Flight	Fluxes	Number of measurements	Correlation radius (km) $\times 0.5$	Variability factor, V	Averaging scale to obtain $\alpha=5\%$ at $\beta=0.95$ (in km)
Above the layer	D $\uparrow$	13	25	0.3	60
	A		25	0.25	60
Inside the layer	Q	5	1.5	0.2	25
	D $\uparrow$		2.5	0.2	25
	A		1.0	0.15	10
Under the layer	Q	9	3.5	0.5	100
	D $\uparrow$		2.5	0.5	100
	A		1.5	0.3	30

In Fig. 1 the average autocorrelation functions for fluxes of short-wave radiation are presented, and also for the short-wave albedo inside the layer. We may note that even in conditions of stratocumulus cloud cover the correlation decreases quite rapidly and in this case a certain weakly expressed periodicity is observed.

In Fig. 2 the average spectral densities  $S(f)$  are represented for fluxes of short-wave radiation in the interval of frequencies  $f$  from 0.015 to 0.6  $\text{km}^{-1}$ . On the curve of the spectral density of the flux of total radiation inside the layer, by a dashed line, the two small maxima are designated which are observed in the majority of cases, but, however, for confirmation of their reality the material is still inadequate. In Fig. 3 the spectral densities are given in logarithmic coordinates. In the cases under consideration, the spectral densities are not described by the ratio  $S(f) = bf^{-c}$  with a constant exponent  $c$ , with the exception of the flux of total radiation under the clouds, for which the given relation is true when  $c = 1.3$ . /123

Cumulus cloud cover. All the measurements were conducted with intra-mass cloud cover of the form Cu hum (Cu fr), Cu med, Cu cong of 1-8 points and, as a rule, below the clouds. In this case, the total radiation flux was recorded, and also the presence of clouds in the direction of the zenith along the flight path. Altogether in 1968, 19 successful realizations were obtained. The results obtained in the conditions indicated above turned out to practically coincident, and we did not succeed in observing any dependence of

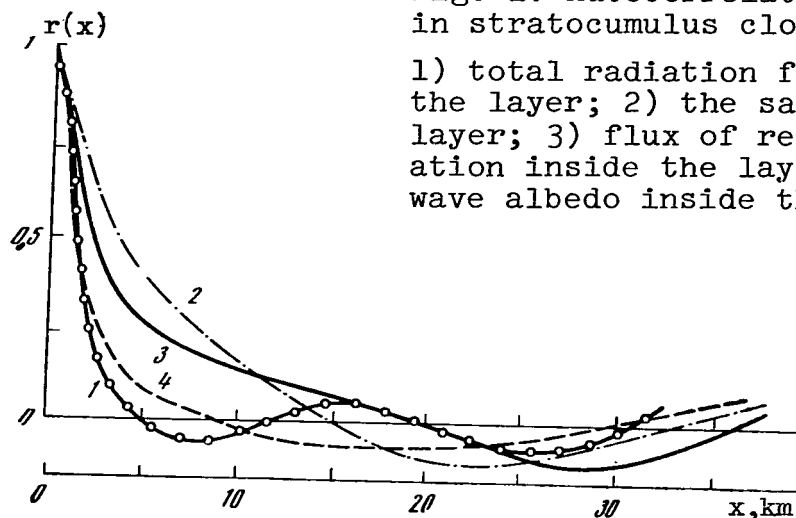


Fig. 1. Autocorrelation functions in stratocumulus cloud cover.

1) total radiation flux inside the layer; 2) the same, below the layer; 3) flux of reflected radiation inside the layer; 4) short-wave albedo inside the layer.

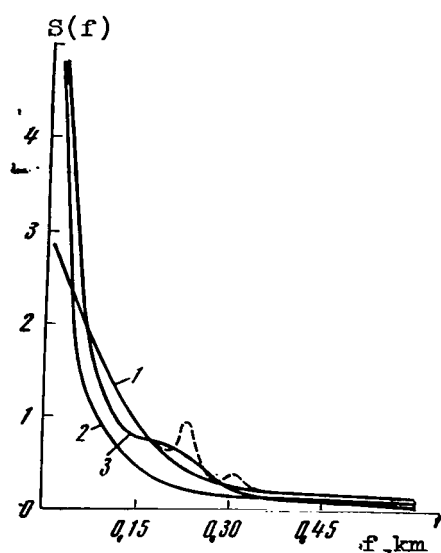


Fig. 2. Spectral densities in stratocumulus cloud cover.

1) total radiation flux inside the layer; 2) the same, below the layer; 3) flux of reflected radiation inside the layer.

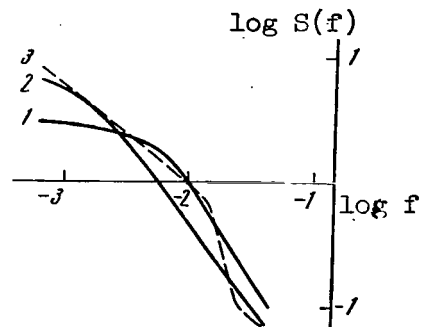


Fig. 3. Spectral densities in stratocumulus cloud cover on a logarithmic scale.

For symbols, see Fig. 2.



the statistical characteristics upon the point number or the form of cloud cover. This contradicts the ground observation data concerning the total radiation flux in cumulus cloud cover, but agrees well both with ground and aircraft measurements with a narrow-angle detector and apparently can be attributed to the small amount of averaging in space in flight at a short distance from the lower boundary of the clouds. On the basis of what has been said, we will consider only the averaged characteristics below. The average correlation radius  $x_{0.5}$  is equal to 0.8 km, the variation factor is 0.3. The necessary averaging scale for obtaining an average flux with a relative error  $\alpha = 5\%$  with a reliability  $\beta = 0.95$  is of the order of 30 km. In Fig. 4 the average autocorrelation function is given, and in Fig. 5 the spectral densities of the total radiation flux of flights below the clouds. In cumulus cloud cover the latter is approximated well by the expression  $S(f) = bf^{-c}$  at  $c = 0.62$ . /125

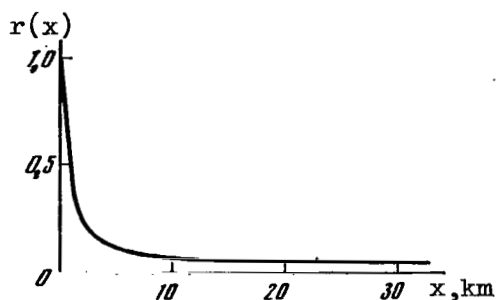


Fig. 4. Autocorrelation function of the total radiation flux below the layer of cumulus clouds.

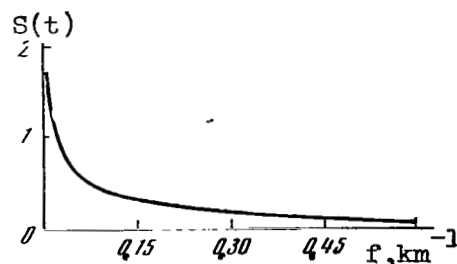


Fig. 5. Spectral density of the total radiation flux below the layer of cumulus clouds.

According to measurement with a narrow-angle detector on the flight path, the distributions of individual clouds and openings according to dimensions were found. Their average distribution is presented in Fig. 6. As is apparent, small clouds with openings predominate. With a growth of dimensions the probability of them monotonously decreases. Aside from this, according to measurements with the narrow-angle detector random functions were subjected to analysis, these random functions being a sequence of square pulses, where level 1 corresponds to the presence of clouds and level 0 to their absence. The autocorrelation function and the spectral density of such a function were found, and also their average value (the average absolute cloud cover along the flight path) and dispersion. The autocorrelation function obtained coincides with the

autocorrelation function for fluxes of total radiation presented in Fig. 4. The latter is entirely natural if we take into consideration the fact that during the flight directly below the clouds, because of the small amount of averaging, the notation of the total radiation flux is very similar to a series of square signals with "clear sky" and "cloud" levels.

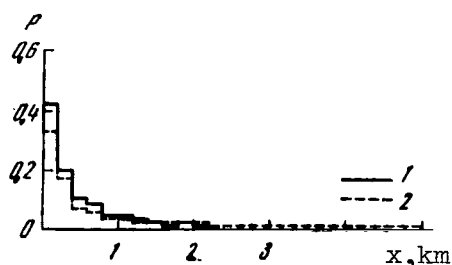


Fig. 6. Distribution of dimensions of clouds (1) and openings (2) along the flight path in a case of cumulus cloud cover.

In conclusion we must direct attention to the fact that the structure of the radiation field measured by a detector with an angle of view of  $180^\circ$  depends strongly upon the distance from the boundary of the cloud layer, in view of the different averaging with respect to area. Therefore, only results obtained at the same distances from the clouds may be compared directly with each other. If the purpose is the study of the structure of the field of clouds and the radiation field directly at its boundaries, it is advisable to use narrow-angle detectors, since in this case the results are practically independent of the distance between the detector and the layer of clouds and we may freely compare ground and aircraft data.

## STRUCTURE OF THE FIELD OF CUMULUS CLOUDS

Yu. R. Mullamaa, V. K. Pyldmaa, and M. A. Sulev

For purposes of studying the structure and distribution of intra-mass cumulus clouds, at the IFA AN ESSR ground recording of the coverage of the sky by clouds in the direction of the zenith and the sun was conducted, and, jointly with the Ukr. NIGMI, aircraft measurements of the presence of clouds in the direction of the zenith (or nadir) on the flight path were performed. A correlation and spectral analysis of the segments of cloud fields in time and space was performed. The results of aircraft investigations are presented in [IV.22]. /126

We may obtain an analytical formula for the autocorrelation function of the process of the appearance of clouds in a section of the cloud field. Under the assumption that the time or space section of the cloud field was obtained by means of limitation of the normal random function from the zero level, the autocorrelation function has the form [1]

$$r(t) = \frac{2}{\pi} \arcsin r_1(t), \quad (1)$$

where  $r_1(t)$  is the autocorrelation function of the normal random process.

At the same time, the experimentally determined autocorrelations functions of the presence of clouds in a section (cross-section) of the cloud field are well approximated by the formula

$$r(t) = \frac{2}{\pi} \arcsin e^{-\alpha(t)}. \quad (2)$$

As was noted in ref. [IV.22], the correlation function of the total radiation in flights below the clouds coincides with the function of the presence of clouds and openings at the zenith. Consequently, formula (2) also describes the spatial autocorrelation of the total radiation well in measurements directly below cumulus clouds. We will also note that the total radiation at the surface of the earth is also described by formula (2), but more roughly, since the latter does not consider the variability of the scattered radiation and the contribution of the direct radiation arriving through the semi-transparent parts of the clouds [IV.20].

The spectral densities of the presence of clouds and openings, calculated according to the autocorrelation functions in the range of linear frequencies  $f$  from 0.12 to 2.4 min<sup>-1</sup>, are well approximated by the formula  $(f) \sim f^{-k}$ , where  $k$  varies within limits from 5/3 to 4/3. The dependence of  $k$  upon  $n_0$  in steady-state fields of cumulus cloud cover is shown in Fig. 1. It is apparent that the exponent  $k$  turns out to be least at  $n_0 = 5$ . In considering clouds as convective elements, we may compare the spectra obtained with the spectra of the pulsations of turbulent fluxes in an inertial sub-interval. It is interesting that in all the spectra of cumulus clouds observed the exponent  $k$  is less than in an inertial sub-interval [2]. The following hypothetical explanation of this fact is possible. The steady-state field of cumulus clouds is maintained by the influx of external energy (basically by the latent heat of condensation), which counteracts turbulent decay in the inertial sub-interval. As a result, the exponent  $k$  decreases. With a growth of cumulus clouds it must be less, and in decay greater, in comparison with the values given in Fig. 1. However, we must note that the exponent  $k$  is only slightly sensitive to the growth and decay of cumulus clouds and the accuracy of its determination is low. Therefore, the use of it for determination of the rate of development or decay of the fields of cumulus clouds is scarcely probable.

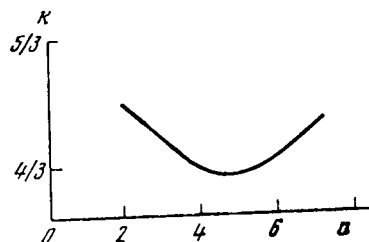


Fig. 1. Exponent  $k$  of the spectral density as a function of the point number of cloud cover at the zenith.

For the distribution characteristic of the duration of the coverage of the zenith by clouds, the probability densities  $p(t)$  of the relative number of openings or clouds were determined. The latter demonstrate what fraction of the general number of openings or clouds in a time or space cross-section has a duration  $t$  or a length  $x$ .

The probability densities of the number of openings and clouds obtained from the experiment are well approximated by the function

$$p(t) = \frac{\alpha}{\pi} \frac{e^{-\alpha t}}{(1 - e^{-2\alpha t})^{1/2}}. \quad (3)$$

Formula (3) was obtained theoretically under the same assumptions as formula (2), i.e., under the assumption that the normal random process is simultaneously also a Markov process [3]. Formula (3) is inapplicable at  $t \rightarrow 0$ . According to ground measurements at  $n_0 = 5$ , the value of  $\alpha = 0.3$  occurs.

The experimentally determined probability densities of the number of clouds as a function of their duration are given in Fig. 2. The probability densities of ground and aircraft measurements coincide if, on the average, 1 minute of ground measurements corresponds to 0.4 km in space.

An analogous picture is also observed for openings, if we replace the average point number of the cloud cover by the average probability of a free sighting line. Short openings and small clouds are encountered most frequently. Curves 1 and 2 characterizes cloud cover to zenith sighting angles of  $50^\circ$ . At large zenith angles, the lateral parts of the clouds [IV.22] play an important role. Under their influence the openings decrease, and the shortest of them are overlapped, i.e., the clouds join together, and the more so if the sighting direction is closer to the horizon. For a comparison in Fig. 2 the density of the number of openings at a zenith sighting angle  $\vartheta = 80^\circ$  and  $n = 2$  is shown.

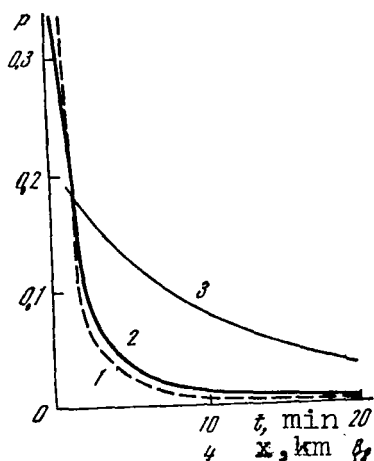


Fig. 2. Probability density of the number of clouds and openings as a function of their duration  $t$  (length  $x$ ). 1) average point number of cloud cover at zenith,  $n_0=1$ ; 2)  $n_0=9$ ; 3) at a zenith sighting angle  $\vartheta=80^\circ$  at  $n_0=2$ .

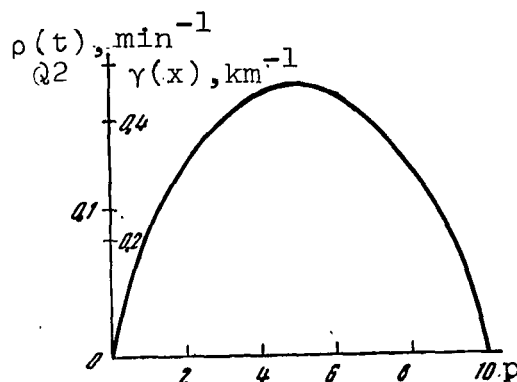


Fig. 3. Frequency of openings or clouds as a function of the point number of cloud cover at the zenith.

As is apparent, the distribution density of the number of openings or clouds depends slightly upon the average point number of cloud cover at the zenith. The frequency of openings or clouds,  $\gamma$ , i.e. their number per unit of time in ground measurements or per unit of length in aircraft measurements, is more sensitive to the variation of the point number at the zenith. Under the same assumptions as formula (1), the frequency of the clouds and openings is expressed by the formula

$$\gamma(n_0) = \frac{1}{2\pi} \frac{\sigma_{z'}}{\sigma_z} \exp \{-\arg \operatorname{erf} |1 - 2n_0|\}^2, \quad (4)$$

where  $\sigma_z$  and  $\sigma_{z'}$  are the square roots of the dispersions of the normal random surface and its derivative. According to our measurements  $\frac{1}{2\pi} \frac{\sigma_{z'}}{\sigma_z} = 0.18$ . Fig. 3 demonstrates that the frequency is at the maximum with a point number at the zenith of  $n_0 = 5$ . With variations of the point number within limits from 1 to 9 the frequency varies by up to a factor of two, in the first approximation turning out to be symmetrical relative to  $n_0 = 5$ .

Thus, cumulus cloud cover may be modeled by a normal random /129 function, limited from below. A good agreement of such a model with the experimental data is observed. Short openings and cross-sections of clouds that are small in dimensions are most frequently encountered. In this case the average number of clouds or openings per unit interval is greatest at an average point number  $n_0 = 5$  in the direction of the zenith.

## REFERENCES

1. Tikhonov, V. I., Statisticheskaya radiofizika (Statistical Radiophysics), Moscow, "Sov. radio", 1966.
2. Monin, A. S. and Yaglom, A. M., Statisticheskaya gidromekhanika (Statistical Fluid Mechanics), Part 2, Moscow, 1967.
3. Stratonovich, R. L., Izbrannyye vorposy fluktuatsiy v radiotekhnike (Selection of Problems of Vibration in Radio Engineering), Moscow, "Sov. radio", 1961.

# ON THE TRANSMISSION OF SOLAR RADIATION BY STRATIFORM CLOUD COVER AS A FUNCTION OF THE STATISTICAL CHARACTERISTICS OF ITS STRUCTURE

Yu. R. Mullamaa

The light regime in a light-scattering medium is connected nonlinearly with the characteristics of the medium ordinarily used in transport theory—the scattering and absorption factors, the scattering indicatrix, and the optical thickness. As a consequence of this, the description of the light regime of heterogeneous media by means of a transport equation with average characteristics of the medium brings with it a systematic error that is frequently impossible for the researcher to estimate.

In this work the transparency  $\Phi$  of the optically dense cloud layer is considered, as a function of the variability of its optical thickness, caused by variations of the altitude of the lower and upper boundaries, the absolute humidity, and the microstructure. G. V. Rozenberg's formula for calculation of the transparency of optically thick media [1] is well adapted for such a type of investigation:

$$\Phi = \frac{c_1}{1 + c_1(\bar{\tau} + \tau)}, \quad (1)$$

where

$$c_1 = \frac{1}{3} + \mu_0 \quad \text{or} \quad c_1 = \left( \frac{1}{3} + \mu_0 \right) \left[ \frac{1 + 2A}{3} + (1 - A)\mu \right]$$

respectively, for the flux and intensity;  $c_2 = \frac{1-A}{l}$ ,  $\bar{\tau}$  and  $\tau$  are /130  
the average optical thickness of the layer and its deviation from the mean;  $A$  is the albedo of the underlying surface;  $l$  is a parameter characterizing the degree of elongation of the scattering indicatrix;  $\mu_0$  and  $\mu$  are the cosines of the zenith angle of the incident and scattered radiation, respectively. Formula (1), strictly speaking, is applicable for a description of the propagation of light in plane-parallel homogeneous optically thick layers ( $\bar{\tau} + \tau \geq 5$ ) along a horizontal. For the study of the fluctuation of the transparency of real clouds according to formula (1) it is required that the scales of the heterogeneities of the cloud cover greatly exceed the length of the free path of a photon in the cloud. The possibility of such an approach is provided by the fact that the characteristic scale of the heterogeneities of the cloud cover, as is well known, is considerably greater than



the length of the free path of a photon in the cloud. The small-scale heterogeneities encountered in natural conditions in such a consideration are smoothed out and averaged; in essence, consideration of their contribution is a problem of the future. In the analysis it is assumed that the optical thickness of the stratoform cloud cover, considered as a random function, is normally distributed, which, apparently, is plausible, since the optical thickness is formed under the joint effect of several randomly varying parameters: the altitude of the upper and lower boundaries, the absolute humidity, and the microstructure.

In these assumptions, the transparency density function is expressed in the form

$$p(\Phi) = \frac{c_1}{\sqrt{2\pi} c_2 \sigma_\tau \Phi^2} \exp \left[ -\frac{1}{2\sigma_\tau^2} \left( \frac{c_1}{c_2 \Phi} - \frac{1}{c_2} - \bar{\tau} \right)^2 \right]. \quad (2)$$

The transparency density distribution functions, depending upon the average optical thickness and its dispersion, are given in Fig. 1. In the calculations it was assumed that  $c_2 = 0.1$  and  $\mu_0 = 0.5$ . As is apparent, the transparency density distribution function is more asymmetrical if the dispersion of the optical thickness is greater. In this case, the distribution function is extended in the direction of larger values of the transparency. With an increase in  $\bar{\tau}$ , the maximum in the transparency distribution shifts toward lesser values of  $\Phi$  and the probability of the maximum brightness increases. The transparency mode does not coincide with the transparency at the average optical thickness, but is shifted toward larger optical thicknesses, and the greater this is the greater its dispersion and the less its average magnitude, i.e.,  $\Phi_{\text{mode}} < \bar{\Phi}$ .

In Fig. 2 the dependence of the difference  $\Delta\tau = \tau(\Phi_{\text{mode}}) - \bar{\tau}$  upon the dispersion  $\sigma_\tau^2$  at  $\tau = 15$  is given. On the other hand, the optical thickness corresponding to the average transparency  $\bar{\Phi}$  is less than the average optical thickness  $\tau(\bar{\Phi}) < \bar{\tau}$ .

As is well known, the average transparency and the dispersion of the transparency may be found according to the formulas

$$\begin{aligned} \bar{\Phi} &= \int_0^1 \Phi p(\Phi) d\Phi, \\ \sigma^2 &= \bar{\Phi}^2 - \bar{\Phi}^2 = \int_0^1 \Phi^2 p(\Phi) d\Phi - \left[ \int_0^1 \Phi p(\Phi) d\Phi \right]^2. \end{aligned} \quad (3)$$

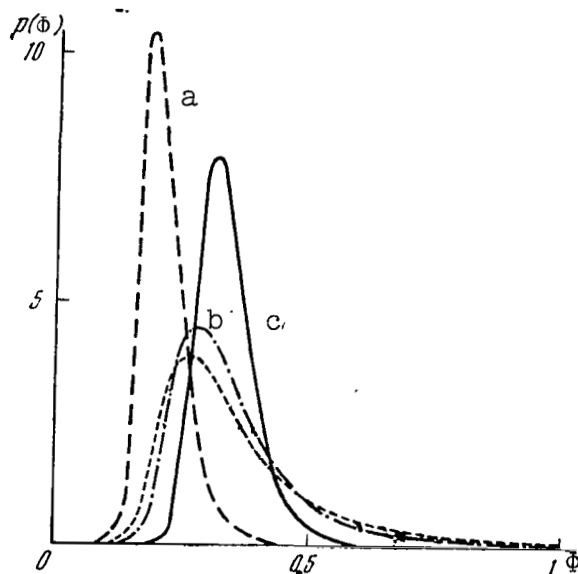


Fig. 1. Transparency distribution function.

- a)  $\bar{\tau}=30$ ,  $\sigma_{\tau}^2=64$ ; b)  $\bar{\tau}=15$ ,  $\sigma_{\tau}^2=64$ ;  
 c)  $\bar{\tau}=15$ ,  $\sigma_{\tau}^2=16$ ; d)  $\bar{\tau}=15$ ,  $\sigma_{\tau}^2=100$ .

However, expressions (3) do not integrate in the analytical form.

The average transparency and dispersion are expressed in approximation in the form

$$\Phi = \frac{c_1}{1 + c_2 \bar{\tau}} [1 + c_2 \bar{\tau}^2] = \frac{c_1}{1 + c_2 \bar{\tau}} \left[ 1 + \left( \frac{c_2}{c_1} \right)^2 \Phi^2(\bar{\tau}) \bar{\tau}^2 \right], \quad (4)$$

$$c = \frac{c_2}{1 + c_2 \bar{\tau}},$$

$$\sigma_{\Phi}^2 = \left( \frac{c_2}{c_1} \right)^2 \left( \frac{c_1}{1 + c_2 \bar{\tau}} \right)^4 \sigma_{\tau}^2. \quad (5)$$

As is apparent from formula (4) the average transparency coincides with the transparency at the average optical thickness only in the limiting case, when the dispersion of the optimum thickness approaches zero. In all other cases it is greater than this would be according to formula (1) at the average optical thickness. Thus, by calculating the average optical thickness according to the average transparency, we obtain systematically understated values.

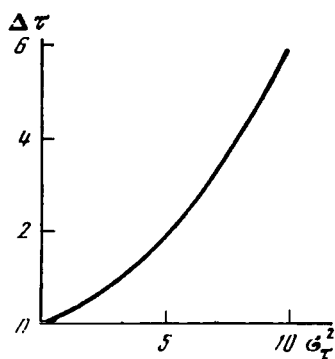


Fig. 2.  $\Delta\tau$  as a function of the dispersion  $\sigma_{\tau}^2$  at  $\bar{\tau} = 15$ .

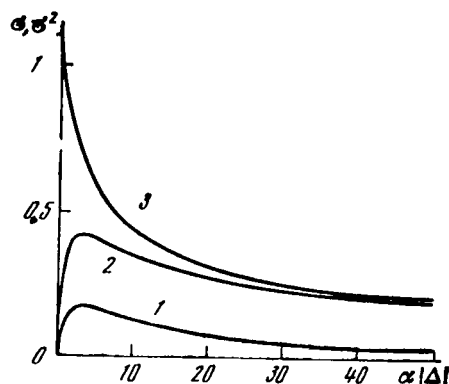


Fig. 3. Dispersion (1), mean square deviation (2), and variability factor (3) of the dispersion of the correction factor as a function of the averaging  $\alpha|\Delta|$ .

The dispersion of transparency (5) in the first approximation depends linearly upon the dispersion of the optical thickness and is proportional to the fourth power of the transparency at the average optical thickness.

In ground or aircraft measurements of the fluxes of radiation by the detector, averaging is performed according to the region of space not providing, generally speaking, for obtaining the averaged values for the fluxes. We will find the dependence between the thickness  $\bar{\tau}^{\Delta}$  and the transparency  $\bar{\phi}^{\Delta}$ , averaged according to region  $\Delta$ , increasing from 0 to infinity.

Analogously with formula (4) we obtain

$$\bar{\phi}^{\Delta} = \frac{c_1}{1 + c_2 \bar{\tau}^{\Delta}} [1 + c_{\Delta}^2 \sigma_{\tau_{\Delta}}^2], \quad (6)$$

where

$$c_{\Delta} = \frac{c_2}{1 + c_2 \bar{\tau}^{\Delta}}, \quad a_{\Delta} \sigma_{\tau_{\Delta}}^2 = \bar{\tau}^{2\Delta} - [(\bar{\tau}^{\Delta})^2 - (\bar{\tau})^2].$$

The dispersion  $\sigma_{\tau_{\Delta}}^2$  is a random function and, consequently, the functional connection (6) between  $\bar{\tau}^{\Delta}$  and  $\bar{\phi}^{\Delta}$  is random in nature.

By averaging  $\sigma_{\tau_{\Delta}}^2$ , we obtain the average magnitude of the dispersion /133

$$\overline{\sigma_{\tau_{\Delta}}^2} = \sigma_{\tau}^2 - \sigma_{\tau_{\Delta}}^2. \quad (7)$$

By substituting (7) into formula (6), we obtain the connection between  $\bar{\Phi}^\Delta$  and  $\bar{\tau}^\Delta$  at the average magnitude of the correction factor in brackets.

$$\bar{\Phi}^\Delta = \frac{c_1}{1 + c_2 \bar{\tau}^\Delta} [1 + c_3 (\sigma_\tau^2 - \sigma_{\tau\Delta}^2)]. \quad (8)$$

For estimation of the random nature of the functional connection in formula (6) we calculate the dispersion of the dispersion  $\sigma_{\tau\Delta}^2$ . Under the assumption that the optical thickness has a correlation function of the form  $r(t) = e^{-\alpha|t|}$ , the dispersion of the dispersion  $\sigma_{\tau\Delta}^2$  is expressed, in approximation, as

$$\sigma_{\tau\Delta}^2 \leq \sigma_\tau^4 \left[ \frac{2}{1 + \alpha\Delta} - 2 \left( \frac{2}{2 + \alpha\Delta} \right)^2 \right] \quad (9)$$

or

$$\frac{\sigma_{\tau\Delta}^2}{(\sigma_\tau^2 - \sigma_{\tau\Delta}^2)^2} \leq \left( \frac{1}{1 - \frac{2}{2 + \alpha\Delta}} \right)^2 \left[ \frac{2}{1 + \alpha\Delta} - 2 \left( \frac{2}{2 + \alpha\Delta} \right)^2 \right]. \quad (10)$$

In Fig. 3 the dispersion  $\sigma_{\sigma_2}^2$  is given in units  $\sigma_\tau^4$ , the mean square deviation in units  $\sigma_\tau^2$ , and the variability factor

$$\sigma_{\sigma_2}^2 / (\sigma_\tau^2 - \sigma_{\tau\Delta}^2).$$

As is apparent from Fig. 3, the random nature of the functional connection (6) is greatest in averaging according to space  $\Delta$  if  $\alpha\Delta \lesssim 1$ . With an increase in the averaging scale the random nature of the connection (6) decreases slowly and with a decrease in scale rapidly.

For cirrus clouds the factor in brackets in formula (4) varies from 1.05 to 1.15. Consequently, in calculating the transparency according to the average optical thickness we obtain results systematically decreased by 10%, on the average. In calculating the average optical thickness according to the average transparency, we obtain a magnitude that is 20% less than the true value.

In summary, we note that for a description of the light regime in fluctuating media, it is inadequate to know the average characteristics of the medium. It is necessary to know their dispersions, correlation functions, and, in the solution of certain problems, also the distribution functions.

By means of a method analogous to the one described, we may obtain both the functional connections of the intensities or fluxes of radiation with the fluctuating albedo or the parameters of the extension of the indicatrix. By using the methods of moments, we /134 may analogously obtain also the connection between the correlation functions and the spectral densities.

## REFERENCE

1. Rozenberg, G. V., "Optical properties of thick layers of a homogeneous scattering medium", Collection: Spektroskopiya svetorasseivayushchikh sred (Spectroscopy of Light Diffusing Environments), Minsk, Izd-vo AN BSSR, 1963.

## ON THE COVERAGE OF THE SKY BY CLOUDS

O. A. Avaste, Yu. R. Mullamaa,  
Kh. Yu. Niylik, and M. A. Sulev

At the present time there are two basic opportunities of determining the cloud cover: ground and satellite observations. In ground observations, the quantity of clouds is expressed as the fraction of coverage of an imaginary hemisphere with its center at the point of observation. Since in the given case the quantity and distribution of the clouds depend upon the vertical and horizontal coordinates of the observation point, we will call the cloud cover determined in such a manner "relative". A widely used method is to define cloudiness in terms of points on a scale, which are found by multiplying the fraction of sky covered by 10. By projection of the clouds on an imaginary sphere with its center at the center of the earth (or, with a plane-parallel model of the atmosphere, onto a horizontal surface), we obtain the so-called absolute cloud cover. In other words, absolute cloud cover is the quantity of cloud cover at the zenith over the territory under consideration. Satellite photographs of clouds, which are obtained by means of photography at relatively small angles to the vertical, give magnitudes that are close to the absolute cloud cover.

We should note that both ground and satellite observations of the point number of the cloud cover do not contain any information concerning the dependence of the probability of coverage of the sky by clouds upon the zenith sighting angle. At the same time, the radiation regime of the atmosphere (such as, for example, the duration of sunshine, fluxes of scattered radiation, etc.) is determined mainly not only by the quantity of the cloud cover, but also by the thickness of individual clouds and by their distribution throughout the sky.

Thus, the problem of the determination of various characteristics of cloud cover and ascertainment of their interrelationship, and also the selection of appropriate cloud characteristics for determination of the radiation field in the atmosphere, is a very urgent one. For this purpose, a cycle of theoretical investigations was performed at the IFA AN ESSR. /135

The quantity of relative cloud cover, according to estimates [1], in clouds of the lower and middle levels as a function of their altitude, is practically entirely determined by the cloud field with a radius of 15-25 km above the observation point.

Averaging throughout the sky on such scales turns out to be inadequate for providing the stability of the magnitude of the

relative cloud cover. With an approach to the layers of cloud cover in observation from aircraft and balloons, the averaging scale decreases and as a result the random variability of the relative point number increases. According to estimates performed the deviations of the momentary values from the mean may reach as much as  $\pm 3$  points [1]. Therefore, for reliable determination of the average relative point number of the cloud cover, an additional averaging of ground observations or spatial averaging according to the results of observations from several points is required. In other words, the cloud field as a whole is characterized only by averaged values of the parameters being used. In a case of necessity of the study of the variability of the cloud cover, we should apply dispersion-harmonic analysis to it [IV.22-23].

Three calculation schemes are given below for determination of the averaged values of the probability of coverage of the sighting direction and the point number of the relative cloud cover as a function of the absolute cloud cover and as a function of the nature of the distribution of the clouds throughout the sky.

In all these models, the following assumptions were made: the atmosphere is plane-parallel, the field of cloud cover is homogeneous and isotropic, the height of the lower boundary of all the clouds in the cloud system is the same.

In model I [2,3] an additional assumption was made, that the cloud is approximated by cylinders with a base radius  $q$  and a thickness  $h$ , which on the plane of the lower boundary of the clouds are distributed according to Poisson's law.

In model II [4] the clouds are approximated by straight cylinders with an arbitrary configuration of the bases. The distribution of them on the plane of the lower boundary of the clouds is arbitrary.

In addition it is assumed that the horizontal and vertical dimensions of the clouds, and also the distance between them, are independent of each other. This assumption is made for the purpose of simplification of calculation formulas; in principle it is possible to derive formulas of model II for a case when the geometrical characteristics of the clouds depend upon each other.

In model III [5] the clouds are modeled by a continuous random Gaussian surface, bounded at a certain level from below.

We will give the calculation formulas for determination of the averaged values of the probability of coverage of the direction



of sighting ( $\bar{n}_\vartheta$ ) and the relative cloud cover ( $\bar{n}$ ) for various models 136. As is well known,  $\bar{n}_\vartheta$  and  $\bar{n}$  are associated with each other in the following manner:

$$\bar{n} = \int_0^{\pi/2} \bar{n}_\vartheta \sin \vartheta d\vartheta. \quad (1)$$

The quantities  $\bar{n}_\vartheta$  and  $\bar{n}$  in model I are calculated according to the formulas

$$\bar{n}_\vartheta = 1 - \exp[-\gamma_p(\pi q^2 + 2qh \lg \vartheta)], \quad (2)$$

$$\bar{n} = n_0 - (1 - n_0) G(k), \quad (3)$$

where  $n_0$  is the quantity of the absolute cloud cover over the plane under consideration;  $\gamma_p$  is the density of the centers of clouds distributed on this plane according to Poisson's law ( $\gamma_p$  is functionally connected with the point number of the clouds [6]);  $q$  is the radius of the clouds,  $h$  is the thickness of the clouds, and  $\vartheta$  is the sighting angle.

The parameter  $k$  is determined as the statistical average according to the formula

$$k = 2\gamma_p / \pi q \quad (4)$$

and

$$G(k) = \frac{\pi k}{2} [H_0(k) - Y_0(k)], \quad (5)$$

where  $H_0(k)$  is a zero-order Struve function;  $Y_0(k)$  is a second-level zero-order Bessel function (a Weber function).

In model II for determination of  $\bar{n}_\vartheta$  the following formula was obtained

$$\bar{n}_\vartheta = 1 - \gamma \int_0^\infty p(l) dl \int_{h \lg \vartheta}^\infty (l - h \lg \vartheta) p(l) dl, \quad (6)$$

where  $\gamma$  is the frequency of the clouds upon the route being investigated (the average number of the clouds per unit of length);

$p(\ell)$  is the probability density of cloud openings ( $\ell$ );  $p(h)$  is the probability density of the vertical thickness of the clouds.

In model III  $\bar{n}_\theta$  is calculated in the following manner:

$$\bar{n}_\theta = n_0 \exp \{-n_0 [N(\theta) - 1]\} - \exp \{-n_0 [N(\theta) - 1]\}, \quad (7)$$

where

$$N(\theta) = \frac{1}{2} \operatorname{erf} \frac{\operatorname{ctg} \theta}{\sigma_z' \sqrt{2}} + \frac{\sigma_z'}{\sqrt{2\pi} \operatorname{ctg} \theta} \exp \left[ -\frac{\operatorname{ctg}^2 \theta}{2\sigma_z'^2} \right], \quad (8)$$

where  $\sigma_z'^2$ , is the dispersion of the derivative from a normal random surface; erf is the probability integral.

In models II and III the relative cloud cover  $\bar{n}$  is obtained according to formula (1).

The models I-III given above contain parameters determined experimentally.

In model I:  $n_0$  is the absolute cloud cover,  $p(q)$  is the /137  
probability density of the cloud elements,  $p(h)$  is the probability density of the thickness of the clouds.

In model II:  $\gamma$  is the frequency of the clouds in a cross-section of the track under consideration,  $p(\ell)$  is the probability density of cloud openings,  $p(h)$  is the probability density of the thickness of the clouds.

In model III:  $n_0$  is the absolute cloud cover,  $\sigma_z'^2$ , is the dispersion of the derivative from a random surface.

Let us compare the models developed.

An advantage of models I and II should be considered, the fact that they make it possible to follow the effects of the influence of the geometrical structure of the cloud field on the magnitude of the relative cloud cover easily. Model I makes it possible to derive analytical formulas for calculation of the probability that in the direction  $\theta$  in the solid angle  $\Omega$  there is not one cloud element [3]. In model II the calculation of the quantity  $\bar{n}_\theta$  is performed on the basis of values of  $\gamma$ ,  $p(\ell)$ , and  $p(h)$  assigned or experimentally determined without any sort of limitation relative to the distribution of the clouds. An

advantage of model III is the quite general form of the cloud field—a random Gaussian surface.

The results of the calculations according to the three models explained coincide with an accuracy up to the errors of measurement of the initial parameters.

Among the shortcomings and limitations of the methods we should note:

1. Models I and II use a quite rough approximation of the clouds by straight cylinders. In model I, in addition, it is assumed that the bases of the cylinders are circles.

2. In models I and II the probability density of the thickness of the clouds  $p(h)$ , which it is difficult to determine experimentally, enters into the initial parameters. However, this difficulty may be overcome by using the dependence between the dimensions of the bases and their thickness from the experimental data [3] or by using the average thickness of the cloud system [4], with a judicious selection of which the errors are very small [4].

Model I gives slightly exaggerated results at  $n_0 > 0.6$ . This is caused by the fact that cumulus clouds are not randomly distributed, as is assumed in the Poisson model, but correlation dependences are observed (for example, the so-called cloud series, a cluster of clouds at large relative coverage, etc.). On the other hand, with a limiting decrease of the point number of cover at the zenith ( $n_0 \rightarrow 0$ ) the cloud elements obtained theoretically by limitation of the random Gaussian surface from below are distributed in space according to Poisson's law. The latter explains the good agreement of all the models at small values of  $n_0$ .

In model III a certain difficulty arises in the determination of the dispersion  $\sigma_z^2$ , which is calculated indirectly according to formula (7) on the basis of experimental data for  $n_0$  and  $\bar{n}$ .

However, it turns out that the dispersion of the derivative from a random Gaussian surface is 1.4 on the average and increases insignificantly with a growth of the absolute cloud cover. If  $\sigma_z^2$  is assumed to be independent of the point number  $n_0$ , then  $\sigma_z^2$  becomes a constant which can be much more readily determined. In this work  $\sigma_z^2$  was determined with the use of photographs of the sky obtained by means of a spherical mirror. The observations were performed at Tyraver (near Tartu) and near Moscow (at Zvenigorod) [IV.20].

/138

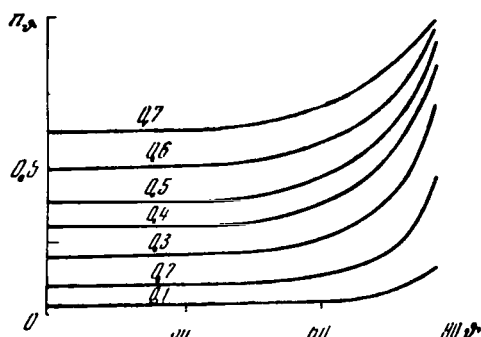


Fig. 1. Average coverages of the direction of sightings by clouds according to formula (2) at magnitudes of relative cloud cover of 0.1-0.7 as a function of the zenith angle.

In Fig. 1 the averaged values of the coverage of the sky are given as a function of the zenith angle and the sighting angle at magnitudes of the "relative" cloud cover from 0.1 to 0.7. These curves were calculated according to formula (7) at  $\sigma_z^2 = 1.4$ . It is apparent that the coverage of the direction of sighting begins to increase considerably, beginning with a zenith angle of about  $50^\circ$ . According to investigation [4] (model II in this work) a curve resembling the one given in Fig. 1 was obtained with an average thickness of the clouds of about 0.1-0.2 km.

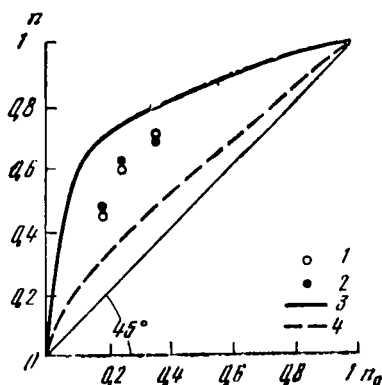


Fig. 2. Dependence of the averaged magnitudes of the relative cloud cover upon the magnitudes of the absolute cloud cover.

Curves are results of the calculations for a theoretically assigned function  $p(\lambda)$  at two variations of the vertical thickness of the clouds (0.1 and 1 km); 1) results of the calculations according to experimentally determined magnitudes of  $\gamma$  and  $p(\lambda)$ ; 2) the same magnitude, calculated according to method I [formulas (3)-(5)]; 3)  $h=1.0$  km; 4)  $h=0.1$  km.

The determination of the dependence of the averaged values of the relative cloud cover  $\bar{n}$  upon the magnitudes of the absolute cloud cover according to various calculation schemes (models I-III) demonstrates that the magnitudes of  $\bar{n}$  are always greater

than the corresponding magnitudes of  $n_0$ . These divergences are the maximum at medium point numbers of the cloud cover and depend considerably upon the vertical thickness of the clouds. As an example, in Fig. 2 the magnitudes of the "relative" cloud cover, averaged according to various routes, as a function of the quantity of the absolute cloud cover (according to model II [4]), are presented. The curves represent the results of calculations according to formulas (1) and (6) under the assumptions that  $h = \text{const}$  and  $p(l) = \text{const}$  for two variations of the vertical thickness of the clouds ( $h = 0.1$  and  $h = 1$  km). The results of the calculations according to the experimentally determined functions  $p(l)$  are plotted by dots. In this case it was assumed that the vertical thickness of each cloud on the plane of the cross-section is equal to the length of its horizontal dimension. In the given case the averaged magnitudes of the relative cloud cover exceed the corresponding magnitudes of the absolute cloud cover by 2-3 points on the average. This is also confirmed by calculations according to model I. According to model III maximum divergences of about 1.5 points were obtained. /139

We should emphasize that the averaged magnitudes of the "relative" cloud cover are determined mainly by the value of the frequency of openings [ $\gamma$  in formula (6)] and to a much lesser degree than this whether the cloud openings are the same or differ strongly from each other [4]. Consequently, in calculations according to model II reliable data are required for the determination of  $\gamma$  and the function  $p(l)$  is determined only tentatively. This circumstance considerably simplifies the accumulation of experimental initial data for the calculation.

We will now summarize.

Within the limits of the accuracy of the determination of initial experimental parameters, calculations according to the three methods explained coincide, and therefore the selection of one method or another in each specific case is determined basically by the available experimental data and by the purposes of the investigation. The parameters of model III are determined more easily from the experiment than the parameters of models I and II.

In cumulus clouds, the coverage of the direction of sighting by the clouds begins to increase considerably at zenith distances  $\theta > 50^\circ$ . As a consequence of this, for example, the duration of sunshine decreases with a decrease in the altitude of the sun, with an unchanged state of the cloud cover.

A point number of cumulus cloud cover, measured from an artificial earth satellite, is always less than the relative point number at the earth's surface, which it is necessary to bear in mind in the use of satellite data for ground conditions.

## REFERENCES

1. Niylik, Kh. Yu., "On certain characteristics of cloud cover", Collection: Radiatsiya i oblachnost' (Radiation and Cloudiness), IFA AN ESSR, Tartu, 1969.
2. Avaste, O. A., "Increase in cloud cover at the horizon in a case of ground observation", Collection: Radiatsiya i oblachnost' (Radiation and Cloudiness), IFA AN ESSR, Tartu, 1969.
3. Avaste, O. A., "Method of calculating the coverage of the sky by the lateral parts of cloud elements", Collection: Radiatsiya i oblachnost' (Radiation and Cloudiness), IFA AN ESSR, Tartu, 1969.
4. Niylik, Kh. Yu., Yu. R. Mullamaa, M. A. Sulev, "On the coverage of the sky by clouds", Collection: Radiatsiya i oblachnost' (Radiation and Cloudiness), IFA AN ESSR, Tartu, 1969.
5. Mullamaa, Yu. R., "On the coverage of the sky by cumulus clouds", Collection: Radiatsiya i oblachnost' (Radiation and Cloudiness), IFA AN ESSR, Tartu, 1969.

## CONCLUSION

We will list the basic results of the theoretical and experimental investigations described. /140

### I. Long-Wave Radiation

Various integral transmission functions of the gaseous components of the atmosphere are compared, which are used in radiation calculations, and a new transmission function constructed on the basis of more complete spectral data [I.1].

It was ascertained that in the most important range of the masses of the underlying substances all the transmission functions agree with an accuracy of up to 10%.

The integral transmission function for a cloudy atmosphere,  $\Phi_{\text{cloud}}$ , considering absorption by cloud particles and atmospheric gases at a given space-time distribution of the density of gases and the absolute humidity, was calculated. By means of  $\Phi_{\text{cloud}}$  it became possible to dispense with prior assumptions concerning black radiation of the cloud boundaries, to consider the variation of the radiation field in the process of the origin, development, and destruction of clouds [I.2, I.3], and the continuous spatial distribution of the fluxes. Powerful heat (radiation) sources inside the clouds near their boundaries were investigated, which is impossible in the "black" approximation, and also other characteristic regions of the radiation influx, depending upon the factors determining them [I.2 and I.3].

It was ascertained that the "black" approximation describes influxes near the cloud boundaries (outside the cloud) with an error of the order of 50%; as the distance from the cloud increases the error rapidly decreases. The influx to the entire column of the atmosphere or to the entire column of the layer over the cloud in this approximation is calculated with an error not exceeding 10%, and the influx to the cloud layer with an error not exceeding 20%; the relative error of the calculation of the influx to the entire layer below the cloud is very great, which is not too essential since this influx is small [I.3] at  $z_{n.g} \leq 5$  km.

Special attention was paid to the calculation and investigation of the behavior of the influx to thick atmospheric layers, in accordance with small vertical resolution in problems of the general circulation of the atmosphere. It was ascertained that the cloud layer as a whole is a high-capacity heat sink, providing /141



approximately half or more (in multi-layer cloud cover) of the general radiation cooling of the atmosphere [I.1].

Much attention is devoted in this collection to approximate methods of calculating thermal radiation in comparison with more accurate methods [I.3,4,5]. Formulas were proposed for description of the structure of local heat (radiation) sources at the cloud boundaries, their general heat content, and also the influx to the entire layers below the cloud, in the cloud, between the clouds, and above the cloud [I.3]. The error of the formulas in individual cases may reach 50%, but, however, they are attractive for their simplicity and physical clarity. In [I.4] approximate algorithms for calculating long-wave radiant fluxes and the influx, obtained from physical and mathematical considerations, were studied. In [I.5] calculations according to these methods are compared with more accurate methods using integral and spectral transmissions functions and thus the sequence of methods of decreasing accuracy (at a known error) and increasing simplicity is established.

Natural limitations of the accuracy of radiation calculations originate because of errors of measurement of the meteorological field. In [I.6] it was demonstrated that the contemporary accuracy of measurement of temperature is adequate for calculation for the long-wave radiant influx to the troposphere and the lower stratosphere with an error not exceeding 10%. Such an error is provided by the accuracy of measurement of the humidity in conditions of the lower troposphere. The error of calculation of the influx at higher levels rapidly increases due to imperfect methods of measuring the humidity. In conditions of broken cloud cover, the values of the radiation fluxes depend upon the horizontal distribution of the clouds.

As a consequence of the great degree of blackness, of even very thin clouds (with an absolute humidity of  $0.03-0.05 \text{ g/m}^3$ ) the basic parameter of cloud cover in calculations of fluxes of long-wave radiation is the quantity of clouds. In this case, calculation of counter-radiation with an error less than 3% requires a knowledge of the zonal number of points of cloud cover, i.e., the detailed distribution of the clouds throughout the sky [I.7]. Calculations on the basis of data concerning the general number of points of cloud cover guarantee an error of the determination of the counter-radiation of the atmosphere of the order of 5-10% as a function of the nature of the distribution of the clouds throughout the sky.

In [I.7] possibilities of the determination of averaged values of the counter-radiation of the atmosphere (with respect to time or with respect to a certain territory) are considered and the accuracy of the methods proposed is estimated.

For check and confirmation of the results of the numerical experiments and theoretical investigations performed, long-wave radiant fluxes in the 50-3000 m layer were measured in St-Sc clouds with a detailed resolution with respect to altitude [I.8].

The measurements were conducted onboard aircraft by means of /142 two types of instruments: a standard actinometric apparatus and radiation thermal elements designed by B. P. Kozyrev. The mean square deviation of the results of measurements in both cases did not exceed 10%, on the average. The measurements demonstrated the good convergence of the average profiles of the influxes calculated according to averaged data from measurements of the temperature, relative humidity, and absolute humidity, and according to averaged data from measurements from the fluxes. A systematic difference was observed between the measured and calculated fluxes above the clouds, which did not appear in the influxes.

## II. Short-Wave Radiation

The behavior of fluxes of visible solar radiation,  $0.4 \leq \lambda \leq 0.75$  micron, and infrared solar radiation,  $0.75 \text{ micron} \leq \lambda \leq 4 \text{ microns}$  is considered, and also direct and scattered solar radiation, in cloudless conditions at the level of the earth's surface as a function of the turbidity (pollution) and humidity of the atmosphere [II.10]. The total solar radiation flux arriving at the surface of the earth varies by not more than 30 and 15% with variation of the turbidity and humidity of the atmosphere, respectively, within limits of possible climatic variations of these quantities. The distribution of the influx with respect to altitude was investigated, as a function of the content of water vapor and its distribution. Approximation formulas were obtained for the total flux of solar radiation arriving at the surface of the earth, and the influx in the free atmosphere with consideration of the variation of pressure according to altitude.

The same results and methods of the calculation of the fluxes and influxes of solar radiation may be used in stratoform cloud cover if the albedo of the clouds is known. Calculation of the non-monochromatic albedo in the infrared range of wavelengths with consideration of absorption by the gaseous components is a difficult task. The solution of this problem within the framework of the classic theory of radiation transfer is impossible, since the determination of the true length of the path of the photons in the cloud is required. The first results of a work performed in this direction are presented in [II.11]. The values of the albedo in the basic bands of the absorption spectrum of water vapor and the integral albedo in a case of dense clouds with normal incidence of the sunbeams were calculated. The quantity of the solar radiation absorbed by the cloud layer was determined.

Experimental investigations of the structure of the short-wave radiation field in stratoform St and Sc clouds are presented in [II.12,13]. In these works the averaged vertical profile of the balance of radiant fluxes and the influx in the clouds was obtained. The average reflection and absorption capability of the clouds was experimentally determined, as a function of the thickness of the cloud layer and the position of the sun.

In broken cloud cover the dependence of the flux of direct solar radiation upon the zonal number of points of cloud cover in the angular zone containing the sun is ascertained, and the dependence of the scattered radiation upon the general relative number of points of cloud cover [II.19,21]. The duration of sunlight as a parameter of cloud cover more representative than the number of points with relationship to the average fluxes of direct radiation and total radiation is considered [II.21]. /143

### III. Turbulent and Radiant Heat Transfer in the Boundary Layer of the Atmosphere

As is well known, the boundary layer of the atmosphere (up to the level of the formation of clouds) may be heated by radiation, turbulence, and advective influxes of heat. In order to ascertain the significance of each of these factors, they were measured in the 50-500 m layer from onboard an aircraft in conditions of well-developed convection [III.14,15].

It turned out that all the types of heat transfer listed give an influx of the same order of magnitude. Together with this the equation of heat transfer, as a rule, does not close. Additional investigations and works to increase the accuracy of the measurements of each of the components of heat transfer were required. In particular, a methodology was developed and for the first time measurements were made of the spectra of turbulent heat fluxes in the boundary layer of the atmosphere. The results of these measurements made it possible to estimate the scales of the heterogeneities responsible for the turbulent heat transfer and to determine the requirements imposed upon the frequency characteristics of the measuring apparatus and the necessary averaging time in such a type of measurements [III.14].

It was demonstrated that the spectra of turbulent heat fluxes in well-developed convection over the steppe in the 50-500 m layer have maxima corresponding to the dimensions of the heterogeneities from 300 m at an altitude of 50 m and up to 1100 m at an altitude of 500 m [III.14].

For the determination of radiation heat influxes in a thin layer, the accuracy of existing methods is inadequate, in connection with which the development of a modulation method of measurement of the balance was begun.

Measurements of radiant short-wave and long-wave fluxes in the boundary layer over the steppe and the sea [III.15] in well-developed atmospheric pollution made it possible to estimate the radiation variations of the temperature and to divide the absorption of solar energy by water vapor and by the aerosols roughly, in approximation. The latter turned out to be comparable with the former and in certain cases was predominating.

It was observed that at a high degree of superheating of the soil (of the order of  $20-30^{\circ}$ ) relative to the air at the surface of the earth, which is characteristic for summer ground conditions, the long-wave radiation heats the entire boundary layer directly, and in this case heating by solar radiation decreases. A hypothesis was advanced concerning the regulating role of the aerosol in the ratio between long-wave and short-wave heat transfer in the surface layer.

#### IV. Statistical Structure of Radiation Fields in Clouds

/144

Real cloud cover is heterogeneous in space, variable in time, and may be considered as a random process, in connection with which the radiation field also becomes random.

An especially important task is study of the statistical structure of the radiation field in cumulus clouds and its parametrization. The fact is that medium-scale cumulus clouds may be considered in problems of large-scale dynamics only on the basis of statistical connections with other meteorological fields. Also, obviously, the corresponding radiation field must be described.

For the solution of this problem a cycle of ground operations was performed for recording the variability in time of the fluxes of short-wave radiation and the characteristics of cloud cover [IV.16-21,23].

For the study of the spatial variability of the total short-wave radiation flux and the reflected short-wave radiation flux over and under the clouds and the structure of the cloud cover, investigations aboard aircraft were conducted [IV.16-23].

The time and space series of values of radiation fluxes and the characteristics of the cloud cover obtained were considered

as realizations of the random functions and subjected to statistical analysis on a digital computer. The average values, dispersions, correlation functions, spectral densities, and distribution functions of the probability density, as well as the variability factors, were calculated. The accuracy of the statistical characteristics obtained was estimated. Thus, in measurements of radiation fluxes in the atmosphere in conditions of a relatively homogeneous cloud cover of St, As, Ac, Sc, averaging of not less than 20-60 minutes is required in ground measurements and not less than 15-40 km in aircraft measurements [IV.16,18]. An adequate increase in the scales of space and time averaging makes it possible to decrease the dispersion of the mean by an order of magnitude [IV.16-18,22]. In cumulus cloud cover the necessary averaging scale is located within limits of 40-100 min and increases with the increase in the number of points of the cloud cover. The averaging scales and measurements of the vertical profile of the radiation fluxes must be of the order of 100 km, which exceeds the technically realistic scale. As a result, with an adequately high degree of accuracy we succeed in constructing only the experimental radiation model of the "average stratoform cloud" and achieve a good agreement only with calculations also based on averaged profiles of temperature, relative humidity, and absolute humidity [I.8, II.12].

For determination of the dispersion, correlation function, and spectral density, longer realizations are required. In cumulus cloud cover the optimum duration amounts to 1.5-2 hours, in stratus cloud cover of various forms 2-4 hours, and sometimes up to 10 hours [IV.17,20]. The necessity of such a long period of observation or corresponding spatial scales sometimes makes it impossible /145 to study the radiation field in clouds within the framework of the theory of steady-state random functions.

Investigations of the structure of total radiation fluxes at the earth's surface [IV.19,21] demonstrated that the dispersion of the flux in cumuliform clouds exceeds the dispersion in stratoform cloud cover by almost an order of magnitude. The dispersion of the fluxes in intra-mass cumulus cloud cover is the maximum at a medium number of points of cloud cover. The probability densities of the total radiation strongly depend upon the number of points of cloud cover. In continuous cover (overcast) the distribution of the probability density has a monomodal form and with a lesser number of points of cloud cover, a bimodal form. The proximity of the autocorrelation functions at a higher number of points of various forms of cloud cover is a general rule. The autocorrelation functions of direct and total radiation also turn out to be very close.

By means of aircraft measurements we succeeded in accumulating adequate material for the study of stratocumulus and cumulus clouds

[IV.22,23]. The structure of the fluxes, because of different averaging throughout the area, depends upon the distance of the radiation detector from the cloud layer. Usually in aircraft measurements the averaging throughout space is less than in ground measurements with respect to time, and therefore the dispersion of the fluxes is greater and the correlation decreases more rapidly. Nevertheless, the characteristics of the radiation fields and cloud fields, obtained according to aircraft and ground measurements, are close, and supplement each other [IV.16]. For cumulus cloud cover the dependence of autocorrelation functions and distribution functions of the probability density and the spectral density upon the number of points of cloud cover was studied in detail.

The dependence of the statistical parameters of the radiation field upon the duration of sunshine was considered [IV.20].

It was demonstrated that this parameter is not identical to the number of points of cloud cover, as this is usually assumed in meteorology, and contains in itself more information concerning the radiation properties of the clouds than a point of cloud cover.

The structure of the cloud fields was studied in greatest detail for a case of intra-mass cumulus cloud cover [IV.20,23,25]. The optical properties of the atmosphere in cumulus cloud cover are determined not only by the quantity (points) of clouds, but also by their thickness (vertical development), distribution throughout the sky, dimensions, etc. Because of the considerable vertical dimensions of cumulus clouds, the probability of coverage of the sky begins to increase essentially at a zenith distance of the order of  $50^\circ$ , which leads to a decrease in the duration of sunshine with a decrease of the altitude of the sun, with an unchanged state of the cloud cover. Theoretical models were constructed for calculation of the coverage of the sky in the sighting direction [IV.25] which agree well with the experiment [IV]. The time and space recurrences of the coverage of the sun by clouds in the direction of the zenith demonstrate that small openings and short cross-sections of the clouds are most frequently encountered. In this case, the /146 average number of clouds or openings per unit of length is greatest at a medium number of points of cloud cover in the direction of the zenith. Autocorrelation for recurrence of the clouds decreases much more rapidly than for total radiation. In the frequency range from  $0.06$  to  $1.2 \text{ min}^{-1}$ , or from  $0.15$  to  $3.0 \text{ km}^{-1}$ , the spectral densities are well approximated by a power function, and the exponent is the maximum at a medium number of points [IV.23]. The noticeable role of the semi-transparent parts of cumulus clouds in the formation of the total radiation flux was ascertained [IV.20].

On the basis of experimental investigations, the effects of the quantity and distribution of cumulus cloud cover throughout the sky on the averaged magnitudes of the counter-radiation of the atmosphere [I.7] were calculated.

The effect of fluctuations of the optical thickness of cirrus cloud cover on radiation transmission was theoretically considered [IV.24]. In a fluctuating thickness of the cloud cover the radiation transmission is greater than in a homogeneous layer having the same average optical thickness.

## ABSTRACTS OF ARTICLES

UDC 551.521

"Integral Function of the Transmission of Thermal Radiation" /149  
Gradus, L. M., Kh. Yu. Niylik, and Ye. M. Feygel'son, Collection:  
Teploobmen v atmosfere, "Nauka", 1972, p. 1.

The integral transmission function in a cloudy atmosphere, considering the distribution of the absolute humidity of clouds in space and time, and also that of the gaseous absorbing substances, was obtained and presented by approximation formulas. If there are no clouds, this transmission function is one of the variations of an integral transmission function for water vapor and carbon dioxide gas, constructed according to somewhat refined initial data and compared with other transmission functions used in calculations of radiant fluxes. 1 table, 1 illustration, 5 references.

UDC 551.521; 551.576

"Features of Long-wave Radiation Influx in Stratoformous Cloud Cover (Numerical Experiment)", Petrova, L. V. and Ye. M. Feygel'son, Collection: Teploobmen v atmosfere, "Nauka", 1972, p. 7.

The vertical profile of the long-wave radiant influx of heat in the troposphere is calculated as a function of the levels of arrangement, thickness, and quantity of cloud layers, of the distributions of temperature and relative humidity, of the distribution of the absolute humidity of the clouds, and of the average dimensions of the drops. The numerical experiment performed made it possible to study separately the role of each of the factors listed with the others preserved as constants. The structure of the radiation cooling and heating near the cloud boundaries inside the cloud was studied in detail. It was demonstrated that the radiation energy effect of weak cloud cover is not small with an absolute humidity that is an order of magnitude less than the average absolute humidity of stratoform clouds. 1 table, 3 illustrations, 6 references.

UDC 551.521

"A Cloud as a Heat Sink", Ye. M. Feygel'son, Collection: Teploobmen v atmosfere, "Nauka", 1972, p. 16.

A cloud layer resembles a heat sink because its radiation cooling is great, amounting to approximately half the general cooling of the entire column of the atmosphere, and depends slightly upon the thickness of the cloud. It is demonstrated that cooling is basically concentrated near the upper boundary of the cloud layer and is partially compensated by heating near the lower boundary. Simple and physically clear approximate formulas were obtained for calculation of radiant influxes to the boundary layers of the cloud, to the entire column of the cloud layer, the layer



above the cloud, and the layer below the cloud. The error of the assumption of the equivalence of the cloud to black radiation was estimated, and the boundaries of the applicability of this approximation were determined. 1 table, 2 illustrations, 6 references.

UDC 551.521

"Some Approximate Methods of Calculating Radiant Heat Transfer in a Cloudless Atmosphere", Ginzburg, A. S. and Ye. M. Feygel'son, Collection: Teploobmen v atmosfere, "Nauka", 1972, p. 26.

Simplified methods of calculating the fluxes of long-wave radiation and influx of heat are discussed in connection with large-scale problems of dynamic meteorology. The calculation method considering heat transfer with the underlying surface and cooling in space is considered, and also a method based on the assumption of the  $\delta$ -shaped nature of the second derivative of the transmission function. It is indicated that these methods may be extended to a case of cloud conditions. 3 references.

UDC 551.521

"Comparison of Various Methods of Calculating the Field of Long-wave Radiation", Ginzburg, A. S. and Kh. Yu. Niylik, Collection: Teploobmen v atmosfere, "Nauka", 1972, p. 30.

Results of successively more simplified calculations of fluxes and influxes of heat are compared with data from spectral calculations. For three models of the atmosphere, fluxes of long-wave radiation at levels 0, 1, 2, 4, 6, and 10 km, and influxes of heat to the kilometer layers throughout the entire column of the troposphere are given. Possible sources of errors of various methods are considered and the magnitudes of these errors are estimated and also the general errors of the method. 1 table, 8 references.

UDC 551.521

"Estimate of the Error in Calculation of Fluxes and Influxes of Thermal Radiation due to Errors of Initial Meteorological Parameters", Niylik, Kh. Yu., Collection: Teploobmen v atmosfere, "Nauka", 1972, p. 39.

An estimate was made of errors of calculation of fluxes and influxes of thermal radiation of the atmosphere originating as a consequence of errors of the initial meteorological data. It is demonstrated that the accuracy of measurement of the atmospheric temperature that can be achieved at the present time is entirely satisfactory for calculation of integral radiation fluxes, but, however, it is necessary to increase the accuracy of the measurements of the characteristics of relative humidity. 2 tables, 6 references.

UDC 551.576

"On Calculations of the Thermal Radiation of the Atmosphere in Broken Cloud Cover", Niylik, Kh. Yu., Collection: Teploobmen v atmosfere, "Nauka", 1972, p. 46.

Possibilities of the calculation of fluxes of counter-radiation of the atmosphere in broken cloud cover are considered and analyzed. Simple formulas are proposed for determination of averaged values of fluxes of the thermal radiation of the atmosphere throughout a territory. 5 references.

UDC 551.521.3

"Vertical Profiles of Fluxes of Long-wave Radiation in a Cloud Atmosphere (Measurements and Calculations)", Goysa, N. I., V. D. Oppengeym, and Ye. M. Feygel'son, Collection: Teploobmen v atmosfere, "Nauka", 1972, p. 50.

The results of a series of measurements of long-wave radiation fluxes and effective radiation in cloud conditions from an aircraft in the daytime are given, as obtained by means of radiation thermoelements and a Yanishevskiy balance gauge. On the basis of 25 vertical profiles of the effective radiation in single-layer St clouds an experimental radiation model of the "average stratoform cloud" was constructed. Calculations were made of the radiation fluxes and influxes by means of an integral transmission function of a cloudy atmosphere, and results of the calculations were compared with data from measurements. 1 table, 1 illustration, 7 references.

UDC 551.521.3

"Transfer of Solar Radiation in the Atmosphere", Avaste, O. A., Collection: Teploobmen v atmosfere, "Nauka", 1972, p. 54.

A brief survey is given of the basic results in the investigation of fluxes and influxes of short-wave radiation obtained by the author in 1960-1969. The method of calculation of the fluxes and influxes in a cloudless and a cloudy atmosphere is considered. The results of calculation of the geographical distribution of the diurnal sums of direct solar radiation absorbed are given. It is demonstrated that in the use of the average value of the cosine of the zenith angle of the sun for a given calendar day the errors (in winter) in the high latitudes reach 60%. In the presence of continuous cloud cover (overcast) the absorption of short-wave radiation in the cloud layer, layer above the cloud, and layer below the cloud was estimated. In the layer below the cloud considerably less solar radiation is absorbed than in the same layer in a clear sky. Formulas are given for calculation of the average flux and influx of solar radiation in broken cloud cover. 5 tables, 4 illustrations, 15 references.

UDC 551.521.3

"On the Calculation of the Integral Flux and Influx of Solar Radiation", Avaste, O. A., L. D. Krasnokutskaya, and Ye. M. Feygel'son, Collection: Teploobmen v atmosfere, "Nauka", 1972, p. 67.

The dependence of the flux of solar radiation striking the earth's surface upon the pollution of the atmosphere and the content of water vapor was investigated. The visible and infrared regions of the spectrum are considered separately. Approximate formulas are given for calculation of this flux and the corresponding influx in cloudless conditions. 1 table, 2 illustrations, 5 references.

UDC 551.521

"Reflection, Transmission, and Absorption of Radiation by Clouds in the Absorption Bands of Water Vapor", Krasnokutskaya, L. D., and L. M. Romanova, Collection: Teploobmen v atmosfere, "Nauka", 1972, p. 72.

The spectral and integral albedos, transmission, and absorption of the solar radiation by a homogeneous, monodispersed stratoform cloud in the infrared region of the spectrum, 0.7-3.5 micron, were calculated. For the calculations, the distributions of light departing from the cloud were used, along the path, and also experimentally obtained transmission functions of water vapor. The quantities indicated were obtained for an optical thickness of the cloud  $\tau_0 = \infty, 30, 20$ , and densities of water vapor  $p_v = 1$  and  $5 \text{ g/m}^3$ . 2 tables, 17 references.

UDC 551.501:52

"Average Vertical Structure of the Field of Short-wave Radiation in Stratoform St and Sc Cloud Cover", Goysa, N. I. and V. M. Shoshin, Collection: Teploobmen v atmosfere, "Nauka", 1972, p. 92.

According to data from actinometric sounding of the lower troposphere (up to 3 km) in the presence of single-layer stratus and stratocumulus clouds (25 cases) averaged vertical profiles of the absolute humidity, transmission, and absorption factors of short-wave radiation, short-wave albedo, balance of short-wave radiation, radiation influxes of heat, and rates of radiation heating due to short-wave radiation in the cloud-forming layer containing the "average" stratoform cloud were constructed. It was demonstrated that the basic parameters are: the thickness (vertical development) and absolute humidity of the "average" cloud, which agree well with the statistical characteristics obtained by other authors on the basis of a large volume of material from observations. The profiles of the radiation characteristics indicated above were obtained for an ideal case (albedo of the underlying surface equal to zero) and for individual real values of the albedo. 3 tables, 1 illustration, 4 references.

UDC 551.501:52

"Experimental Investigations of Fluxes of Solar Radiation in the Lower Troposphere in St and Sc Clouds", Goysa, N. I. and V. M. Shoshin, Collection: Teploobmen v atmosfere, "Nauka", 1972, p. 78. /151

Data from 112 vertical soundings of St-Sc cloud layers are analyzed. A quantitative characteristic of the dependence of the albedo, relative transmission, effective absorption capability, and also the attenuation factor, scattering factor, and absorption factor upon the basic parameters of the cloud cover: vertical development, water reserve, and upon the altitude of the sun,  $h_0$ , was obtained. The diurnal rate of radiation heating of St-Sc as a function of their vertical development in the cold season of the year at latitudes of 45, 50, and 55° was estimated. A cloud with a vertical development of 350 m is heated due to absorption of short-wave radiation by 0.4 degree/day in December and by 3.5 degrees/day in April at a latitude of 55°, the corresponding magnitudes at a latitude of 45° amount to 1.0 and 4.0 degrees/day, 6 tables, 2 illustrations, 19 references.

UDC 551.511.33

"On the Closing of the Equation of Heat Flux in the Boundary Layer of the Atmosphere (According to Experimental Data)", Tsvang, L. R., Collection: Teploobmen v atmosfere, "Nauka", 1972, p. 100.

A survey of works performed in the IFA with respect to measurements of turbulent, radiation, and advective influxes of heat is given, and also concerning measurements of the spectra of turbulent heat fluxes at altitudes from 2.5 to 500 m.

UDC 551.521.3

"Determination of the Radiation Heat Flux in the Boundary Layer of the Atmosphere", Oppengeym, V. D. and G. P. Faraponova, Collection: Teploobmen v atmosfere, "Nauka", 1972, p. 107.

Data are given relative to fluxes of short-wave and long-wave radiation in the daytime and nighttime over the steppe and over the sea, measured from an aircraft by means of radiation thermoelements. The magnitudes of the radiation variation of the temperature for the lower layers of the troposphere up to an altitude of 1500 m were calculated. 1 table, 1 illustration, 1 reference.

UDC 551.521

"Some Problems of the Methodology of Measurement of Average Fluxes of Short-wave Radiation in Cloud Cover", Mullamaa, Yu. R., V. K. Pyldmaa, and M. A. Sulev, Collection: Teploobmen v atmosfere, "Nauka", 1972, p. 111.

In measurements of the variable process, one reading taken

separately is random in nature, and therefore for obtaining reliable information a certain averaging is required. On the basis of experimental material it was demonstrated that in measurements of fluxes of short-wave radiation in a cloudy atmosphere averaging throughout a space of 25-100 km is required and the optimum discretization spacing is located within limits of 0.4-7.0 km. Adequate averaging in space or time makes it possible to decrease the dispersion of the average radiation flux by an order of magnitude in comparison with one reading taken separately. For a further decrease in the error, a considerable increase in the averaging scale is required, which is usually practically impossible. Thus, in measurements of the average radiation fluxes in natural conditions the accuracy of the result obtained is determined not only by the accuracy of the instruments but primarily by the nature of the variability of the quantity being measured. 4 illustrations, 3 references.

UDC 551.521; 551.576

"On the Accuracy of the Averaging of Total Radiation Fluxes", Pyldmaa, V. K., Collection: Teploobmen v atmosfere, "Nauka", 1972, p. 119.

The nature of the variability of the field of total radiation in time depends upon the form and quantity of the clouds and therefore also the accuracy of the determination of average fluxes of radiation depends upon the parameters of the cloud field. By using experimental data concerning the variability of the radiation field, the degree of accuracy of averaging of the fluxes of total radiation in certain specific conditions of cloud cover that it is possible to achieve is considered. 5 illustrations, 2 references.

UDC 551.521; 551.576

"On the Methodology of the Study of the Statistical Structure of Ground Fluxes of Solar Radiation in Cloudy Conditions", Timanovskaya, R. G. and Ye. M. Feygel'son, Collection: Teploobmen v atmosfere, "Nauka", 1972, p. 125.

Estimates of the steady-state nature of the process of the variability in time of total radiation fluxes at the surface of the earth according to data from continuous recordings of actinometric measurements are given. The maximum period of observations is determined that is adequate to obtain reliable characteristics of the statistical structure of the fluxes in conditions of cumulus cloud cover and continuous cloud cover of various forms. 1 table, 2 illustrations, 2 references.

UDC 551.521; 551.576

"Total Radiation at the Surface of the Earth in Various Conditions of Cloud Cover", Pyldmaa, V. K. and R. G. Timanovskaya, Collection:

Teploobmen v atmosfere, "Nauka", 1972, p. 131.

The variability in time of fluxes of total radiation at the surface of the earth in various forms and number of points of cloud cover is investigated. Certain statistical parameters of the total radiation field in cumulus cloud cover are considered. 3 tables, 5 illustrations, 1 reference.

UDC 551.576

"Some Parameters of Cumulus Clouds Obtained According to Photographs of the Sky and from Ground Actinometric Measurements", Timanovskaya, R. G. and Ye. M. Feygel'son, Collection: Teploobmen v atmosfere, "Nauka", 1972, p. 138.

/152

According to photographs of the sky and from ground actinometric measurements the interrelationship of the general number of points of cumulus clouds and the zonal number of points in the direction to the sun with the duration of sunshine is discussed. 2 tables, 4 illustrations, 5 references.

UDC 551.521; 551.576

"Fluxes of Solar Radiation at the Surface of the Earth in Cumulus Cloud Cover", Timanovskaya, R. G. and Ye. M. Feygel'son, Collection: Teploobmen v atmosfere, "Nauka", 1972, p. 146.

The statistical structure of fluxes of direct and total radiation at the surface of the earth as a function of the state of cumulus cloud cover is investigated, characterized by the general number of points of cover and by the duration of sunshine. 2 tables, 10 illustrations, 3 references.

UDC 551.521; 551.576

"Spatial Structure of the Field of Short-wave Radiation in Strato-cumulus and Cumulus Cloud Cover", Sulev, M. A. Collection: Teploobmen v atmosfere, "Nauka", 1972, p. 152.

An airborne investigation was made of the spatial variability of the fields of short-wave radiation and cloud cover for clouds of the Sc and Cu forms. Average statistical characteristics of the fields indicated are given (autocorrelation function, spectral density, variability factor). In a case of Sc the correlation radius for radiation fluxes varies within limits from 1.5 to 35 km, the variability factor from 0.15 to 0.5. With Cu the average correlation radius is equal to 0.8 km, the variation factor to 0.3. 1 table, 6 illustrations.

UDC 551.576

"Structure of the Field of Cumulus Clouds", Mullamaa, Yu. R., V. K. Pyldmaa, and M. A. Sulev, Collection: Teploobmen v atmosfere, "Nauka", 1972, p. 161.

A theoretical analysis was made of ground and airborne measurements of the presence of clouds in the direction of the zenith.

By modeling the cumulus cloud cover of the normal random surface, limited from a certain level, analytical formulas were obtained for the autocorrelation function, probability density of the number of openings in clouds as a function of their duration (or length), frequency of openings or clouds, i.e., their number per unit of length or unit of time. A good agreement of the model with the experimental data is observed. 3 illustrations, 3 references.

UDC 551.576

"On the Transmission of Solar Radiation by Stratoform Cloud Cover as a Function of the Statistical Characteristics of its Structure", Mullamaa, Yu. R., Collection: Teploobmen v atmosfere, "Nauka", 1972, p. 166.

The variability of the transparency of an optically dense cloud layer is theoretically considered as a function of the variability of its optical thickness, caused by the variability of the altitude of the lower and upper boundaries, the absolute humidity, and the microstructure. In the analysis it is proposed to consider the optical thickness of stratoform cloud cover as a normal random function. It was found that the probability density function is asymmetrical and extended toward the side of greater transparency. Approximate formulas were derived for consideration of the dependences of the average transparency and transparency dispersion upon the average optical thickness and its dispersions. It turns out that the average transparency is a direct function of the dispersion of the optical thickness and an inverse function of the average optical thickness. The dispersion of the transparency in the first approximation depends linearly upon the dispersion of the optical thickness and is proportional to the transparency of a homogeneous layer to a power of four at the average optical thickness. For a description of the light regime in heterogeneous media, aside from average characteristics of the media, it is necessary to know their dispersions, correlation functions, and in the solution of certain problems also the distribution functions. 3 illustrations, 1 reference.

UDC 551.576

"On the Coverage of the Sky by Clouds" Avaste, O. A., Yu. R. Mullamaa, Kh. Yu. Niylik, and M. A. Sulev, Collection: Teploobmen v atmosfere, "Nauka", 1972, p. 173.

Three calculation schemes are given for determination of the averaged values of the probability of the coverage of the sighting direction and the number of points of cumulus cloud cover as a function of the average coverage in the direction of the zenith and the nature of the distribution of clouds throughout the sky. A satisfactory agreement is observed between the results obtained

according to various calculation schemes. In cumulus clouds, the coverage of the sighting directions by clouds begins to increase considerably at zenith distances greater than  $50^\circ$ . The number of points of cumulus cloud cover measured from artificial earth satellites is always less than the number of points at the earth's surface, which must be born in mind in the use of satellite data with reference to ground conditions. A satisfactory agreement of the calculated data with the experimental data is observed. 2 illustrations, 5 references.

☆ U.S. GOVERNMENT PRINTING OFFICE: 1974-739-162/147



NATIONAL AERONAUTICS AND SPACE ADMINISTRATION  
WASHINGTON, D.C. 20546

OFFICIAL BUSINESS  
PENALTY FOR PRIVATE USE \$300

SPECIAL FOURTH-CLASS RATE  
BOOK

POSTAGE AND FEES PAID  
NATIONAL AERONAUTICS AND  
SPACE ADMINISTRATION  
451



POSTMASTER: If Undeliverable (Section 158  
Postal Manual) Do Not Return

*"The aeronautical and space activities of the United States shall be conducted so as to contribute . . . to the expansion of human knowledge of phenomena in the atmosphere and space. The Administration shall provide for the widest practicable and appropriate dissemination of information concerning its activities and the results thereof."*

—NATIONAL AERONAUTICS AND SPACE ACT OF 1958

## NASA SCIENTIFIC AND TECHNICAL PUBLICATIONS

**TECHNICAL REPORTS:** Scientific and technical information considered important, complete, and a lasting contribution to existing knowledge.

**TECHNICAL NOTES:** Information less broad in scope but nevertheless of importance as a contribution to existing knowledge.

**TECHNICAL MEMORANDUMS:** Information receiving limited distribution because of preliminary data, security classification, or other reasons. Also includes conference proceedings with either limited or unlimited distribution.

**CONTRACTOR REPORTS:** Scientific and technical information generated under a NASA contract or grant and considered an important contribution to existing knowledge.

**TECHNICAL TRANSLATIONS:** Information published in a foreign language considered to merit NASA distribution in English.

**SPECIAL PUBLICATIONS:** Information derived from or of value to NASA activities. Publications include final reports of major projects, monographs, data compilations, handbooks, sourcebooks, and special bibliographies.

**TECHNOLOGY UTILIZATION PUBLICATIONS:** Information on technology used by NASA that may be of particular interest in commercial and other non-aerospace applications. Publications include Tech Briefs, Technology Utilization Reports and Technology Surveys.

Details on the availability of these publications may be obtained from:

**SCIENTIFIC AND TECHNICAL INFORMATION OFFICE**

**NATIONAL AERONAUTICS AND SPACE ADMINISTRATION**

**Washington, D.C. 20546**